SYNTHESIS OF POLYTHIOPHENE-POLYURETHANE SOFT NANOPARTICLES FOR BIOIMAGING APPLICATIONS

A Thesis Submitted to
The Graduate School of Engineering and Sciences of
İzmir Institute of Technology
in Partial Fulfillment of the Requirements for the Degree of

MASTER OF SCIENCE

in Chemistry

by
Soner KARABACAK

July 2020
İZMİR

ACKNOWLEDGMENTS

Primarily, I would like to state my sincere thankfulness to my advisor Assoc. Prof. Dr. Ümit Hakan YILDIZ for his specialist guidance, recommendation, motivation, amicability and patience not only throughout this journey but also for every moment of life. Also, I would like to thank to Assist. Prof. Dr. Ahu ARSLAN YILDIZ for her precious interpretation and supporting to this thesis.

I want to thank to my co-workers, Sezer ÖZENLER, Müge YÜCEL, and Hakan KAYA for their motivation and helping to this thesis. I wish also would thank to members of Biosens-Bioapps Research Group including Mustafa Umut MUTLU, Dilce İNANÇ, Öykü YILDIRIM KARAMAN, Hüseyin ZEYBEK, Merve Beril DOĞDAŞ for their helping and friendship. Also, I would like to thank to members of Biomimetic Research Group for their helps and supports.

I would like to thank to my lovely girlfriend Bahar DEMİRTAŞ for her encouragement, intellection and supporting during my MSc and my life.

Finally, I would like to express my gratitude for my mother Ayşe KARABACAK and my dear siblings, for their supporting and their love in every moment of life.

This thesis is supported by Scientific and Technological Research Council of Turkey (TÜBİTAK-116Z547 and TÜBİTAK-117F243).

ABSTRACT

SYNTHESIS OF POLYTHIOPHENE-POLYURETHANE SOFT NANOPARTICLES FOR BIOIMAGING APPLICATIONS

In this study, synthesis of fluorescent polythiophene and polyurethane soft nanoparticles carrying them was carried out for bioimaging applications. Conjugated polythiophenes and polyurethane derivatives were obtained by changing their structural properties such as size, charge, and group, and were characterized by nuclear magnetic resonance, infrared spectroscopy, dynamic functional light scattering, fluorescent microscopy, methods. In the study, changing characteristics of polyurethane nanoparticle materials were investigated depending on the synthesis conditions. Synthesis of polyurethane nanoparticles was carried out by miniemulsion polymerization technique and synthesized as nanosphere to be more controllable on nanoparticle size, morphology and stability. The sizes of the polyurethane nanospheres varied in the range from 10 to 500 nm. Polyelectrolyte-polyelectrolyte complexation was investigated using cationic polythiophene-anionic polythiophene for use in bioimaging applications. Synthesized conjugated polythiophenes are divided into two groups as anionic and cationic polythiophenes. In this thesis, three kinds of cationic polythiophene synthesis are included, but poly (1,4-dimethyl-1- (3- ((4-methylthiophene-3-yl) oxy) propyl) piperazine-1-ium bromide) (PT4) was used as cationic conjugated polythiophene in the studies. Anionic polythiophene acetic acid (PTAA) was used as a counter-charged polythiophene. In addition to these studies, dual-mode imaging agents were prepared, consisting of PTAA as fluorescent agent and gadolinium metals as magnetic agent. The bioimaging studies continued under conditions imitating biological systems, and the potential of the proposed bioimaging agents was investigated.

Keywords: Bioimaging Applications, Conjugated Polythiophene-based Polyelectrolytes, Polyurethane Nanosphere, Miniemulsion Polymerization, Polyelectrolyte-Polyelectrolyte Complexes

ÖZET

BİYOGÖRÜNTÜLEME UYGULAMALARI İÇİN POLİTİYOFEN-POLİÜRETAN YUMUŞAK NANOPARÇACIKLARIN SENTEZİ

Bu çalışmada biyogörüntüleme uygulamaları için floresan politiyofen ve onları taşıyan poliüretan yumuşak nanoparçacıkların sentezi gerçekleştirilmiştir. Konjuge politiyofenler ve poliüretan türevleri, boyut, yük, fonksiyonel grup gibi yapısal özellikleri değiştirilerek elde edilmiş ve nükleer manyetik rezonans, kızıl ötesi spektroskopi, dinamik ışık saçılması, floresan mikroskop, metotları ile karakterize edilmiştir. Çalışmada, sentez koşullarına bağlı olarak poliüretan nanoparçacık malzemelerin değişen karakteristik özellikleri araştırılmıştır. Poliüretan nanoparçacıkların sentezi, nanoparçacık boyutu, morfolojisi ve stabilitesi üzerinde daha kontrol edilebilir olması için miniemülsiyon polimerizasyon tekniği ile gerçekleştirilmiş ve nanoküre olarak sentezlenmiştir. Elde edilen poliüretan nanokürelerin boyutları 10-500 nm aralığında değişmektedir. Biyogörüntüleme uygulamalarında kullanmak için katyonik politiyofen-anyonik politiyofen polielektrolit-polielektrolit kompleksleşmesi incelenmiştir. Sentezlenmiş konjuge politiyofenler, anyonik ve katyonik politiyofenler olarak iki gruptadır. Bu tezde üç çeşit katyonik politiyofen sentezine yer verilmiştir ancak poli (1,4-dimetil-1- (3- ((4-metiltiofen-3-il) oksi) propil) piperazin-1-ium bromür) (PT4) çalışmalarda katyonik konjuge politiyofen olarak kullanılmıştır. Anyonik politiyofen asetik asit (PTAA) karşıt yüklü politiyofen olarak kullanılmıştır. Bu çalışmalara ek olarak, floresan ajan olarak PTAA ve manyetik ajan olarak gadolinyum metallerden oluşan çift modlu görüntüleme ajanları hazırlanmıştır. Biyolojik sistemleri taklit eden koşullar altında biyogörüntüleme çalışmaları devam edilerek önerilen biyogörüntüleme ajanlarının potansiyeli araştırılmış ve uygulama alanlarına yönelik ön çalışmalar gerçekleştirilmiştir.

Anahtar Kelimeler: Biyogörüntüleme Uygulamaları, Konjuge politiyofen Bazlı Polielektrolitler, Poliüretan Nanoküre, Miniemülsiyon Polimerizasyonu, Polielektrolit-Polielektrolit Kompleksleri

TABLE OF CONTENTS

LIST OF TABLES

Table **Page**

LIST OF FIGURES

Figure **Page**

Figure **Page**

Figure **Page**

Figure **Page**

Figure **Page**

Figure **Page**

CHAPTER 1

INTRODUCTION

Bioimaging is an excellent method to monitor the biological processes in real-time and noninvasively, as well. Bioimaging method is widely used for improvement of functional therapeutic systems that usually consist of molecular targeting and imaging agents. On the other hand, this method have great attention due to the monitoring of drug delivery to tumors in vivo[1]. Thus, bioimaging applications provide to understand mechanism and function of biological species. To date, several bioimaging applications were improved in order to obtain fluorescence[2-3], magnetic resonance (MRI)[4-5], ultrasound[6], computerized tomography[7], and positron emission tomography[8] images of organs, veins and cells. However, imaging agents used in fluorescence and magnetic resonance imaging makes them powerful techniques due to their biocompatibility, good sensitivity, and high resolution[9].

Fluorescence imaging is used to visualize biological process or structural dynamics of biological systems with fluorescent agents such as organic fluorescent dyes, quantum dots, fluorescent proteins, and conjugated polymers[10]. In this thesis, conjugated polymers were used as fluorescence imaging agent. Conjugated polymers are macromolecules that are qualified by electron delocalization along the backbone. They have overlapping p-orbitals which are creating a system of delocalized π-electrons. Thus, they have interesting and practical optical and electronic properties[11]. There are many conjugated polymers which are reported in the literature. However, conjugated polymers have attracted a great deal of attention after discovery of polyacetylene which prepared the ground to new conjugated polymers[12]. Different conjugated polymers are discovered by oxidative electropolymerization of polypyrole[13]. After that, other conjugated polymers came up for example, thiophene[14], indole[15], pyrene[16], benzene[17], and fluorene[18] etc. Figure 1.1 shows structures of some conjugated polymers. Researches show that conjugated polythiophene has been one of the most widely enquired class of the other conjugated polymers. Polythiophene has many advantages such as low cost, thermal

stability, ease of processing, tunable electrical and optical properties. It is also easily functionalized with a kind of aromatic monomers in order to synthesize copolymers[19].

Conjugated polythiophene has double and single bonds but their conjugated system are nondegenerate. As a result of this condition, an energy band gap is occurred between the highest occupied molecular orbital (HOMO) and the lowest unoccupied molecular orbital (LUMO). That is why, tunable optical band gap on polythiophene backbone has made it significant candidate to develop electronic devices[20]. The unique properties provide conjugated polythiophene to be used in different fields such as organic light emitting diodes[21] (OLED), solar cells[22], field effective transistors (FET)[23], photovoltaic devices[24], and biosensor[25-26], and bioimaging applications[27].

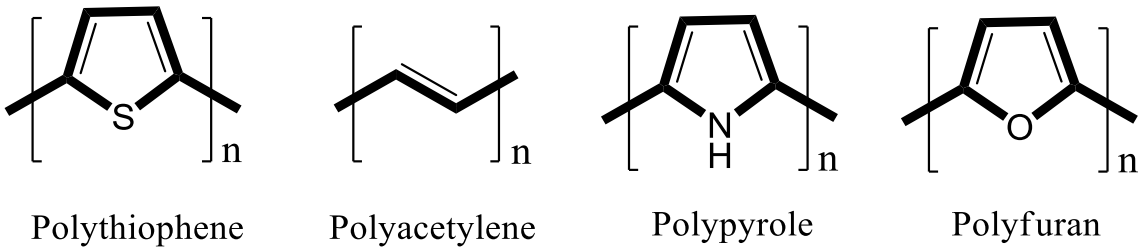

Figure 1.1. Some common conjugated polymer structures.

In this study, basically different conjugated polymers have been synthesized for two purposes. These two main objectives are to examine the formation of polyelectrolyte-polyelectrolyte complexes and to prepare them for use in bioimaging applications by functionalizing the conjugated polymers. For the first purpose, two types of polyelectrolytes (also called conjugated polymers) were synthesized as anionic[28] and cationic[29]. Already the most known feature of polyelectrolytes is that they can form complexes with opposite charges of each other. Although there are many complexation methods, the easiest way is to mix two opposite charged polyelectrolytes in the aqueous solution[30]. Figure 1.2 shows the complexation of anionic and cationic conjugated polymers.

The second and more important goal is to make functional conjugated polymers for use in bioimaging applications. Conjugated polymers have attracted great attention in the fields of chemistry and biology. The reason for this interest is related to its features. Conjugated polymers have high fluorescence brightness, high photostability, low cytotoxity, fast emission rates, high quantum yields, versatile surface modification, good biocompability, and good water solubility [32-35]. These features make conjugated polymers

excellent fluorescent probes for bioimaging applications. Figure 1.3.a shows photographs of some conjugated polymers captured under UV-light. Figure 1.3.b shows brightfield and fluorescence images of macrophage cells stained by the conjugated polymers represented in Figure 1.3.a.

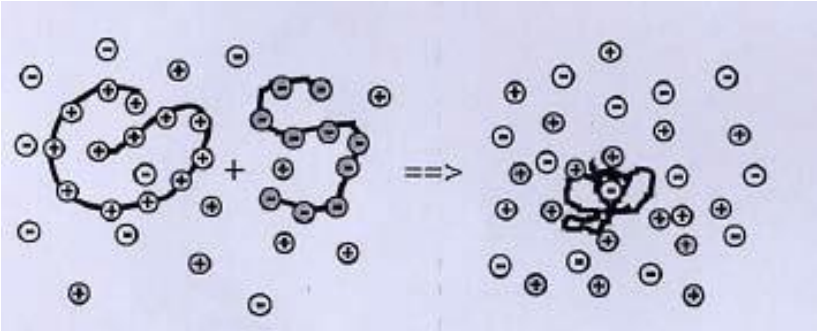

Figure 1.2. Schematic representation of polyelectrolyte(anionic) polyelectrolyte(cationic) complexation.

(Source: Radeva, T., 2001) [31]

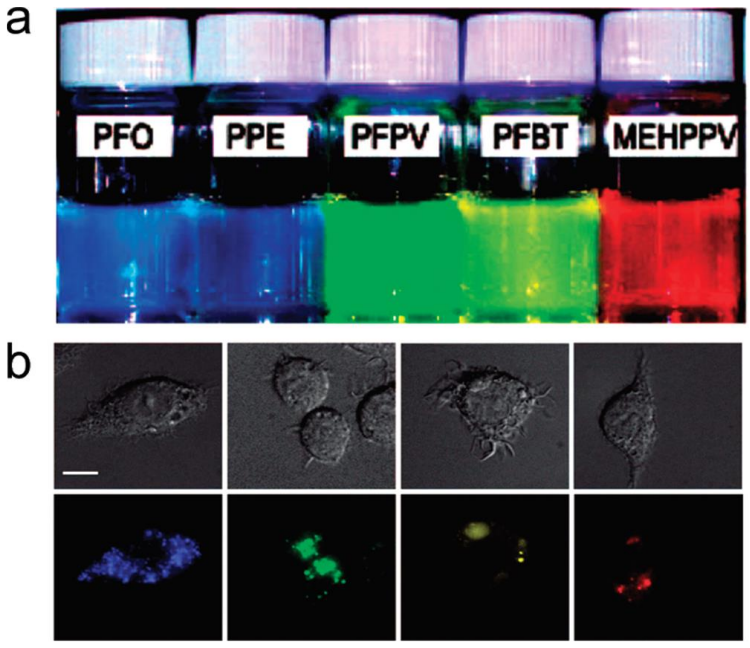

Figure 1.3. a) Photographs of some conjugated polymers taken under UV-light (poly (9,9-dioctylfluorenyl-2,7-diyl (PFO), PPE, poly[{9,9-dioctyl-2,7-divinylene-fluorenylene}-alt-co-{2-methoxy-5-(2-ethylhexyloxy)-1,4-phenylene}] (PFPV), (poly[(9,9-dioctylfluorenyl-2,7-diyl)-co-(1,4-benzo-{2,1′,3}-

thiadiazole)] (PFBT) [37], poly[2-methoxy-5-(2-ethylhexyloxy)-1,4-phenylenevinylene] (MEHPPV) [38], b) Top of the figure b, differential interference contrast images and bottom of the figure b, fluorescence images of macrophage cells.

(Source: Wu, C., 2008) [9]

Nowadays, advanced biotechnology increases the requirements in order to satisfy, therefore, dual-modal fluorescent-magnetic imaging agents gain significance and they are used to visualize biological process. Li et. al. improved this dual-modal bioimaging agents for bioimaging applications. They encapsulated the conjugated polymer (PFVBT: poly[9,9- bis (6′- (*N*,*N*-dimethylamino) hexyl)fluorenyl divinylene - *alt*-4,7-(2,1,3-benzothiadiazole)])) and iron oxide (IOs) nanoparticles with mixture of poly(lactic-*co*-glycolic-acid)-poly(ethylene glycol)-folate (PLGA-PEG-FOL) and PLGA. Demonstration of dual-modal imaging agents were shown in Figure 1.4 [36]. Also, synthesis of dual mode fluorescent-magnetic imaging agent were performed in this thesis. Agents were synthesized by combination of conjugated polymers as fluorescent probe and gadolinium metals as magnetic probe.

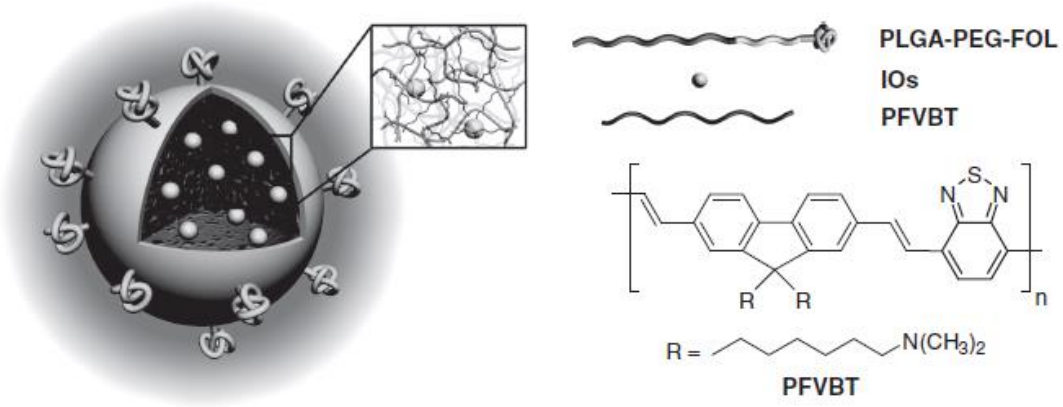

Figure 1.4. Demonstration of dual-modal imaging agents.

(Source: Li, K., et al., 2012) [36]

As can be seen, it has been observed that bioimaging agents are combined with the polymers or attached to its nanosphere surface in order to combine and functionalize as in the above literature example. In this thesis polyurethane was chosen for synthesis of bioimaging agents. Polyurethane provides a multifunctionality, facilitating transport and storage, development the stability of encapsulated product, and increasing the lifetime[39].

Polyurethane are a member of synthetic polymer family which was synthesized with reaction between isocyanate and polyol groups. In the past decade, nanosized polyurethane particles gain huge significance which are widely used as particulate dispersions with size in the range of 10-1000 nm[40-41]. Polyurethane nanoparticles are used for extensive applications in different areas such as agriculture, environment, drug delivery systems, and bioimaging applications. Polyurethane nanoparticles can be named also as polyurethane nanospheres[42]. Polyurethane nanospheres based materials are promising to become functional and technological new nanomaterial in the future[43-47]. Polyurethane nanospheres are prepared by different techniques such as self-assembly, macro/micro/mini emulsion, nanoprecipitation etc.[10]. In this study, miniemulsion technique was used to synthesize nanospheres from polyurethane because miniemulsion technique provides to be more controllable on the structure, morphology, and small size of nanospheres[48-49]. Lately, polyurethane nanospheres was prepared with using miniemulsion technique in some publications[50-52]. Miniemulsion technique is carried out by ultrasonification of materials which includes a hydrophobic monomer, water, surfactant, and costabilizer[53-57]. Figure 1.5 shows a principle of miniemulsion technique that usually consist of two phases.

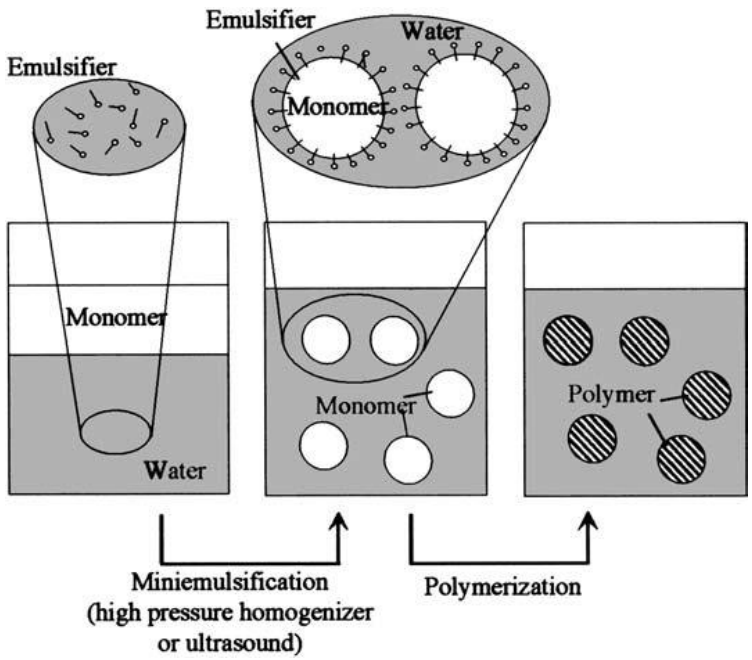

Figure 1.5. Principle of miniemulsion technique.

(Source: Landfester, K., 2003) [41]

In this thesis, there are two different miniemulsion techniques was used for synthesis of polyurethane nanospheres which are two step[48] and one pot[51] miniemulsion technique. Two step miniemulsion technique provides a high molecular weight polyurethane nanospheres. Also, it has more controllable procedure than other techniques. Two step miniemulsion technique was formed as a two-step which are synthesis of NCO-ended prepolymer and preparation of polyurethane dispersions. First step was carried out by reaction of ısophorone diisocyanate and poly (propylene glycol) in toluene. Second step was performed by ultrasonication of oil and water phases and polyaddition reaction with heating. On the other hand, one pot miniemulsion technique includes only ultrasonification of miniemulsion system. Also, polyaddition reaction was performed in order to increase a molecular weight. The difference of one pot miniemulsion technique has easier process than two step miniemulsion technique.

Herein in this thesis, conjugated polythiophene and polyurethane derivatives were synthesized for preparation of bioimaging agents. Also, after conjugated polymers was synthesized, polyelectrolyte-polyelectrolyte complexation was investigated in order to examine effects on the bioimaging applications. In addition to these, various nanospheres was prepared which have different functional properties. Thus, synthesis of polythiophene-polyurethane soft nanoparticles were carried out for bioimaging applications.

CHAPTER 2

MATERIALS AND METHODS

2.1. Materials

3-Bromo-4-methylthiophene (95%, Sigma Aldrich), Copper(II) bromide (99%, Sigma Aldrich), Sodium methoxide (95%, powder, Sigma Aldrich), 1-Methyl-2-pyrrolidinone anhydrous, (99.5% Sigma Aldrich), Methanol (ACS reagent, ≥99.8%, Sigma Aldrich), Sodium Bromide (99%, Sigma Aldrich), Diethyl ether (99.5%, Sigma Aldrich), Magnesium sulfate (97%, Sigma Aldrich), 3-Bromo-1-propanol (97%, Sigma Aldrich), Toluene (ACS reagent ≥99.7%, Sigma Aldrich), Sodium bisulfate anhydrous (Sigma Aldrich), Silica gel (pore size 60 Å, 60- 100 mesh, Merck) , Hexane (95%, Sigma Aldrich), Ethyl acetate (99.7%, Sigma Aldrich), 1,4-Dimethylpiperazine (98%, Sigma Aldrich), Tetrahydrofuran (THF, ACS reagent, ≥99.9%, Sigma Aldrich), Iron(III)chloride (99.9%, Sigma Aldrich), chloroform (≥99%, Sigma Aldrich), Chloroform-d (99.8%, Merck), Deuterium oxide (D_2O, 99.96%, Merck), Dimethylsulphoxide-D (DMSO-D6) (99.96%, Merck), Hydrochloric acid (ACS reagent, ≥37%, Sigma Aldrich), Sodium hydroxide (ACS reagent, ≥97.0%, pellets), 1,4-diazabicyclo [2.2.2] octane (≥99%, Sigma Aldrich), N-allyl-N-methylprop-2-en-1-amine (99%, Sigma Aldrich), 3-Thiophene acetic acid (Acros Organics), Sulfuric acid (Sigma Aldrich), Sodium chloride (Sigma Aldrich), Ethylene Glycol (Merck), 3-Thiophenemethanol (98%, Sigma Aldrich), 3-Thiopheneethanol (Sigma Aldrich), Poly(propylene glycol) (average Mn 1000, Sigma Aldrich), Isophorone Diisocyanate (98%, Sigma Aldrich), Hexadecane (99%), Sodium Dodecyl Sulfate (SDS) (Bioshop), Dibutyltin dilaurate (95%, Sigma Aldrich), 1,4-Butanediol (99%, Sigma Aldrich), Trimethylolpropane (Alfa Aesar), Ethylenediamine (99%, Sigma Aldrich), Ethyl lysine diisocyanate (ELDI) (99%, Alfa Aesar), Polyethyleneimine (PEI) (branched MW 25000, Sigma Aldrich), Pentaerythritol (Sigma Aldrich), DOTA-NHS-ester (Macrocyclics) Gadolinium(III) chloride hexahydrate (Sigma Aldrich), Citric Acid monohydrate (Sigma Aldrich) was purchased.

2.2. Synthesis Conjugated Polymers

2.2.1. Cationic Conjugated Polymers

Conjugated polymers were synthesized as a below steps. Firstly, Precursor 1 was synthesized. Sodium methoxide is a reactant of Precursor 1; 3-Methoxy-4-methylthiophene (PC1) which is so significant for obtaining high efficiency. Also, commercial sodium methoxide have stability problem for usage of long time. That's why, sodium methoxide was synthesized as a solution. 2.67 g sodium metal was washed with hexane in order to purify from oil. Then, 30 ml dry methanol was used in order to dissolve sodium metal in 100 ml round bottom flask for 3 hours at room temperature.

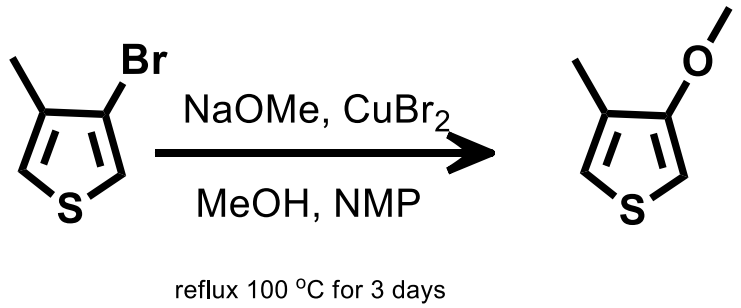

Figure 2.1. Representation of 3-Methoxy-4-methylthiophene (PC1) synthesis.

3-Bromo-4-Methylthiophene (BMT) (0.65 ml, 5.64 mmol), Copper(II)Bromide ($CuBr_2$) (0.5g, 3.48 mmol), 1-Methyl-2-Pyrrolidone (NMP) (2 ml, 20.83 mmol), and sodium methoxide (NaOMe) (4 ml, 25 wt. %, 17.44 mmol) was put into the 50 ml dry-round-bottom flask with magnetic bar (Figure 2.1). The reaction mixture was refluxed at 110 ^oC for 3 days under nitrogen (N_2) atmosphere After 3 days, the reaction mixture was cooled to room temperature and a solution of 0.25 g Sodium Bromide (NaBr) in 10 ml distilled water (DI) was added and stirred vigorously for 1 hour. Filtration and extraction was done with using filter paper and 15 ml diethylether at least 5 times. In this step, TLC paper was used in order to make sure there is no substances. On the other hand, organic phase was washed with pure water in the extraction stage. Magnesium sulfate ($MgSO_4$) was used in order to remove solvent from media. After the purification steps, light-yellow oil product was obtained as a PC1.

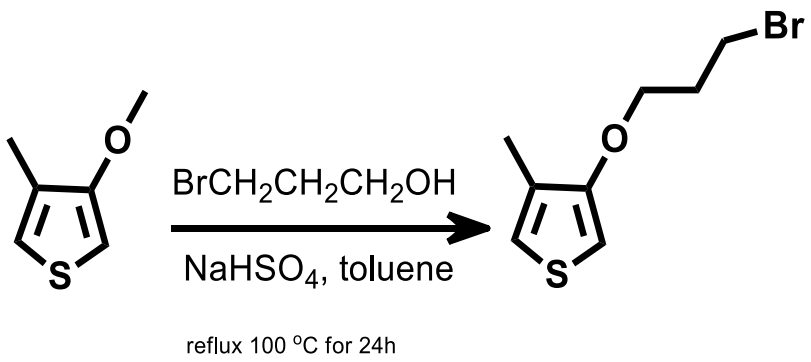

Figure 2.2.Representation of 3-Bromopropoxy-4-methyltiophene (PC2) synthesis.

Mixture of PC1 (80 mg), 3-bromo-1-propanol (200 uL), $NaHSO_4$ (13 mg), and toluene (2 ml) was added into the round-bottom flask. The reaction mixture was refluxed at 100 ^oC for 24 hours under N_2 atmosphere (Figure 2.2). After 24 hours, reaction was ended and cooled to room temperature. Rotary evaporator was used in order to remove toluene. The reaction mixture was extracted with diethylether at least five times, subsequently washed with water. Organic phase was dried with $MgSO_4$ at least three times. Again, rotary evaporator was used in order to remove diethylether. The crude product was purified with column chromatography method. In the column chromatography step, 10 spoon silica gel was mixed with 40 ml hexane and silica gel/hexane mixture was placed into the column. Solvent systems was included hexane and 8:1 hexane-ethyl acetate mixture. The crude product was washed with hexane. Then, hexane was evaporated by rotary evaporator. Eventually, PC2 was obtained in order to use for all kinds of monomer synthesis as a colorless oil.

Three kinds of monomer was synthesized from Precursor 2 (PC2). The monomers are respectively 1-(3-((4-methylthiophen-3-yl) oxy) propyl)-1,4-diazabicyclo [2.2.2] octan-1-ium bromide (M3), 1,4-dimethyl-1-(3-((4-methylthiophen-3-yl) oxy) propyl) piperazin-1-ium bromide (M4), and N-allyl-N-methyl-N-(3-((4-methylthiophen-3-yl) oxy) propyl) prop-2-en- 1-aminium bromide (M5). Monomer reactions was shown in Figure 2.3.

PC2 (80 mg, 0.34 mmol), DABCO (1,4-diazabicyclo [2.2.2] octane) (3.07 mmol, 344 mg), and THF (5 mL) was added into the round bottom flask. The reaction mixture was refluxed at 72 ^oC for 2 days under N_2 atmosphere. When reaction was ended, the crude product was washed with THF and centrifugated at 4000 rpm for 5 min at least three times (Supernatant was separated in each trial). Eventually, after removing supernatant again, precipitate was obtained as a white color and it was dried under vacuum

in desiccator. M4 and M5 was synthesized at the same synthesis and purification procedures with different chemical and amounts. M4 synthesis includes, PC2 (0.27 g, 1.15 mmol), 1,4-dimethylpiperazine (26.45 mmol, 3.7 mL), and THF (10-15 mL) and M5 synthesis includes; PC2 (0.27 g, 1.15 mmol), N-allyl-N-methylprop-2-en-1-amine (26.45 mmol, 3.7 mL), and THF (10-15 mL).

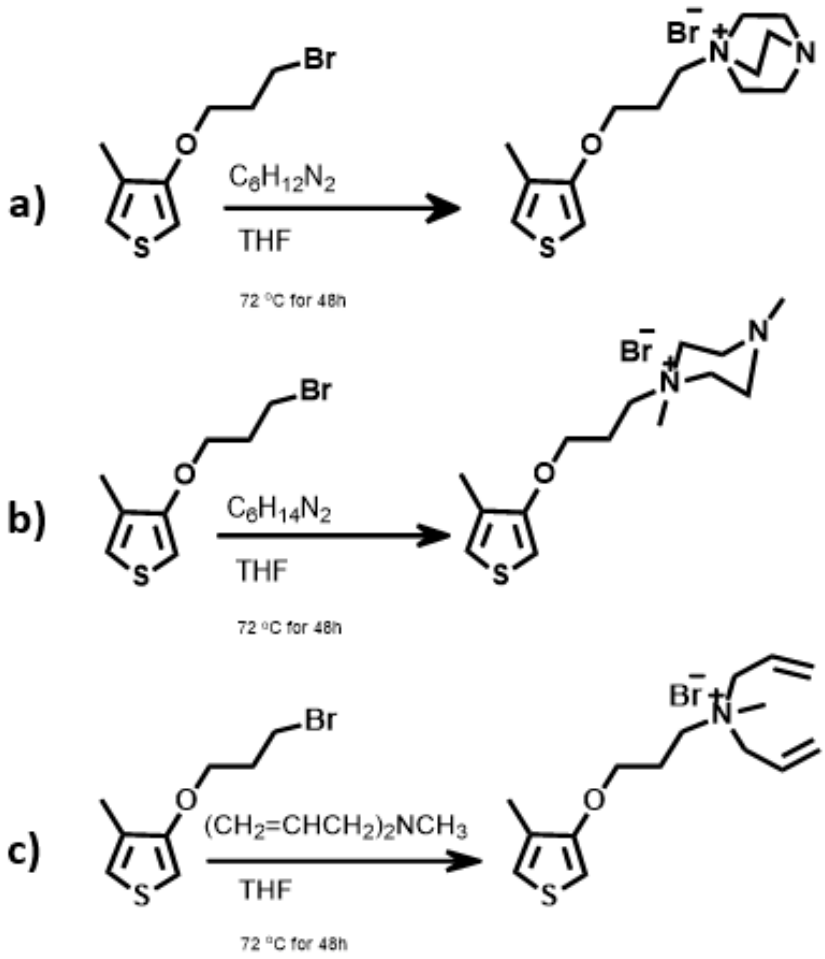

Figure 2.3. Representation of synthesis of monomers, a) M3, b) M4, and c) M5.

After the synthesis of monomers, polymerization step was done for M3, M4, and M5. Approximately each monomer (50 mg, 0.186 mmol) in 2 mL of dry chloroform was dissolved in order to added dropwise to a solution of anhydrous Iron (III) Chloride ($FeCl_3$) (121 mg, 0.744 mmol) in 2 ml of dry chloroform. The reaction was stirred for 24 hours at room temperature under nitrogen atmosphere. After 24 hours, methanol was used to precipitate polymers in solution. Then, precipitated polymers was washed with chloroform and centrifugated at 4000 rpm for 5 min at least three times (Supernatant was

separated in each trial). Finally, after removing supernatant again, precipitate was obtained as a black color and it was dried under vacuum in desiccator. The polymer structures were shown in Figure 2.4.

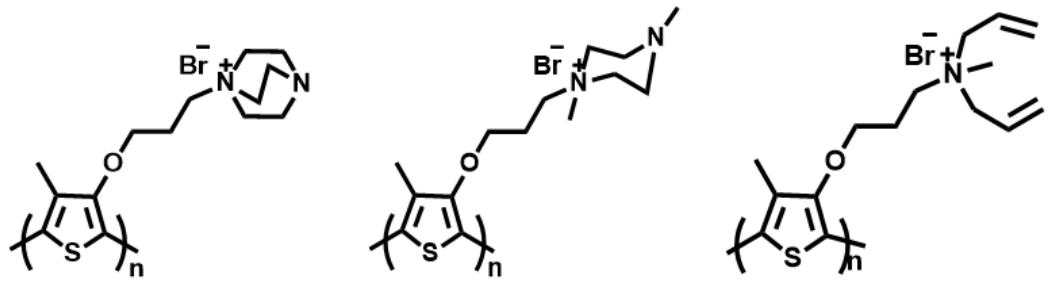

Figure 2.4. Structure of synthesized polymers, a) Poly(1-(3-((4-methylthiophen-3-yl) oxy) propyl)-1,4-diazabicyclo [2.2.2] octan-1-ium bromide) (PT3), b)) Poly(1,4-dimethyl-1-(3-((4- methylthiophen-3-yl) oxy) propyl) piperazin-1-ium bromide) (PT4), and c) Poly(N- allyl-N-methyl-N-(3-((4-methylthiophen-3-yl) oxy) propyl) prop-2- en-1-aminium bromide) (PT5**).**

2.2.2. Anionic Conjugated Polythiophene

Anionic Conjugated polymers was synthesized as a below steps. Firstly, esterification reaction was carried out as shown in Figure 2.5. 3-Thiophene acetic acid, (TAA) (0.5 g, 3.5mmol), Methanol (5 ml), and Sulfuric acid (H_2SO_4) (1 drop) was put into the 50 ml dry-round-bottom flask with magnetic bar and the mixture was refluxed for 24 hours under N_2 atmosphere. As a result of reaction, 3-Thiophene methyl acetate (TMA) was purified. Methanol was evaporated by rotary evaporator. Mixture was extracted with diethyl ether and washed with deionized water. Then, $MgSO_4$ was used in order to dry to mixture. Mixture was filtered to avoid $MgSO_4$. Diethyl ether was evaporated by rotary evaporator. TMA was prepared for other steps.

Polymerization of TMA was carried out as shown in Figure 2.6. Solution of TMA (0.4 g, 2.6 mmol) in 10 ml of chloroform was added dropwise into solution of $FeCl_3$ (1.68 g, 10.4 mmol) in 20 ml chloroform in 50 ml round-bottom flask under nitrogen atmosphere. Reaction temperature was set at 0°C in ice box for 24 hours. After 24 hours,

excess methanol was used to precipitate polymers in the reaction mixture. Then, precipitated polymers was washed with methanol and centrifugated at 4000 rpm for 5 min at least three times (Supernatant was separated in each trial). Finally, after removing supernatant again, precipitate was obtained as a blue-black color and it was dried under vacuum in desiccator. Thus, polythiophene methyl acetate (PTMA) was obtained.

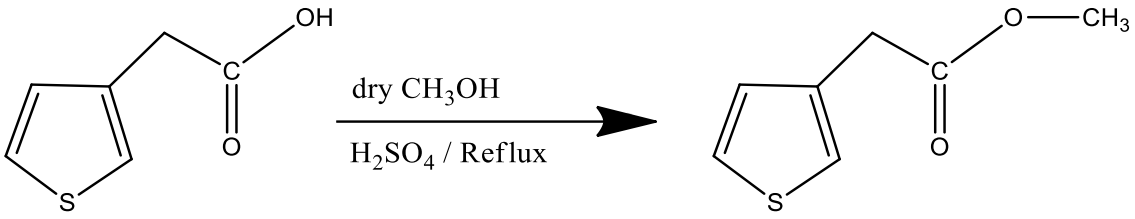

Figure 2.5. Representation of 3-Thiophene methyl acetate (TMA) synthesis.

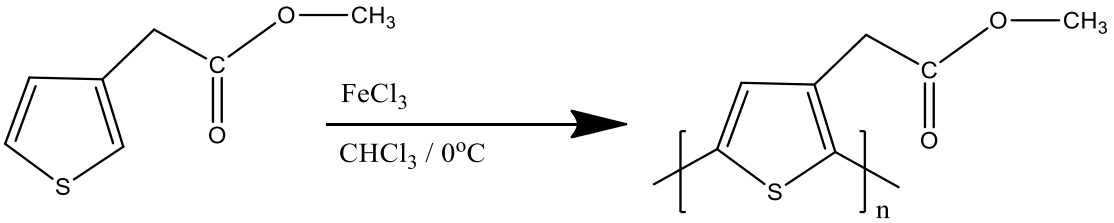

Figure 2.6. Second step of anionic conjugated polythiophene synthesis.

Hydrolysis of PTMA was performed as shown in Figure 2.7. PTMA (50 mg) was dissolved in 5 ml of 2 M NaOH. Reaction condition was adjusted at 100°C for 24 hours. After 24 hours, the mixture was filtered in order to remove solid particles. Diluted Hydrochloric acid (HCl) was used to neutralized liquid phase (Figure 2.8). After neutralization, hydrolyzed polymers was precipitated. Then, precipitated polymers was washed with deionized water (with diluted HCl) and centrifugated at 4000 rpm for 5 min at least three times (Supernatant was separated in each trial). Finally, after removing supernatant again, precipitate was obtained as a black color and it was dried under vacuum in desiccator. Thus, polythiophene acetic acid (PTAA) was obtained.

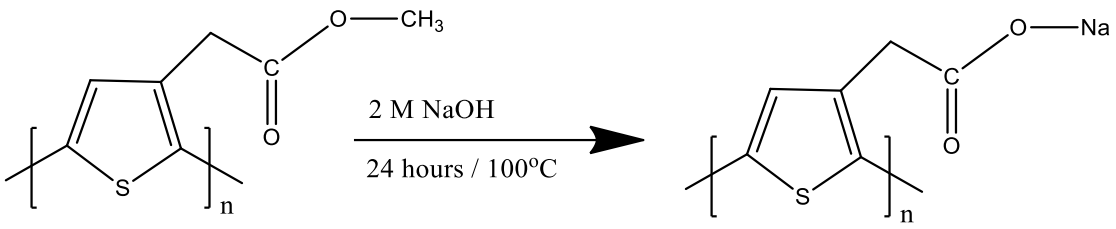

Figure 2.7. Third step of anionic conjugated polythiophene synthesis.

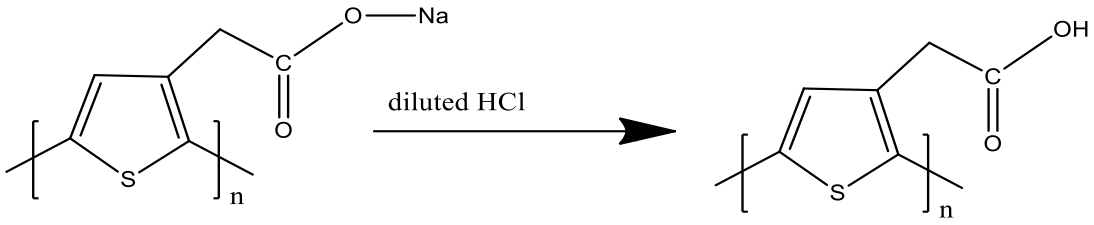

Figure 2.8. Final step of anionic conjugated polythiophene synthesis.

2.2.3. Polymerization of Some Thiophene Derivatives

Firstly, polymerization of 3-thiophenemethanol was carried out as shown in Figure 2.9. Solution of 3-thiophenemethanol in chloroform (0.05 mol/L) was added dropwise into solution of $FeCl_3$ in chloroform (0.02 mol/L) in round-bottom flask under nitrogen atmosphere. Reaction temperature was set at room temperature for 6 hours. After 6 hours, excess methanol was used to precipitate polymers in the reaction mixture. Then, precipitated polymers was washed with methanol and centrifugated at 4000 rpm for 5 min at least three times (Supernatant was separated in each trial). Finally, after removing supernatant again, precipitate was obtained as a reddish-brown color and it was dried under vacuum in desiccator. Thus, polythiophenemethanol (PTM) was obtained.

Secondly, polymerization of 3-thiopheneethanol was carried out as shown in Figure 2.10. Solution of 3-thiophenemethanol in chloroform (0.05 mol/L) was added dropwise into solution of $FeCl_3$ in chloroform (0.02 mol/L) in round-bottom flask under nitrogen atmosphere. Reaction temperature was set at room temperature for 6 hours. After 6 hours, excess methanol was used to precipitate polymers in the reaction mixture. Then, precipitated polymers was washed with methanol and centrifugated at 4000 rpm for 5 min at least three times (Supernatant was separated in each trial). Finally, after

removing supernatant again, precipitate was obtained as a dark-black color and it was dried under vacuum in desiccator. Thus, polythiopheneethanol (PTE) was obtained. Also, like a first two polymerization, PC2 was polymerized as shown in Figure 2.11. Poly-PC2 (PPC2) was synthesized.

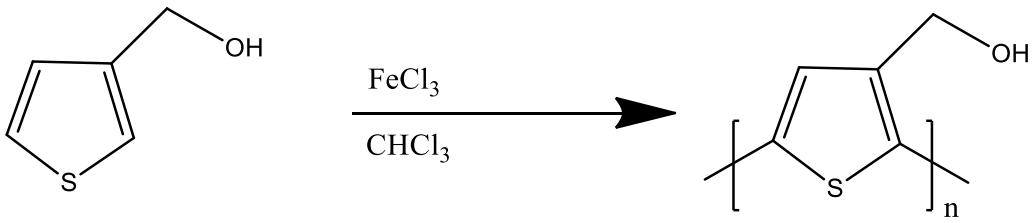

Figure 2.9. Polymerization of 3-thiophenemethanol.

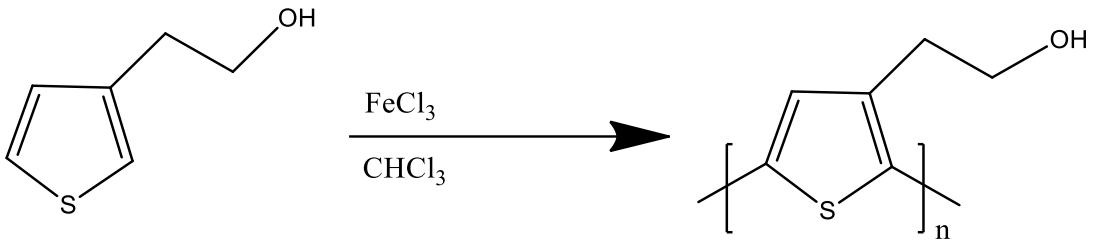

Figure 2.10. Polymerization of 3-thiopheneethanol.

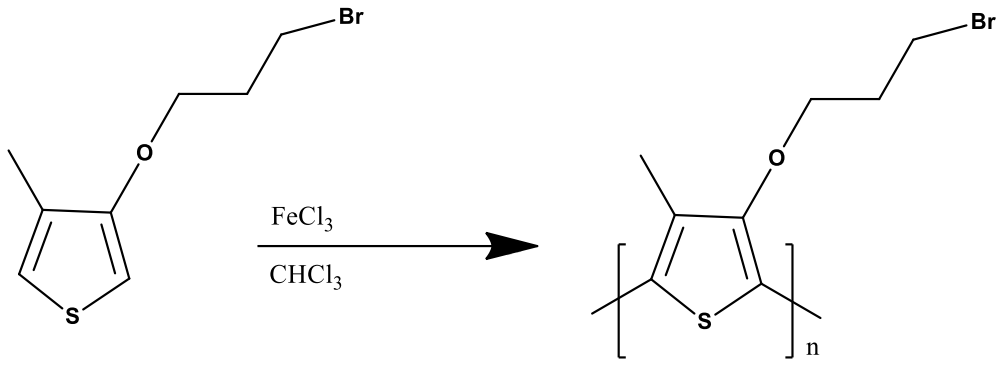

Figure 2.11. Polymerization of PC2.

2.3. Preparation of Polyurethane Nanospheres

Two miniemulsion techniques was performed in order to prepare polyurethane nanospheres in this study. These are two step and one pot miniemulsion polymerization techniques.

2.3.1. Two-step Miniemulsion Polymerization Technique

Two-step miniemulsion technique was formed as two part which are synthesis of prepolymer and preparation of nanospheres. Firstly, synthesis of prepolymer was performed as shown in Figure 2.12. Isophorone Diisocyanate (IPDI) (0.525 ml, 2.5mmol), Polypropylene Glycol 1000 (PPG 1000) (1.245 ml, 1.25 mmol), and toluene (0.832 ml) was put into the 50 ml round-bottom flask and the reaction mixture was refluxed for 2 hours under N_2 atmosphere. Equivalent molar ratios of IPDI/PPG was determined as 2/1. After 2 hours, NCO-terminated prepolymer was cooled to room temperature and stored in refrigerator for preparation of nanospheres.

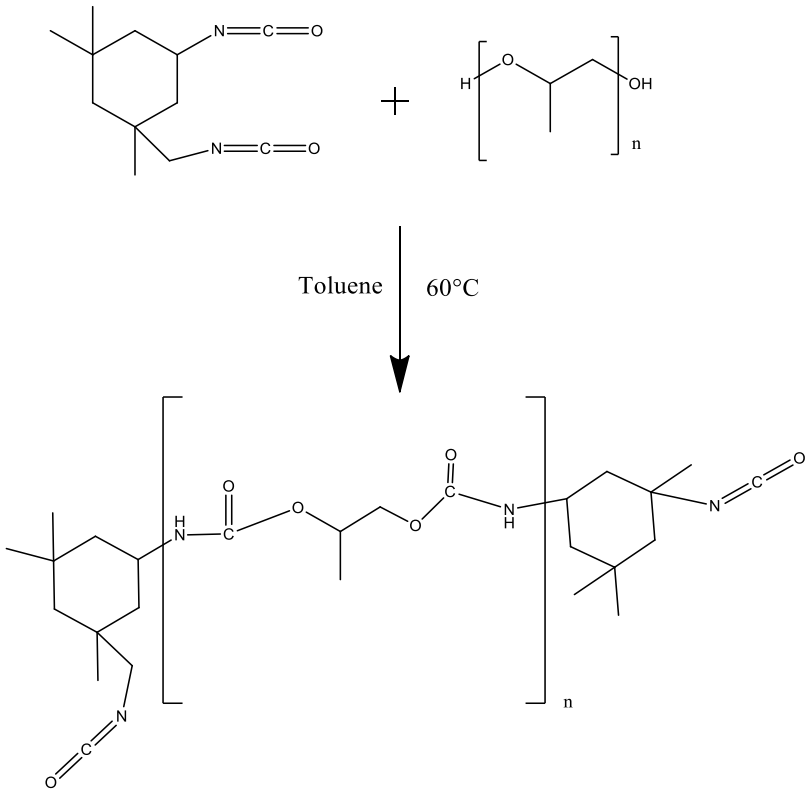

Figure 2.12. Representation of synthesis of prepolymer.

Preparation of polyurethane (PU) nanospheres was carried out with two-step miniemulsion technique as shown in Figure 2.13. Prepolymer, butanediol (BD) (55 uL, 0.625 mmol), hexadecane (HD) (53 µL, 0.180 mmol), Trimethylolpropane (TMP) (84 mg, 0.625 mmol) was put into the 50 ml round-bottom flask with magnetic stirrer as an oil phase. Oil phase was stirred for 5 min. At the same time, water phase was prepared. Sodium dodecyl sulfate (SDS) (40 mg, 0.140 mmol) was dissolved in 20 ml water. The next step includes mixing of oil and water phase for 10 min. Then, mixture was ultrasonicated for 4 min (amplitude %20) by homogenizator. Sonication step was done in ice bath. After ultrasonication, mixture was put into the 50 ml round-bottom flask and the reaction mixture was refluxed at 60 ^{o}C for 3 hours. After 3 hours, miniemulsion solution was cooled to room temperature. Thus, PU nanosphere solution was prepared.

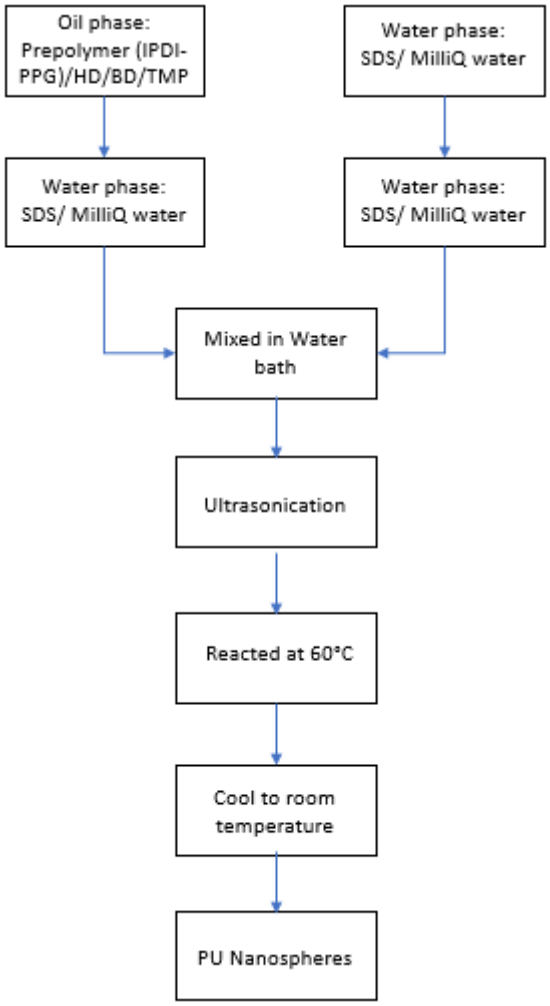

Figure 2.13. Schematic representation of two-step miniemulsion technique.

2.3.2. One-Pot Miniemulsion Polymerization Technique

One-pot miniemulsion polymerization technique was performed as shown in Figure 2.14. Isophorone Diisocyanate (IPDI) (0.263 ml, 1.25mmol), Polypropylene Glycol 1000 (PPG 1000) (1.245 ml, 1.25 mmol), hexadecane (HD) (114 µL, 0.387 mmol), Sodium dodecyl sulfate (SDS) (84 mg, 0.294 mmol) in 10 ml water, and magnetic stirrer was put into the 50 ml round-bottom flask and stirred under room temperature for 1 hour. After 1 hour, pre-emulsion solution was ultrasonicated for 2 min (amplitude %90) by homogenizator in ice bath. After ultrasonication, mixture was put into the 50 ml round-bottom flask and the reaction mixture was refluxed at 60 ^{o}C for 4 hours. After 4 hours, miniemulsion solution was cooled to room temperature. Thus, PU nanosphere solution was prepared.

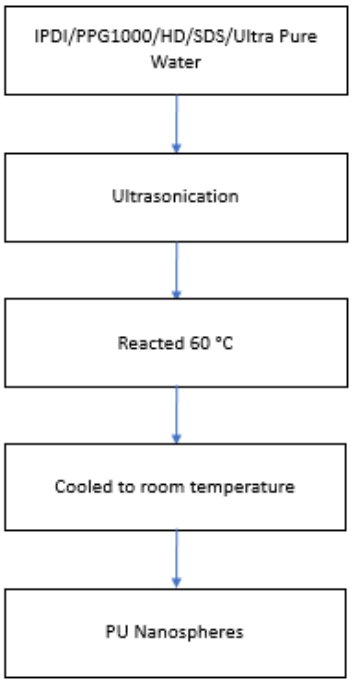

Figure 2.14. Schematic representation of One-pot miniemulsion technique.

2.4. Magnetic Levitation Studies on Nanospheres

Dual mode (Fluorescence and Magnetic) agents was synthesized as shown in Figure 2.15 and Figure 2.16. IPDI/PEI/PTAA-Nanospheres was prepared with one-pot miniemulsion technique as shown in Figure 2.15. IPDI (0.210 ml, 1.00 mmol), and

branched polyethyleneimine 25000 (PEI 25000) (1 g, 0.04 mmol), PTAA (1.25 mg in 250 µl water, pH:9), hexadecane (HD) (114 µL, 0.387 mmol), sodium dodecyl sulfate (SDS) (84 mg, 0.294 mmol) in 10 ml water, and magnetic stirrer was put into the 50 ml round-bottom flask and stirred under room temperature for 1 hour. After 1 hour, pre-emulsion solution was ultrasonicated for 2 min (amplitude %90) by homogenizator in ice bath. After ultrasonication, mixture was put into the 50 ml round-bottom flask and the reaction mixture was refluxed at 60 ^{o}C for 4 hours. After 4 hours, miniemulsion solution was cooled to room temperature. Thus, PU nanosphere solution was prepared.

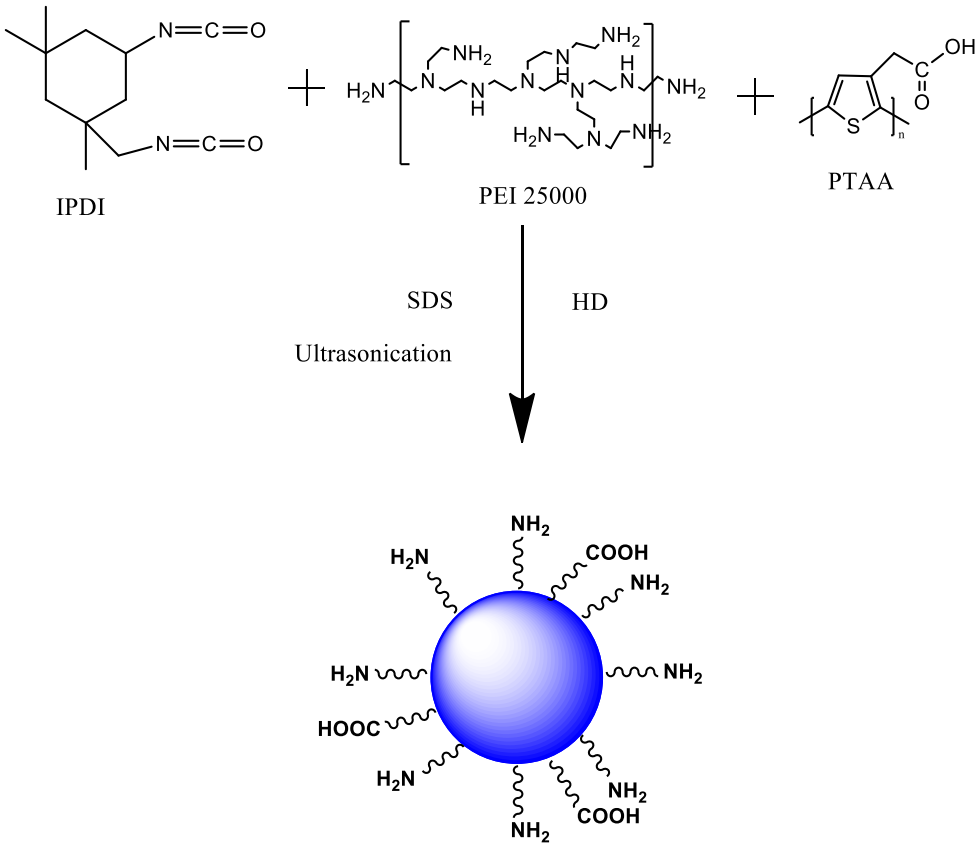

Figure 2.15. First step of dual modal agent synthesis.

After preparing IPDI/PEI/PTAA-Nanospheres, DOTA-NHS (10 mg, 20 µmol) in 100 µl phosphate buffered saline (PBS) solution was added to 100 µl of IPDI/PEI/PTAA-Nanosphere solution with magnetic stirrer and stirred for 1 day. Then, gadolinium (III) chloride hexahydrate ($GdCl_3.6H_2O$) (75 mg, 0.2 mmol) was added to 2 ml citric acid monohydrate solution (230 mg, 0.6 mmol) and stirred for 3 days. After 3 days, 12-14 kDa dialysis tube was used to purification of excess gadolinium metal in solution. That's why,

5 cycles of dialysis (each one for 24 hours) was done against 0.05 M citrate solution (40 ml, pH:7.4). All pH adjustment was done with using NaOH and HCl. After the purification, Gd-DOTA-IPDI/PEI/PTAA-Nanosphere was synthesized as a dual mode agent (Figure 2.16).

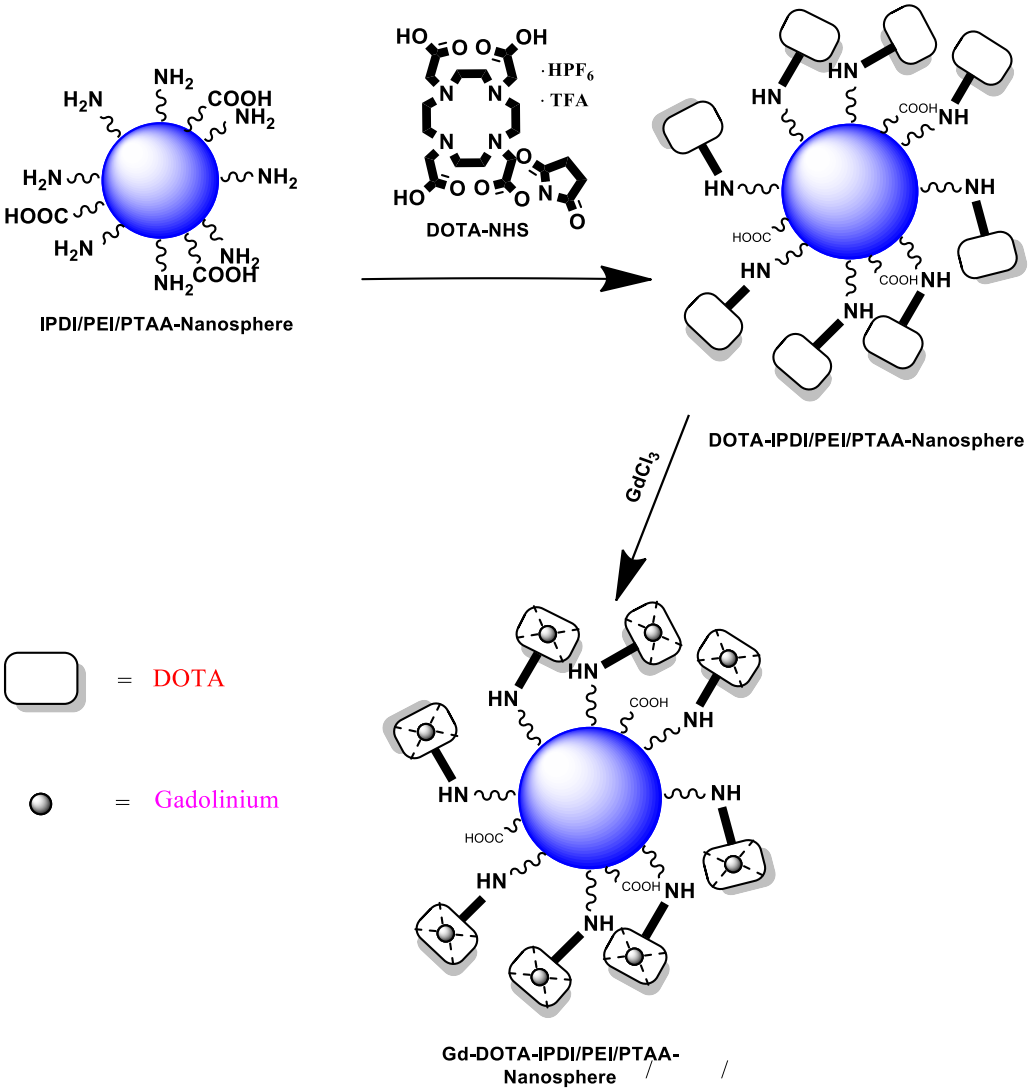

Figure 2.16. Other steps of dual mode agent synthesis.

2.5. Functionalization of Nanospheres

Two techniques was performed in order to functionalize nanospheres in this study. These are EDC-NHS coupling and one pot miniemulsion techniques with conjugated polymer. Procedures of two of them was detailed below topics.

2.5.1. EDC-NHS Coupling Technique on Nanospheres

EDC-NHS coupling technique was performed as shown in Figure 2.17. Firstly, PTAA and Polyethyleneimine derived nanospheres (IPDI/PEI Nanosphere) were reacted with EDC-NHS. For this purpose, 76 mg EDC and 11.5 mg NHS were weighed and dissolved in 1 mL ultra-pure water. Thus, the EDC and NHS concentrations were adjusted as 0.4 M and 0.1 M, respectively. 100 uL of PTAA (0.5 mg) was added to total of 2 ml of EDC-NHS mixture. Also, magnetic stirrer was used in the first step of the reaction for about 30 minutes. The solution was adjusted to pH 9 with using HCl. Finally, PEI nanospheres (NH_2 ended nanospheres) were added to the mixture. The solution was stirred at room temperature for 1 hour. The reaction yielded a product similar to the color of orange.

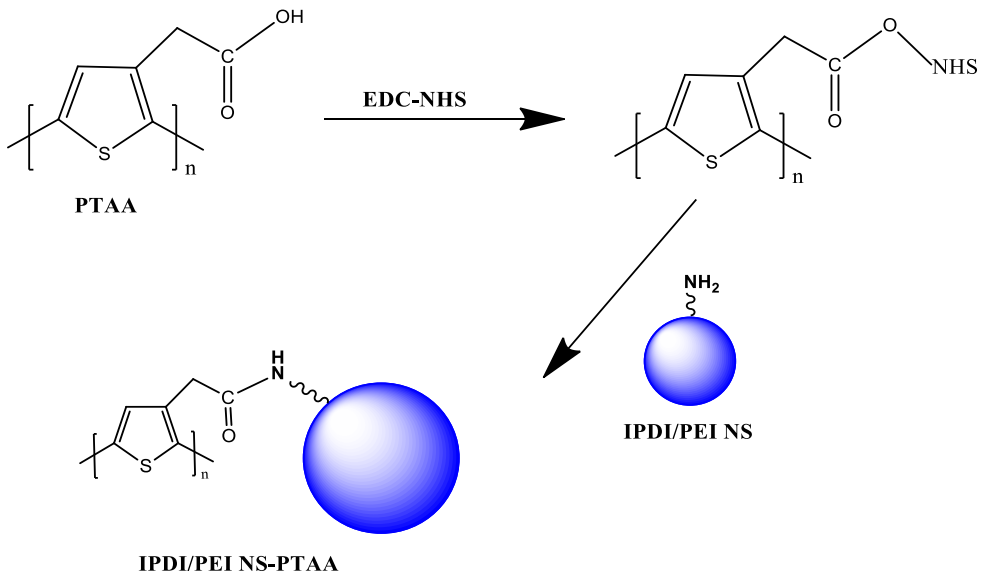

Figure 2.17. EDC-NHS coupling technique on the -NH_2 ended nanosphere.

2.5.2. One pot Miniemulsion Technique with Conjugated Polymer

Functional nanospheres was synthesized in order to form complexation. IPDI/PPG/PTAA-Nanospheres was prepared with one pot miniemulsion technique as shown in Figure 2.18. IPDI (0.290 ml, 1.38 mmol), and polypropylene glycol (PPG 1000) (1.245 ml, 1.25 mmol), PTAA (1.25 mg in 250 µl water, pH:9), hexadecane (HD) (114 µL, 0.387 mmol), sodium dodecyl sulfate (SDS) (84 mg, 0.294 mmol) in 10 ml water,

and magnetic stirrer was put into the 50 ml round-bottom flask and stirred under room temperature for 1 hour. After 1 hour, pre-emulsion solution was ultrasonicated for 2 min (amplitude %90) by homogenizator in ice bath. After ultrasonication, mixture was put into the 50 ml round-bottom flask and the reaction mixture was refluxed at 60 ^{o}C for 4 hours. After 4 hours, miniemulsion solution was cooled to room temperature. Thus, functional PU nanosphere solution was prepared.

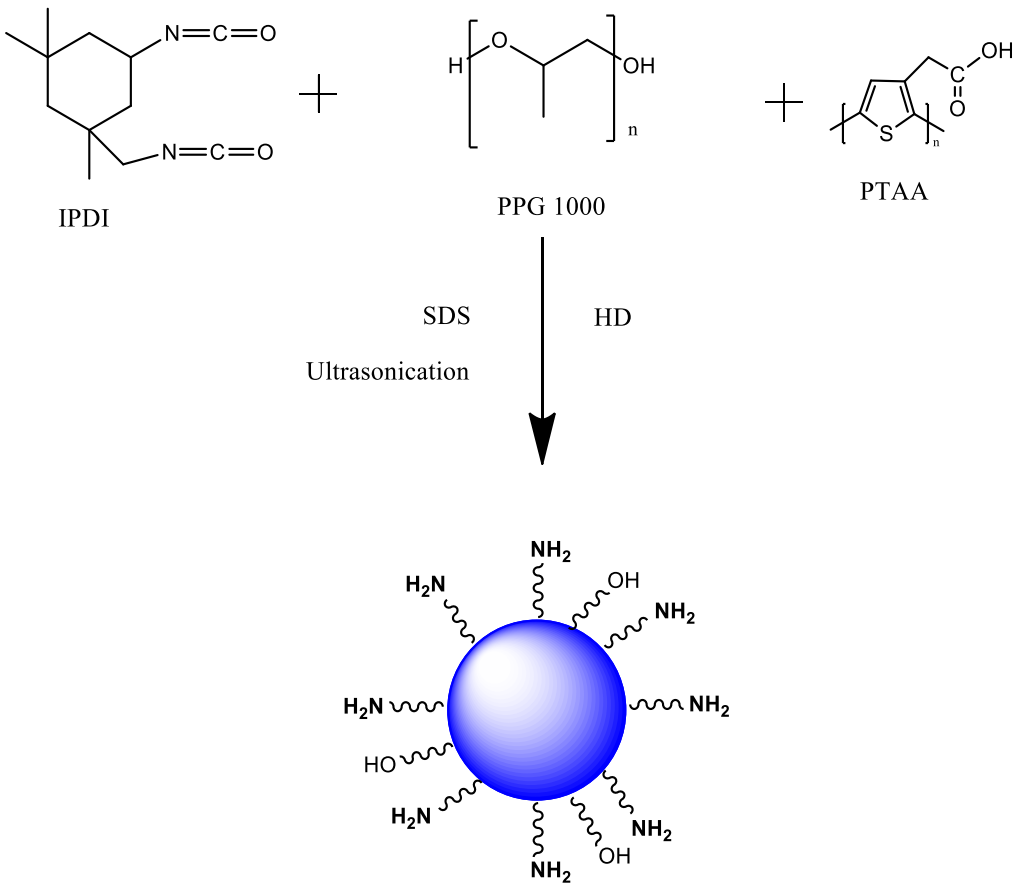

Figure 2.18. Synthesis of functional nanospheres by one pot miniemulsion technique.

2.6. Characterization Tests

After synthesis was completed, the products were characterized with below techniques. In this thesis, there are many characterization methods were used in order to reach to detailed information about the products. Thus, the most reliable knowledge was obtained. Also, some technique information was given about characterization tests in subtitles.

2.6.1. Nuclear Magnetic Resonance (NMR) Analysis

Products were analyzed with ^{1}H NMR (400 MHz) with using deuterium solvents such as $CDCl_3$, D_2O and DMSO-D_6.

2.6.2. UV-Visible Spectrophotometer Analysis

UV-Visible spectral analysis was carried out with using a Shimadzu UV-2550 UV-VIS spectrophotometer. Quartz cuvette was used for all spectral analysis which have light path 1 mm with width 1 cm. Also, range of 200-800 nm was used for scanning. Generally, water was used as solvent for all analysis.

2.6.3. Fluorescence Spectrophotometer Analysis

Varian Cary Eclipse Fluorescence spectrophotometer was used for fluorescence analysis with using a water as a solvent. Also, Quartz cuvette was used for all spectral analysis which have light path 1 mm with 1 cm. Also, range of 400-800 nm was used for scanning.

2.6.4. Scanning Electron Microscopy Analysis

The morphology of the nanomaterials and products was analyzed by Scanning Electron Microscopy (SEM; Quanta 250, FEI).

2.6.5. Dynamic Light Scattering Analysis

Dynamic Light Scattering (DLS) (Zeta sizer Nano ZS, Malvern Instruments) was used in order to determine average size and zeta potential of the products. Quartz cuvettes and disposable cuvettes were used in size measurements, and folded capillary cell was used in zeta potential measurements. Capillary cell has critical significance in order to obtain high accuracy and high precision about the zeta potential results, also, it is specific material for this measurement.

2.6.6. Fluorescence Microscopy Analysis

Zeiss Axio Observer fluorescence microscope was used in order to observe fluorescent and magnetic properties of products. Generally, samples were prepared in well plates.

2.6.7. ICP Optic Emission Spectroscopy Analysis

Elemental analysis was performed with Inductively Coupled Plasma (ICP) Optic Emission Spectroscopy in order to determine the quantity of Gadolinium metal ion.

2.6.8. Quantum Yield Analysis

Quantum yield analysis was determined with Edinburgh Instruments. Reference solution was prepared according to each samples.

2.6.9. FTIR-Attenuated Total Reflectance Analysis

Fourier Transform Infrared-Attenuated Total Reflectance (FTIR-ATR) (Perkin Elmer) was used in order to determine the functional groups of products.

2.6.10. Magnetic Levitation Analysis

Magnetic Levitation analysis was done with using fluorescent nano beads by our designed set up device.

CHAPTER 3

RESULTS AND DISCUSSIONS

3.1. Synthesis and Characterization of Monomers and Their Polymers

Monomer and their polymers were synthesized and characterized. This section explains synthesis of cationic, anionic, and some thiophene derivatives. Also, detailed information was given about synthesis condition in this part.

3.1.1. Cationic Monomers and Their Polymers

The first step is synthesis of Precursor 1 (PC1). PC1 was synthesized and purificated. The yield was computed as %65. Figure 3.1 shows ^{1}H NMR spectrum of PC1. ^{1}H NMR (400 MHz, $CDCl_3$) δ (ppm): 6.85 (1H, d, J= 3.2 Hz), 6.18 (1H, d, J= 3.2 Hz), 3.84 (3H, s), 2.12 (3H, s).

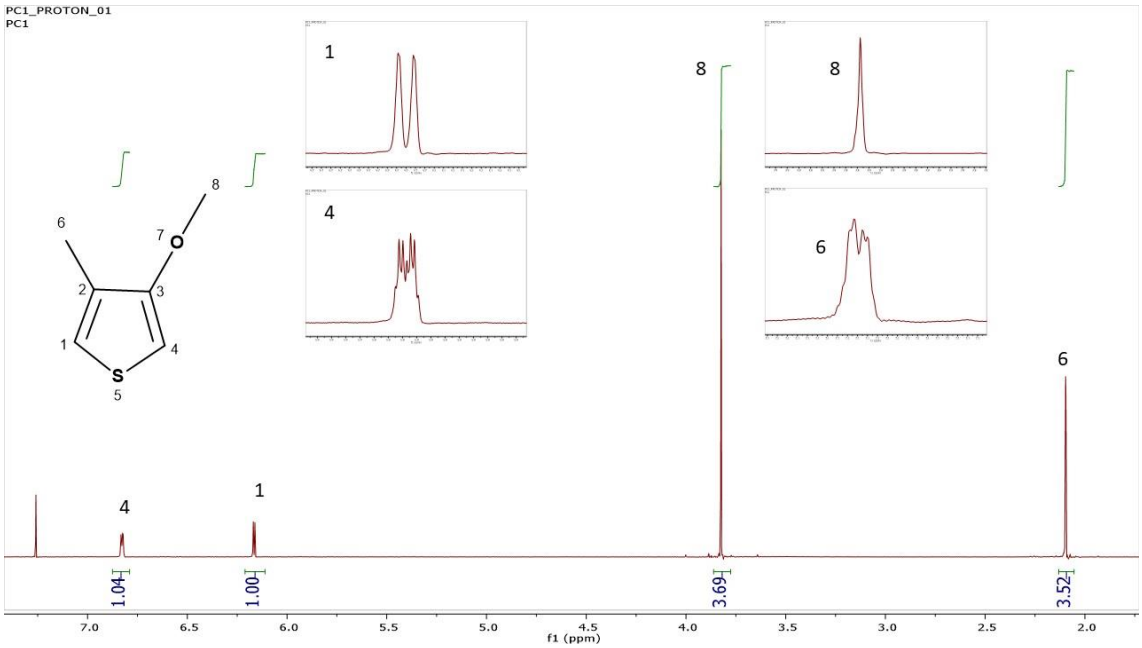

Figure 3.1. ^{1}H NMR spectrum of PC1.

The second step is synthesis of Precursor 2 (PC2). PC2 was synthesized and purificated. The yield was computed as %80. Figure 3.2 shows ^{1}H NMR spectrum of PC2. PC2 was used to synthesize all cationic monomers. ^{1}H NMR (400 MHz, $CDCl_3$) δ (ppm): 6.85 (1H, d, J= 2.7 Hz), 6.18 (1H, d, J= 3.1 Hz), 4.10 (2H, t, J= 5,8 Hz, 6,19 Hz), 3.62 (2H, t, J= 6.2 Hz, 6,5 Hz), 2.35 (2H, p, J= 5.3 Hz, 5.3 Hz, 6.5 Hz, 5.7 Hz), 2.12 (3H, s).

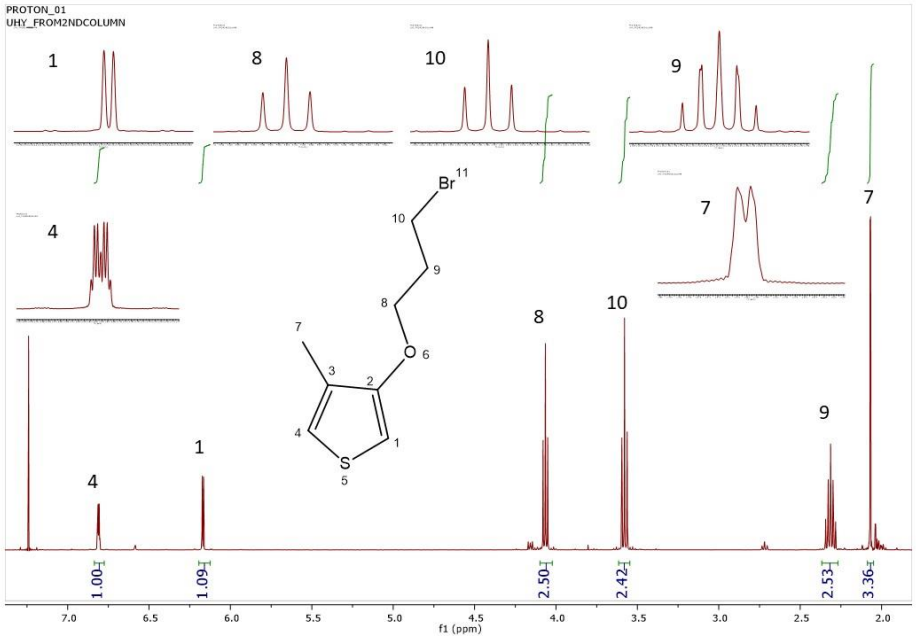

Figure 3.2. ^{1}H NMR spectrum of PC2.

Monomer 3 (M3) was synthesized and purificated. The yield was computed as %80. Figure 3.3 shows ^{1}H NMR spectrum of M3. ^{1}H NMR (400 MHz, $CDCl_3$, δ, ppm) 6.82-6.80 (m, 1H), 6.22 (d, J= 4Hz, 1H), 4.08 (t, J= 6Hz, 2H), 3.82-3.78 (m, 2H), 3.70 (t, J= 8Hz, 6H), 3.25 (t, J= 8 Hz, 6H), 2.37 (t, J= 8Hz, 2H), 2.05 (d, J= 1.2 Hz, 3H).

Monomer 4 (M4) was synthesized and purificated. The yield was computed as %95. Figure 3.4 shows ^{1}H NMR spectrum of M4. Monomer 4 was dissolved with deuteron chloroform in order to perform NMR characterization. According to the result, all specific peaks were observed for monomer 4 in NMR spectrum. ^{1}H NMR (400 MHz, $CDCl_3$, δ, ppm) 6.83-6.82 (m, 1H), 6.22 (d, J= 4Hz, 1H), 4.12 (t, J= 6Hz, 2H), 4.07-4.03 (m, 2H), 3.80-3.75 (m, 2H), 3.64-3.58 (m, 2H), 3.50 (s, 3H), 2.83-2.71 (m, 4H), 2.38 (s, 3H), 2.37-2.31 (m, 2H), 1.58 (s, 3H).

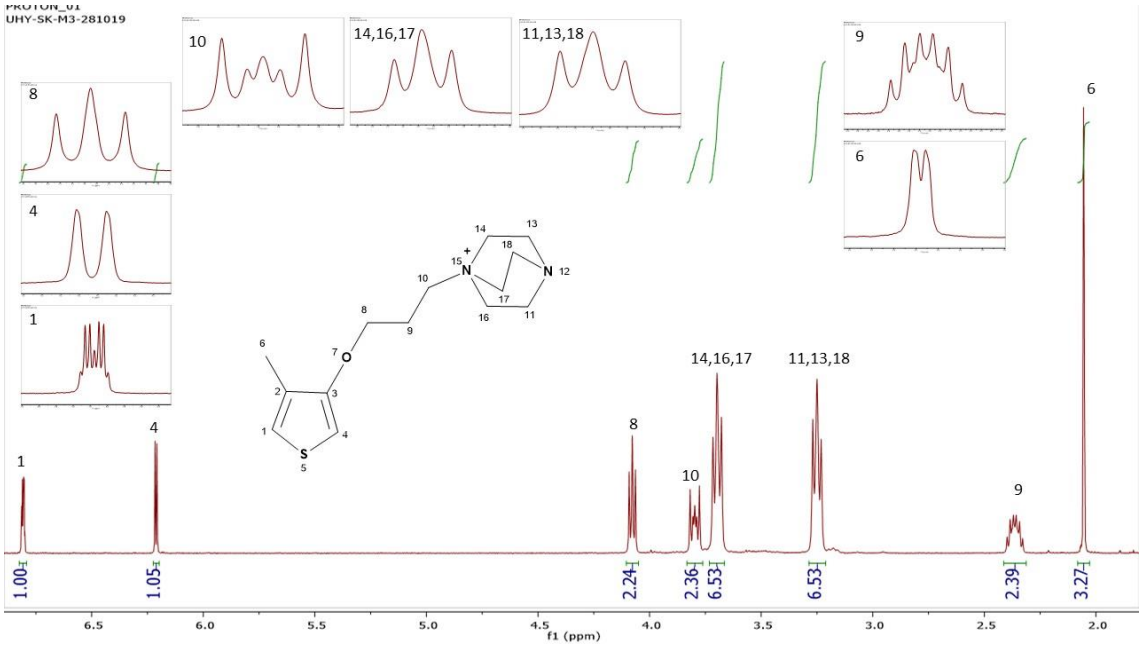

Figure 3.3. ^{1}H NMR spectrum of M3.

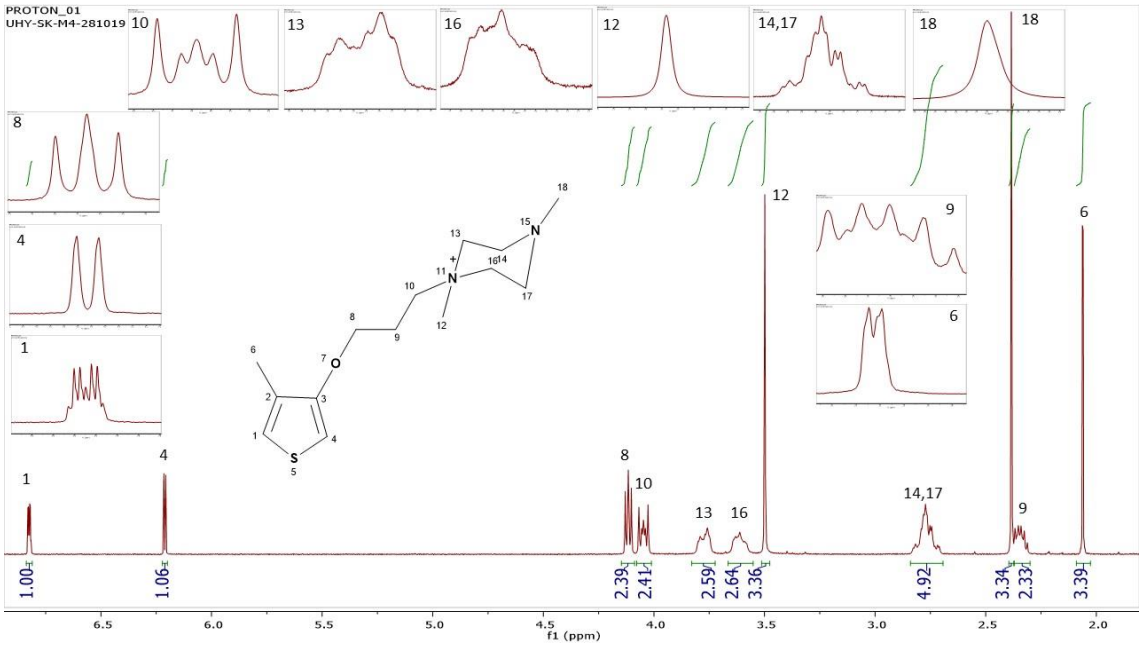

Figure 3.4. ^{1}H NMR spectrum of M4.

Monomer 5 (M5) was synthesized and purificated. The yield was computed as %85. Figure 3.5 shows ^{1}H NMR spectrum of M5. ^{1}H NMR (400 MHz, $CDCl_3$, δ, ppm) 6.83-6.82 (m, 1H), 6.18 (d, J= 3.2 Hz, 1H), 6.04-5.94 (m, 2H), 5.87 (d, J= 0.8 Hz, 1H), 5.83 (d, J= 0.8 Hz, 1H), 5.76 (d, J= 1.2 Hz, 1H), 5.73 (d, J= 1.2 Hz, 1H), 4.41-4.30 (m,

4H), 4.07 (t, J= 5.6 Hz, 2H), 3.63-3.59 (m, 2H), 3.33 (s, 3H), 2.42-2.35 (m, 2H), 2.04 (d, J= 0.8 Hz 3H).

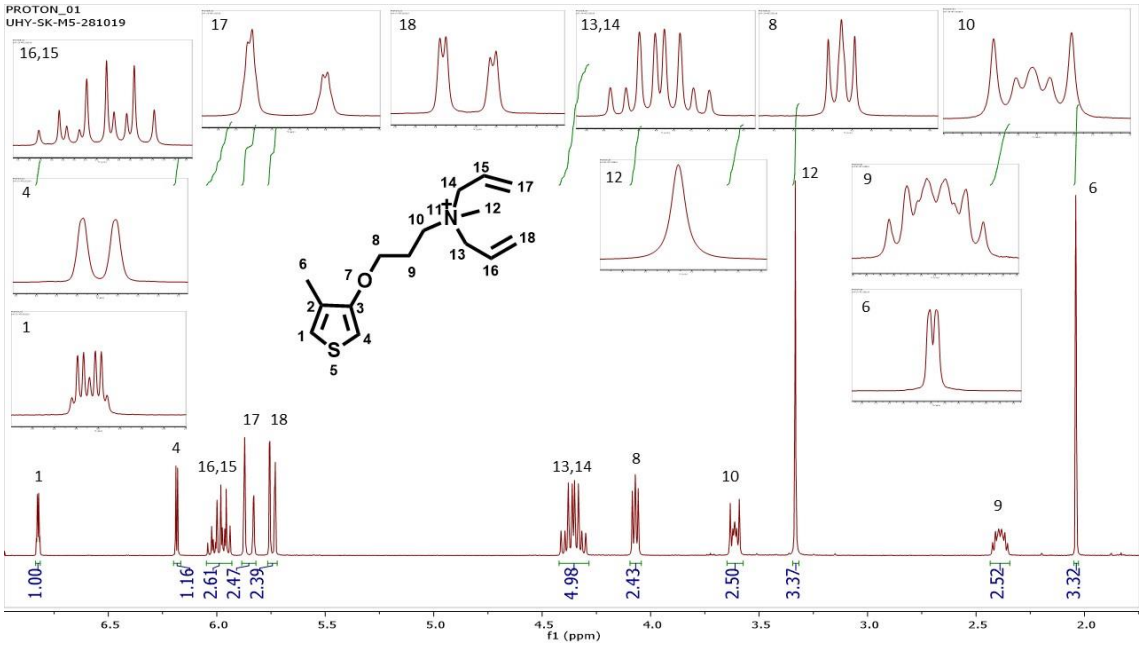

Figure 3.5. ^{1}H NMR spectrum of M5.

Polymerization of all monomers was carried out. Firstly, polymers were characterized by H^1 NMR spectroscopy. All polymers were dissolved in D_2O for analysis of H^1 NMR of PT3, PT4, and PT5. Figure 3.6 demonstrates NMR stack of synthesized polymers. When H^1 NMR spectrum was examined, disappearances of aromatic hydrogen peaks, shifting all signals to high field and band broadening were observed.

Polymers was characterized with UV-Visible spectroscopy as shown in Figure 3.7 which shows the absorbance spectrums of PT3, PT4, and PT5. Respectively, maximum wavelengths are 400 nm (PT3), 395 nm (PT4) and 403 nm (PT5). Behavior of polythiophenes similar to each other in absorbance spectrums but they have only small differences at the maximum wavelength. Also, polymers were characterized by fluorescence spectroscopy as shown in Figure 3.8. According to the spectrums, emission maximum wavelengths was obtained respectively, 534 nm (PT3), 530 nm (PT4), and 532 nm (PT5). When behavior of polythiophenes were examined in emission spectrums, similar to absorbance spectrum, there were minor differences at the maximum wavelength.

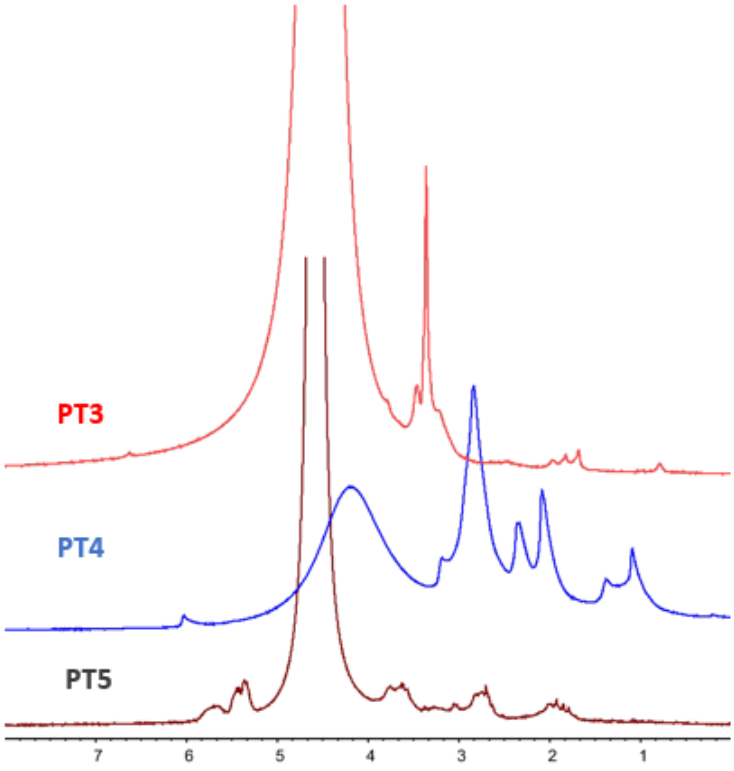

Figure 3.6. H^1 NMR stack of PT3, PT4, and PT5.

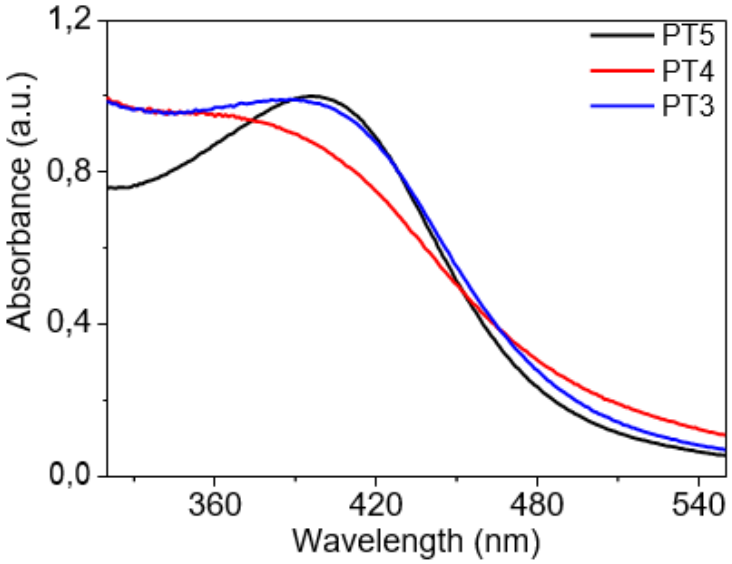

Figure 3.7. UV-Visible absorbance spectrum of PT3-PT4-PT5.

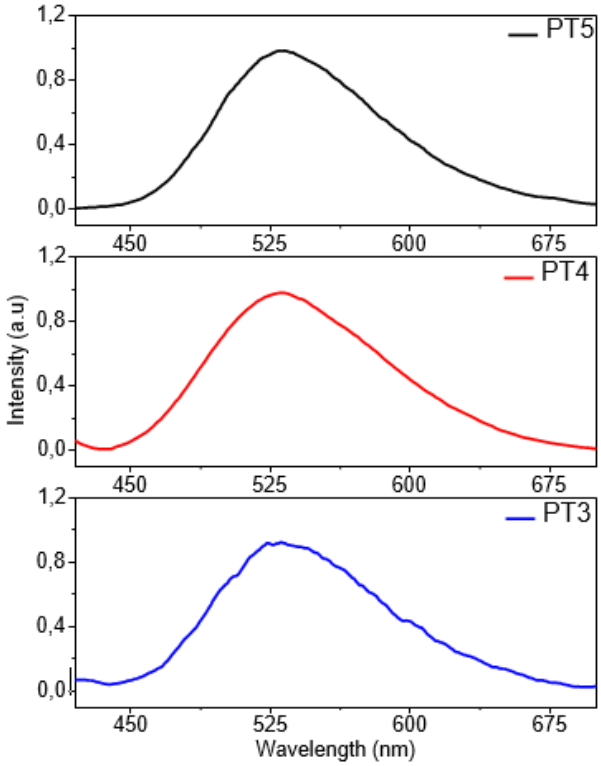

Figure 3.8. Fluorescence emission spectrums of PT3-PT4-PT5.

Generally, PT4 was preferred for applications. Also, PT4 was dissolved in ethylene glycol. The result of this, fluorescence emission of PT4 was increased as shown in Figure 3.9.

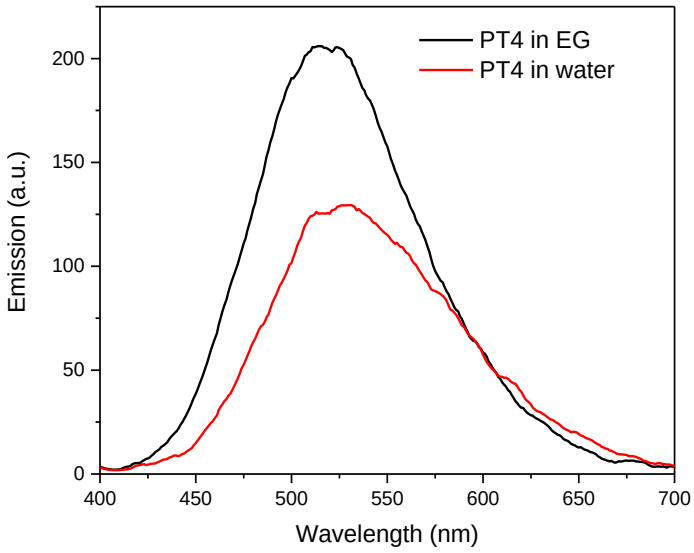

Figure 3.9. Comparison of fluorescence Emissions of PT4 in ethylene glycol and water.

3.1.2. Anionic Polymers

Anionic polymer was synthesized and characterized with using NMR, UV-visible spectroscopy, and fluorescence spectroscopy. Firstly, poly (3-thiophene methyl acetate) (PTMA) was characterized with ^{1}H NMR. Figure 3.10 shows ^{1}H NMR spectrum of PTMA. ^{1}H NMR (400 MHz, $CDCl_3$, δ, ppm) 7.30-7.00 (proton of thiophene ring, m, 1H), 3.70 (s, thiophene ring, 2H), 3.60 (s, methyl, 3H).

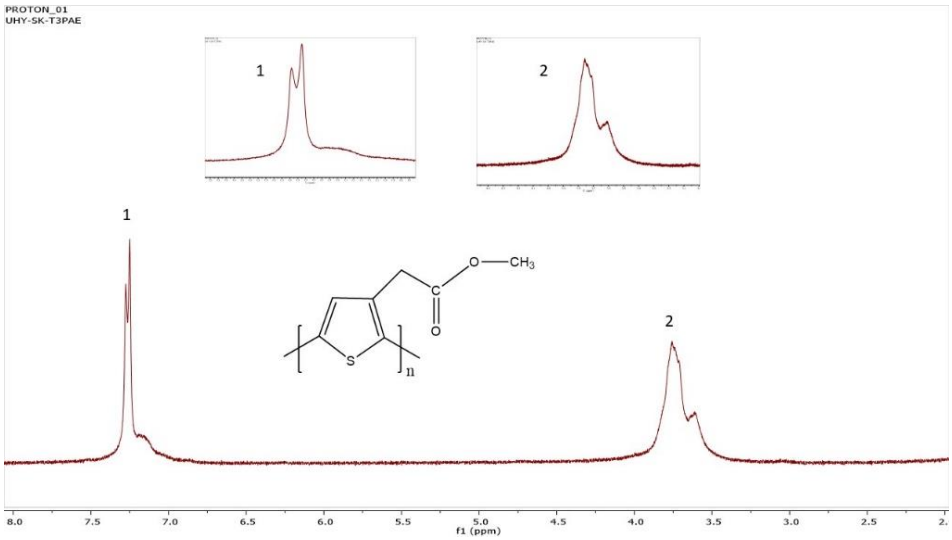

Figure 3.10. ^{1}H NMR spectrum of poly (3-thiophene methyl acetate).

PTAA was synthesized and characterized. FTIR-ATR spectroscopy was performed in order to compare PTMA and PTAA as shown in Figure 3.11. When PTMA and PTAA was compared; aromatic ester (C-O) functional group was observed in PTMA spectra at 1310 cm^{-1} and 1270 cm^{-1} but not in PTAA spectrum. The difference played a key role in characterization of PTAA. The different functional groups were determined by FTIR analysis for PTAA. The most significant peak of the spectrum is broad O-H peak which is seen in 3400-2400 cm^{-1} range. Also, carbonyl peak of carboxyl acid shown in 1700 cm^{-1} which reveals the existing of carboxyl group. On the other hand, other functional groups of PTAA was shown in spectrum. The absorption peak at 3180-2980 cm^{-1} range refers to C-H bond on the ring of thiophene. Also, aliphatic C-H bond was shown at 2980-2780 cm^{-1} range.

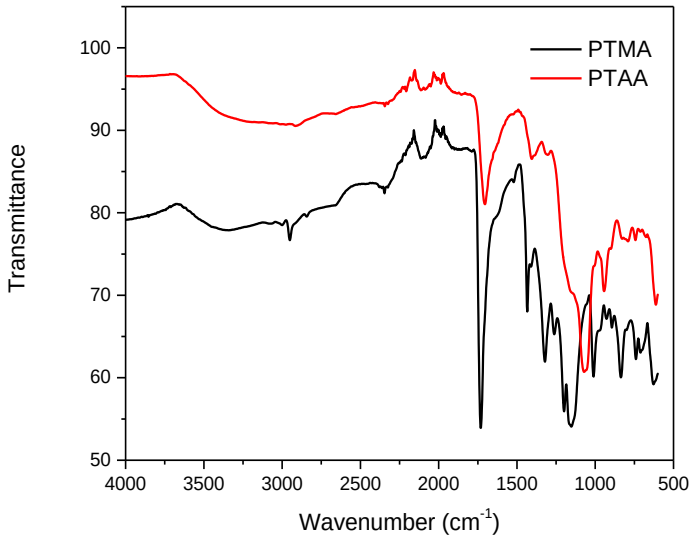

Figure 3.11. FTIR-ATR spectrum of poly (3-thiophene methyl acetate) (PTMA) and polythiophene acetic acid (PTAA).

UV-visible spectroscopy was carried out for PTAA under various pH. The pH was adjusted between pH 3 and 11 at room temperature. When polymer solution was prepared, 1 M NaCl was used for all samples in order to provide a constant ionic strength. The result was shown in Figure 3.12. According to Figure 3.12, PTAA is dissolved more efficiently, when pH is increased, so absorbance intensity is relatively increased at maximum wavelength.

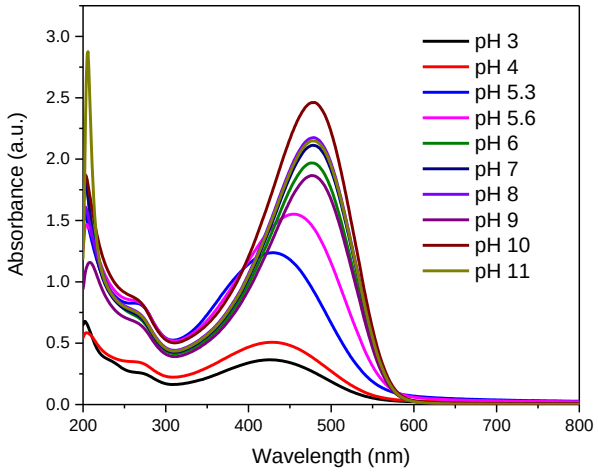

Figure 3.12. UV-visible spectrum of polythiophene acetic acid (PTAA) aqueous solution with 1.0 M NaCl concentrations for pH= 3-11.

When UV-visible spectroscopy was carried out for PTAA under various pH, sharp increase was observed at pH range 5-6 as shown in Figure 3.13 at maximum wavelengths. This condition of PTAA was obtained as a reversible with changing of pH of the solution. According to Figure 3.13, abrupt changes was observed at the range of maximum wavelengths pH 5-6 which demonstrates conformational changes of PTAA.

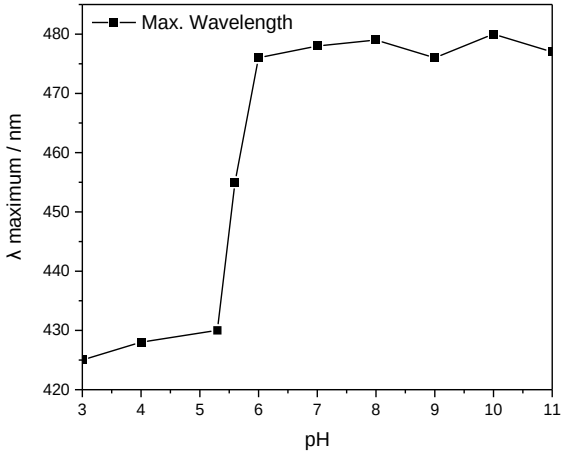

Figure 3.13. UV-visible spectrum of PTAA at maximum wavelengths in different pH values.

Fluorescence spectroscopy was performed under various pH values. At the same way, all anionic polymer solution was included 1 M NaCl in order to provide a constant ionic strength as shown in Figure 3.14. The fluorescence intensity decreases by decreasing pH. Also, after pH 5.3, PTAA was started dissolving, and its fluorescence intensity increased.

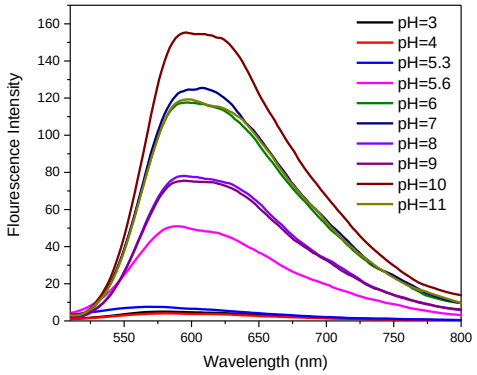

Figure 3.14. Fluorescence spectrum of PTAA aqueous solution with 1.0 M NaCl concentrations for pH= 3-11.

The pH dependence of fluorescence spectrum of PTAA solution was examined in 1.0 M NaCl solutions as shown in Figure 3.15. According to Figure 3.15, maximum wavelength of the emission spectrum shows dramatic increase at the pH range 5-6. The condition was observed to be reversible with changing of pH of the solution.

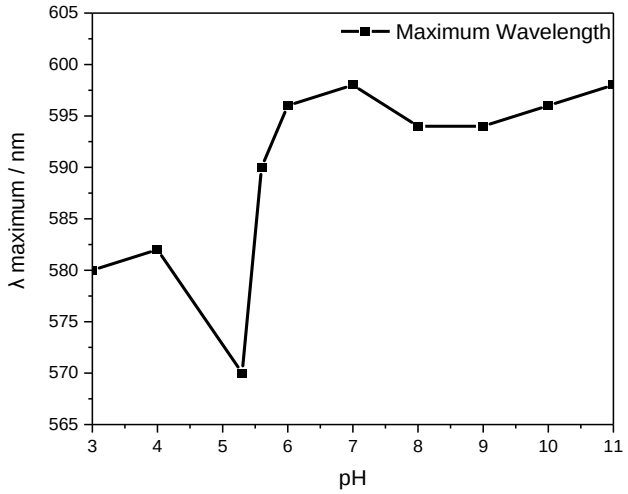

Figure 3.15. Fluorescence spectrum of PTAA at maximum wavelengths in different pH values.

Dynamic light scattering (DLS) analysis was performed for PTAA. Figure 3.16 shows the results of the hydrodynamic radius of anionic polymer. Samples was prepared as 16 x10^{-3} mM concentration in water and analyzed for three times. According to results, average hydrodynamic results was found approximately 12 nm for PTAA.

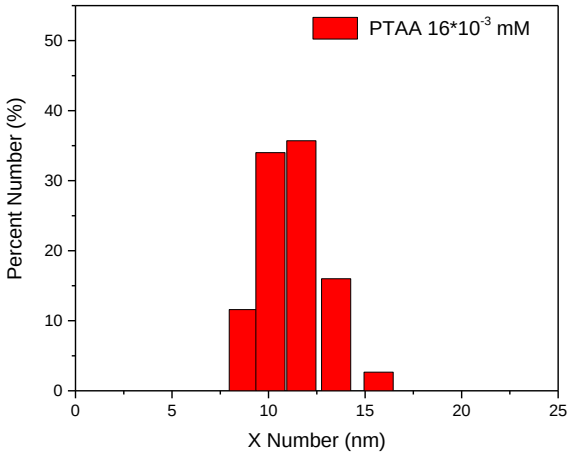

Figure 3.16. Size analysis of PTAA by DLS.

Generally, PTAA was dissolved in water and pH was adjusted to 9 for all utilization. On the other hand, PTAA was dissolved with ethylene glycol (EG) and its characterization was done by UV-visible, Flourescence spectroscopy. Figure 3.17 shows UV-visible absorption spectrum of PTAA in EG at the concentration 0.5 mM. According to Figure 3.17, maximum wavelength of spectrum was obtained as 440 nm. Also, Figure 3.18 shows emission spectrum of PTAA in EG at the concentration 0.5 mM. When Figure 3.18 was examined, maximum wavelength of the spectrum was found as 560 nm. In both absorbance and fluorescence spectrums of PTAA dissolved in EG, it was observed that the maximum wavelength shifts to the left compared to the water-soluble PTAA's spectrums. The reason of this condition is that ethylene glycol is better solvent than water for PTAA. Thus, PTAA chains were dissolved better in ethylene glycol.

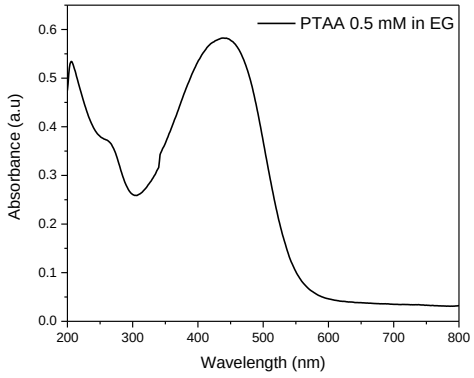

Figure 3.17. UV-visible spectrum of PTAA in EG.

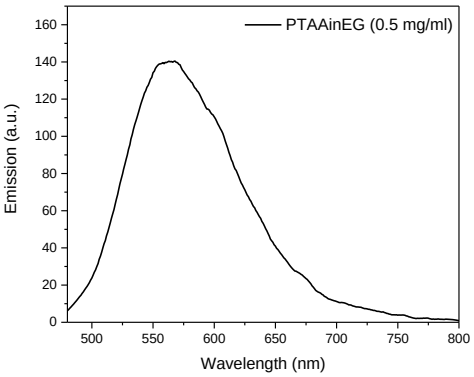

Figure 3.18. Flourescence spectrum of PTAA in EG.

3.1.3. Polymerization of Cationic Thiophene Derivatives

Some Thiophene derivatives was used to synthesize conjugated polymers such as 3-thiophenemethanol, 3-thiopheneethanol, and PC2. Firstly, 3-thiophenemethanol was polymerized and polythiophenemethanol (PTM) was synthesized and characterized. But solubility problem was occurred for PTM. Chloroform and DMF was used in order to dissolve PTM but it was not dissolved efficiently. Although solubility problem was occurred, PTM was characterized by UV-visible spectroscopy as shown in Figure 3.19. According to spectrum, general behavior was not observed. Maximum wavelengths was obtained 353 nm and 368 nm respectively for PTM in chloroform and PTM in DMF.

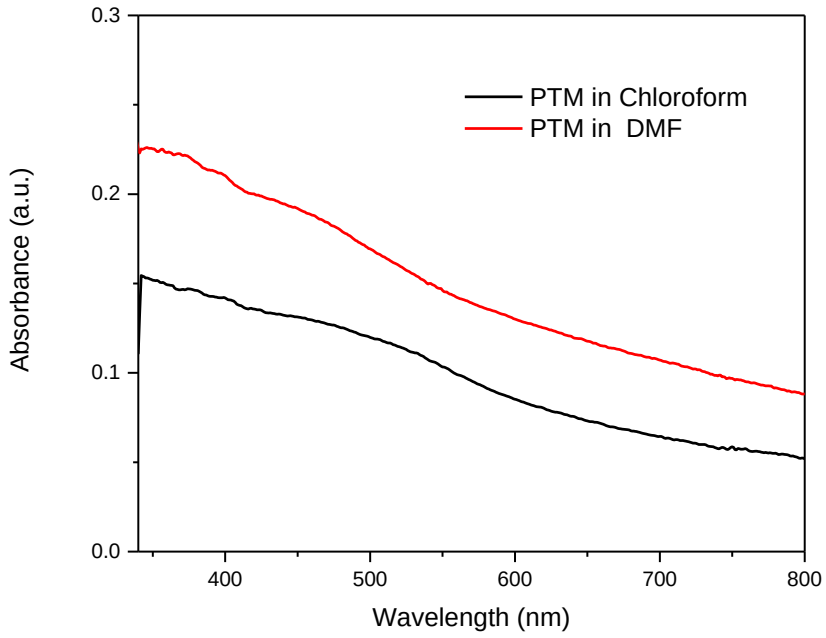

Figure 3.19. UV-visible spectrum of PTM in different solvents (chloroform and DMF).

After synthesis of PTM, polymerization of 3-thiopheneethanol was done in order to obtain more soluble conjugated polymer. Polythiopheneethanol (PTE) was synthesized and characterized by FTIR-ATR and UV-visible spectroscopy. FTIR-ATR spectrum of PTE was shown in Figure 3.20. According to spectrum, characteristic bands was observed for PTE. Hydroxyl group of PTE was seen at 3260 cm^{-1} and shoulder was obtained at 3059 cm^{-1} which refers the =C-H stretching of the thiophene ring. CH_2- group of PTE was seen at 2926 and 2873 cm^{-1}. C-O group of PTE was seen at 1032 cm^{-1}.

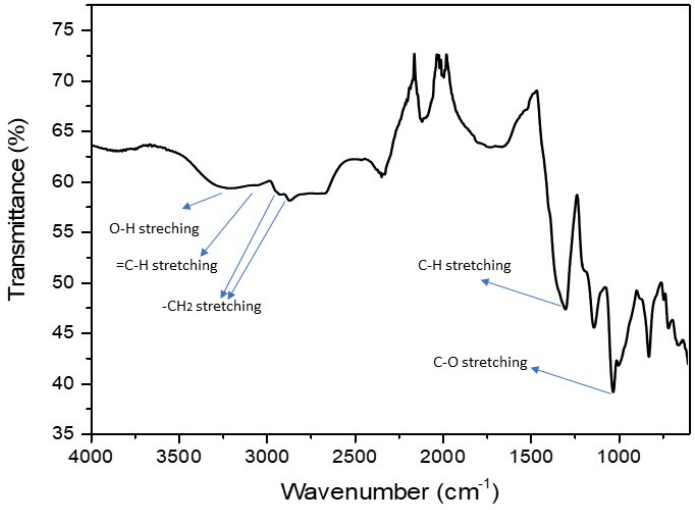

Figure 3.20. FTIR-ATR spectrum of PTE.

Also, PTE was characterized by UV-visible spectroscopy as shown in Figure 3.21. PTE (0.5 mg) was dissolved in 5 ml DMF. Maximum wavelength of PTE was obtained as 425 nm which means there is lower energy for π-π* transitions.

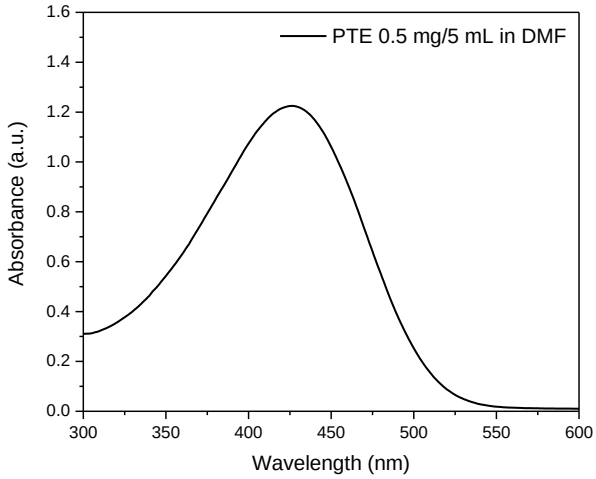

Figure 3.21. UV-visible spectrum of PTE.

After synthesis of PTE, PPC2 was synthesized and characterized by UV-visible and Fluorescence spectroscopy. PPC2 (0.5 mg) was dissolved in 1 ml water. Firstly, UV-visible spectrum was recorded as shown in Figure 3.22. Maximum wavelength of PPC2 was obtained as 404 nm and absorbance intensity was obtained as 0.72 a.u. at the maximum wavelength. Also, fluorescence spectrum was recorded as shown Figure 3.23.

Maximum wavelength of PPC2 was obtained as 542 nm and emission intensity was obtained as 693 a.u. at the maximum wavelength.

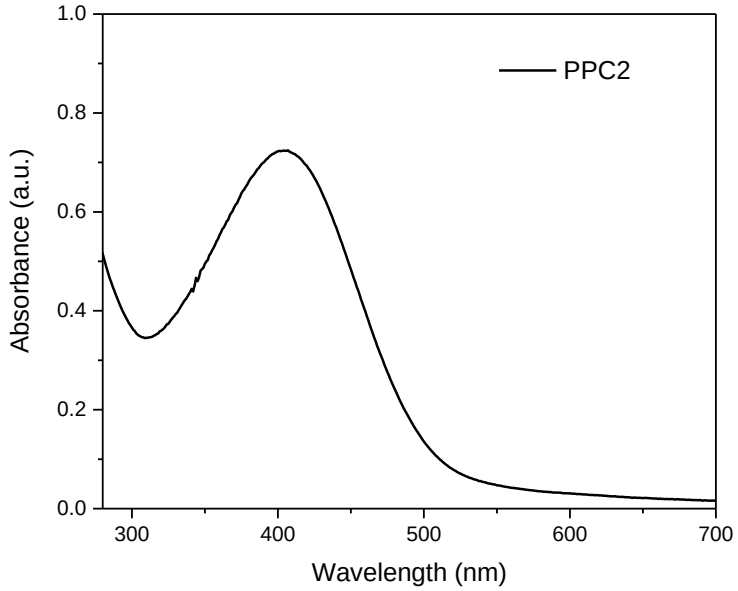

Figure 3.22. UV-visible spectrum of PPC2.

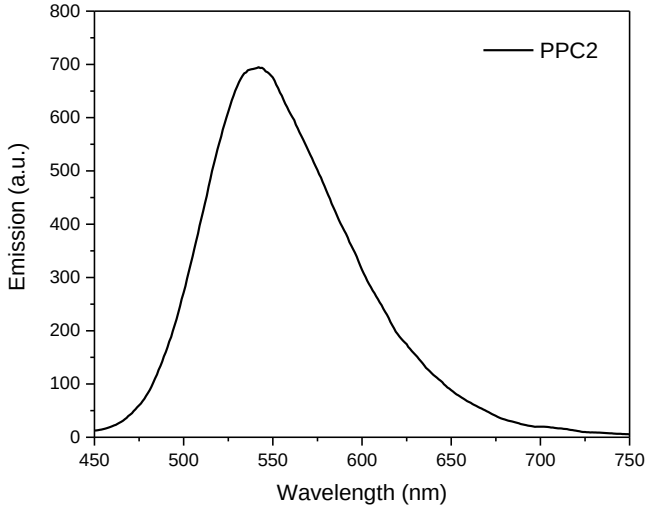

Figure 3.23. Fluorescence spectrum of PPC2.

After synthesis of conjugated polythiophene derivates, PPC2 was chosen for utilization in applications. Since PTE and PTM has low solubility.

3.2. Synthesis and Characterization of Polyurethane Nanospheres

Polyurethane nanospheres was synthesized with two techniques which are two-step miniemulsion and one-pot miniemulsion polymerization. Each technique was examined in different topics in this thesis. Nanospheres was characterized by FTIR-ATR, DLS, SEM analysis.

3.2.1. Two-step Miniemulsion Polymerization Technique

Polyurethane nanospheres was synthesized two-step miniemulsion polymerization. Nanospheres were characterized by FTIR-ATR, DLS, SEM analysis. Two-step technique provide to obtain high molecular weight PU nanospheres. Firstly, prepolymer was synthesized in order to obtain nanospheres. Prepolymer was characterized by FTIR-ATR spectroscopy as shown in Figure 3.24. According to spectrum, characteristic bands was observed for prepolymer. NCO group of prepolymer was seen at 2265 cm^{-1}, also, a band obtained at 1720 cm^{-1} which refers the -C=O stretching. These bands shows an evidence for prepolymer.

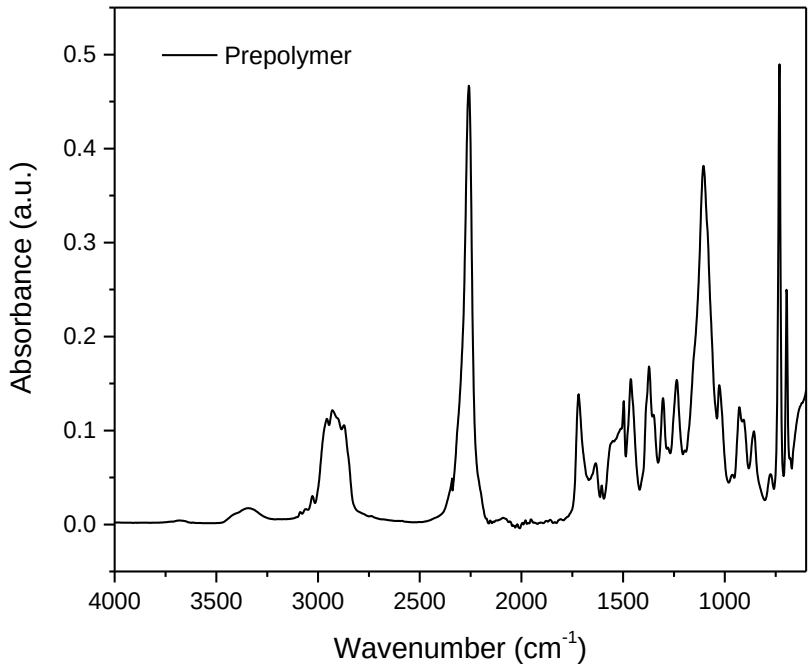

Figure 3.24. FTIR-ATR spectrum of prepolymer.

After synthesis of prepolymer, polyurethane (PU) nanospheres was synthesized with miniemulsion polymerization. Firstly, FTIR-ATR characterization was done for PU nanospheres as shown in Figure 3.25. According to spectrum, disappearance of NCO group, 1720 (-C=O) and 3341 (amide group) cm^{-1} shows an evidence for PU nanospheres.

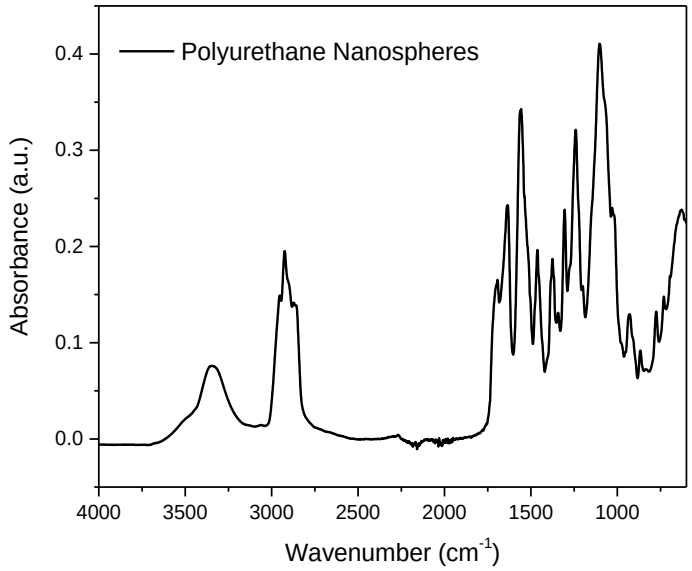

Figure 3.25. FTIR-ATR spectrum of PU nanospheres.

DLS analysis was done in order to measure size of nanospheres as shown in Figure 3.26. According to result, average hydrodynamic radius was measured as approximately 100 nm. In addition to this, SEM analysis was done in order to image nanospheres as shown in Figure 3.27. An image shows that spherical morphology was seen.

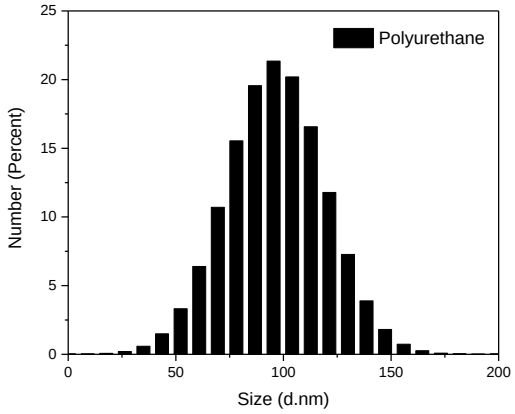

Figure 3.26. Size analysis of PU nanospheres by DLS.

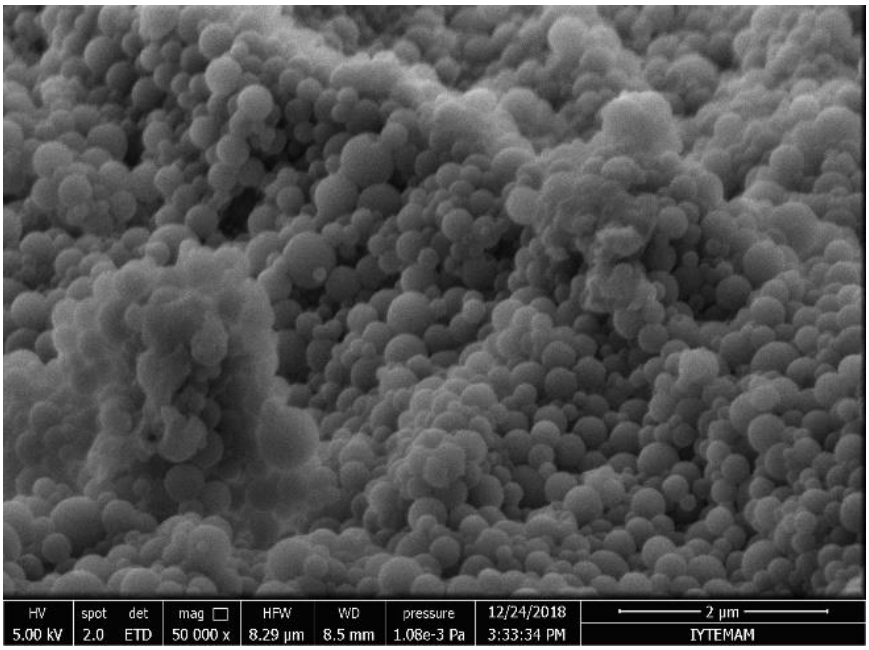

Figure 3.27. SEM image of PU nanospheres.

3.2.2. One-pot Miniemulsion Polymerization Technique

Polyurethane nanospheres was synthesized with using one-pot miniemulsion polymerization technique. PU nanospheres was characterized by FTIR-ATR, DLS, and SEM analysis. One-pot technique has some advantages from two-step technique which are short time, easy procedure and low chemical material. However, two-step technique is more controllable than one-pot technique. According to these criteria, one-pot technique was chosen for synthesis of polyurethane nanospheres. Firstly, PU nanospheres was characterized by FTIR-ATR (Figure 3.28). According to spectrum, characteristic bands was observed for PU nanospheres which are 1720 (-C=O), 3341 (amide group) cm^{-1} and decreasing of NCO groups shows an evidence for PU nanospheres. However, product of one-pot PU nanospheres has more polyurea group (1630 cm^{-1}) than two-step PU nanospheres. The condition was caused to synthesis of low molecular weight PU nanospheres. Process of condition was explained as shown in Figure 3.29. When schematic representation was utilized, first reaction referred the reaction of isocyanate group and diol group which leads to synthesis of polyurethane nanospheres. Second reaction referred the reaction of isocyanate group and water which leads to synthesis of polyurea nanospheres. Also, during the process of forming polyurea nanospheres, CO_2 released.

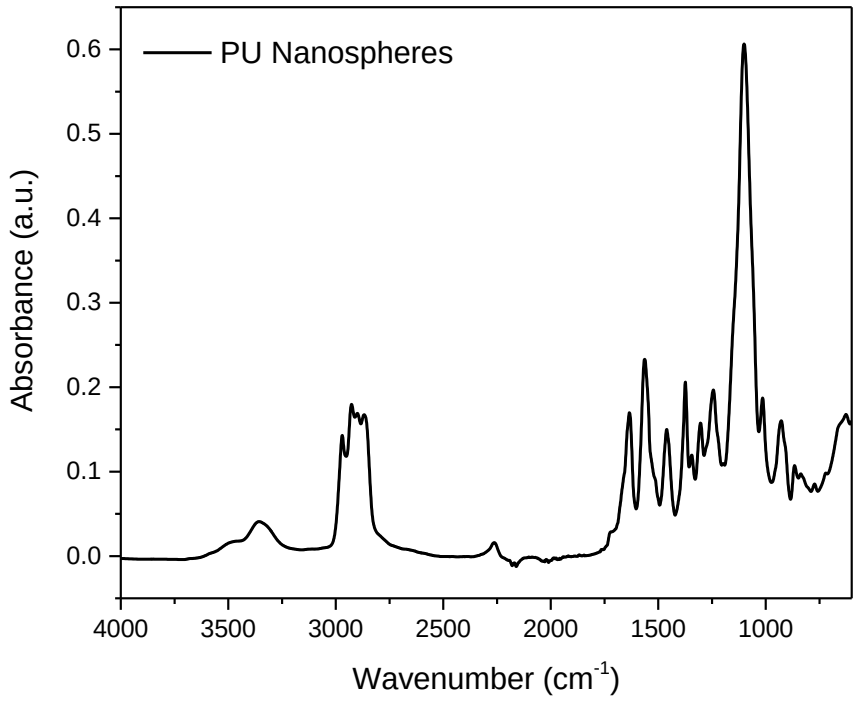

Figure 3.28. FTIR-ATR spectrum of PU nanospheres by One-pot technique.

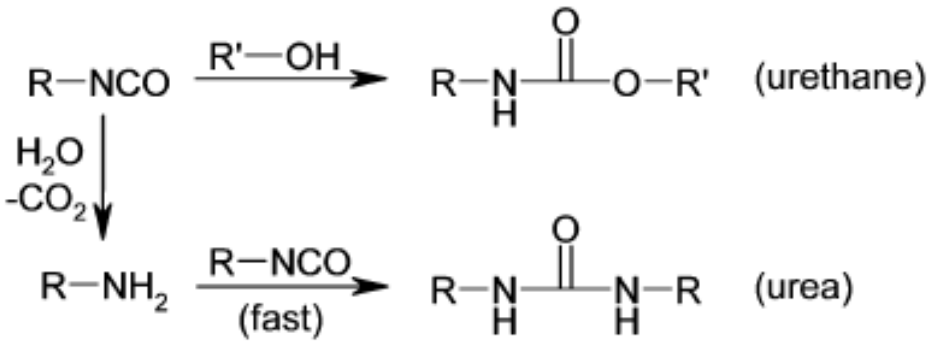

Figure 3.29. Schematic representation of urethane and urea formation.

DLS analysis was done in order to measure size of nanospheres as shown in Figure 3.30. According to result, average hydrodynamic radius was measured as approximately 200 nm. In addition to this, SEM analysis was done in order to image nanospheres as shown in Figure 3.31. An image shows that spherical morphology was seen.

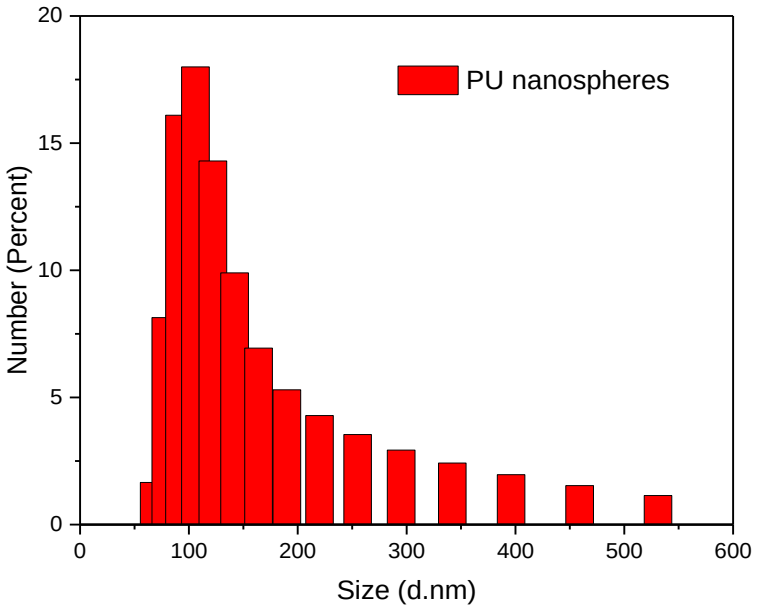

Figure 3.30. Size analysis of PU nanospheres by DLS.

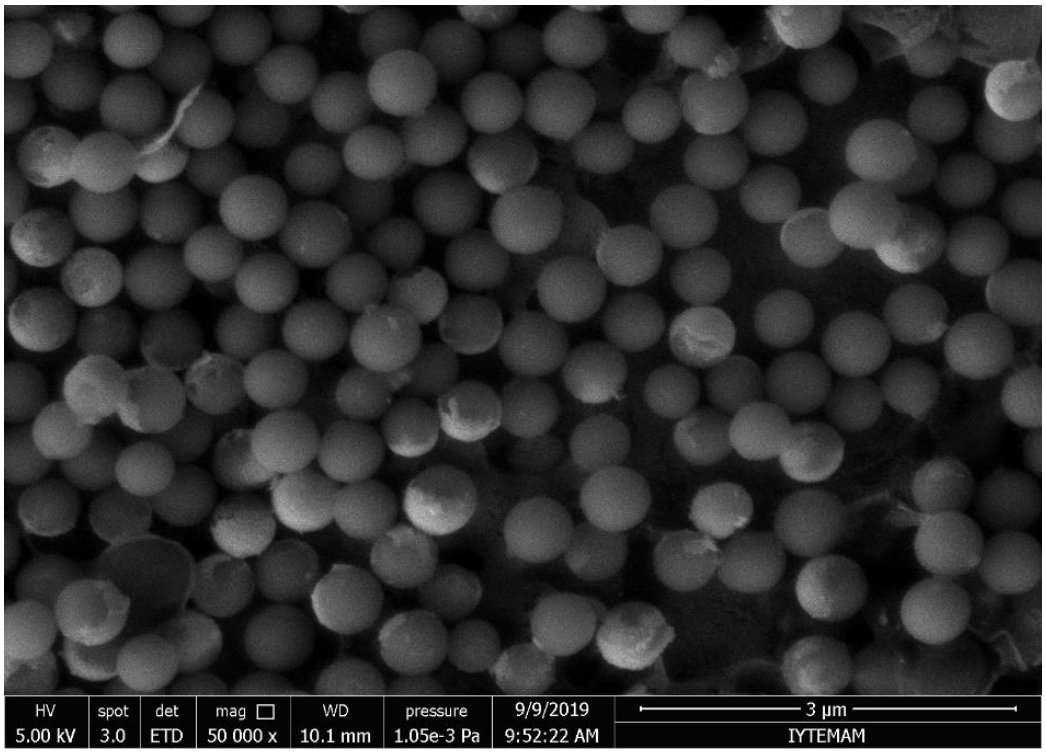

Figure 3.31. An image of PU nanospheres by SEM.

3.2.3. Synthesis and Characterization of Functional Nanospheres

Generally, one-pot miniemulsion polymerization technique was used in order to synthesize functional nanospheres. Therefore, IPDI/PPG ratio was changed for observation of differences on nanospheres. Also, polyethyleneimine, poly-lactic acid-co-glycolic acid (PLGA) were used instead of poly propylene glycol (PPG) for synthesis of functional nanospheres. Firstly, IPDI/PPG ratio was varied by increasing IPDI mole ratio. The changes were monitored by FTIR-ATR analysis. The purpose of this study is to synthesize -NH_2 functional groups on the surface of nanospheres with increasing of isocyanate group in the reaction medium. A correlation between 1 and 1.20 mol IPDI ratios was attempted for this experiment as shown in Figure 3.32. According to spectrums, if isocyanates ratio increases, absorbance intensity of characteristic bands increase proportionally.

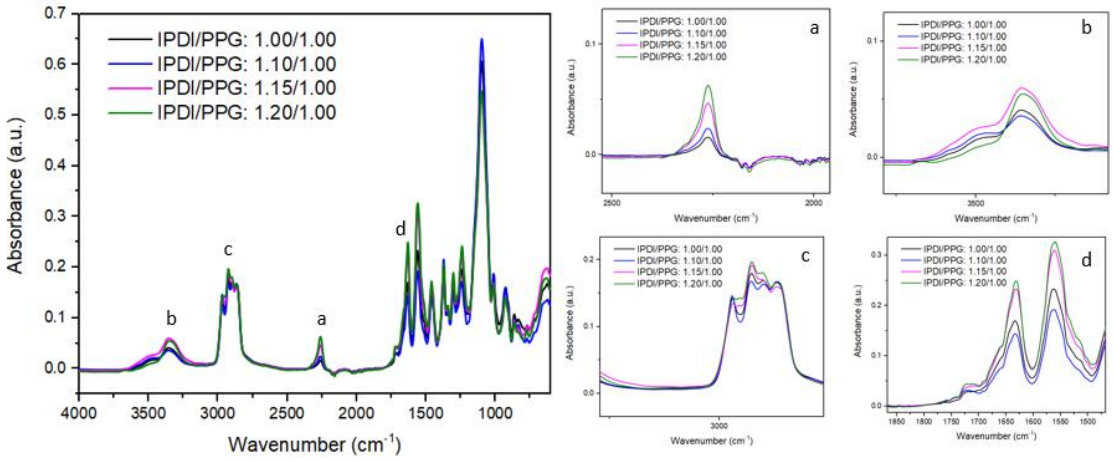

Figure 3.32. Effect of IPDI mole ratio on nanosphere formation; a) NCO band, b) NH2 band, c) C-H band, d) amide band.

After FTIR-ATR characterization, SEM analysis was done in different IPDI/PPG ratio accordingly mol as shown in Figure 3.33. According to images, if mole ratio of IPDI is increases, nanospheres turn into nanocups form. The reason of this situation is related to increasing in the amount of NCO with formation of polyurea. That's why, explosion was caused by release of CO_2 gas. Thus, nanocup structure was obtained. Especially, c and d images shows that 1.10/1.00, and 1.15/1.00 mole ratios are more effective about synthesis of nanocups.

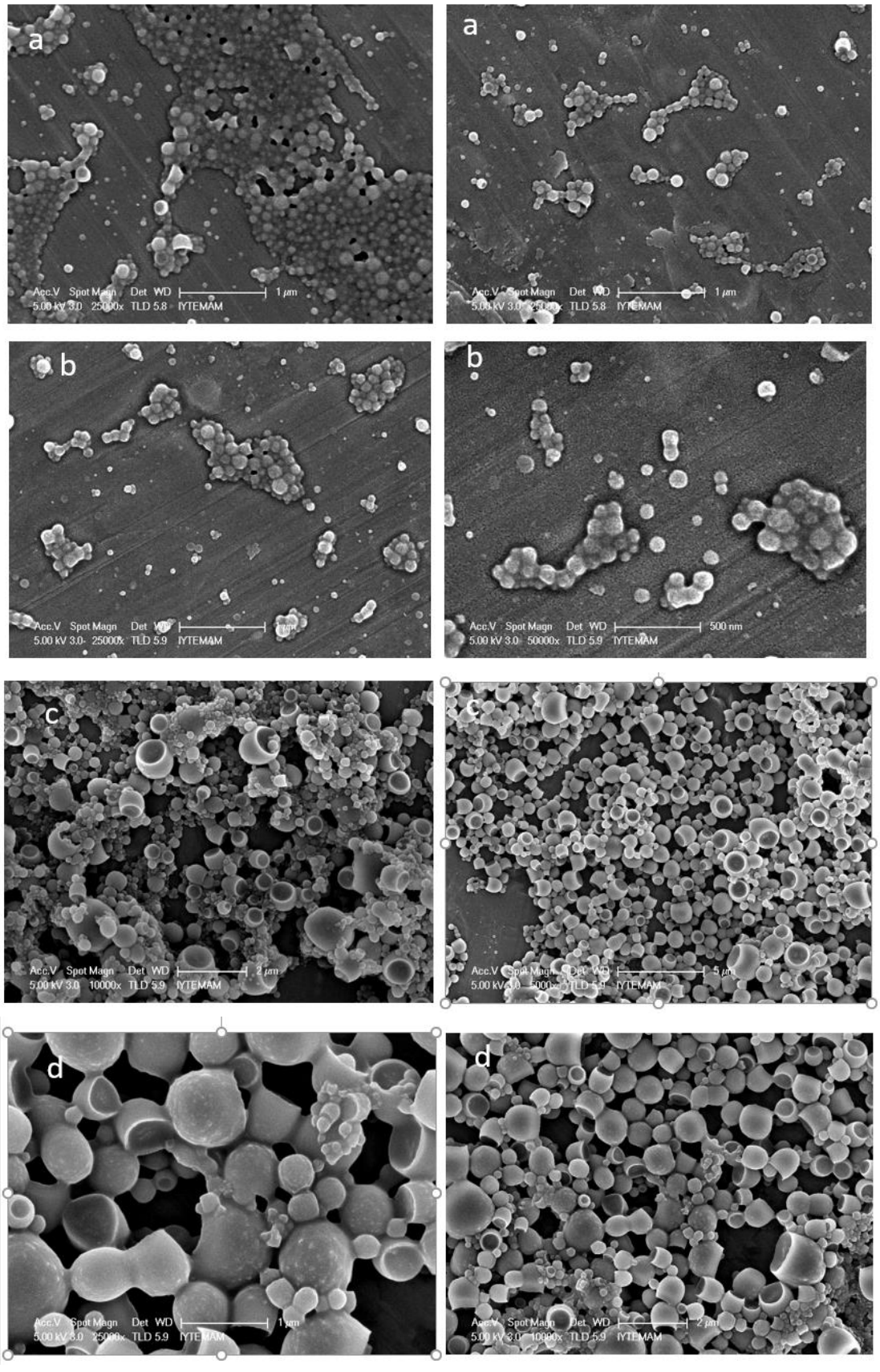
a
Acc.V Spot Magn Det WD 1 μm
5.00 kV 3.0 25000x TLD 5.8 IYTEMAM
a
Acc.V Spot Magn Det WD 1 μm
5.00 kV 3.0 25000x TLD 5.8 IYTEMAM
b
Acc.V Spot Magn Det WD
5.00 kV 3.0 25000x TLD 5.9 IYTEMAM
b
Acc.V Spot Magn Det WD 500 nm
5.00 kV 3.0 50000x TLD 5.9 IYTEMAM
c
Acc.V Spot Magn Det WD 2 μm
5.00 kV 3.0 10000x TLD 5.9 IYTEMAM
c
Acc.V Spot Magn Det WD 5 μm
5.00 kV 3.0 5000x TLD 5.9 IYTEMAM
d
Acc.V Spot Magn Det WD 1 μm
5.00 kV 3.0 25000x TLD 5.9 IYTEMAM
d
Acc.V Spot Magn Det WD 2 μm
5.00 kV 3.0 10000x TLD 5.9 IYTEMAM

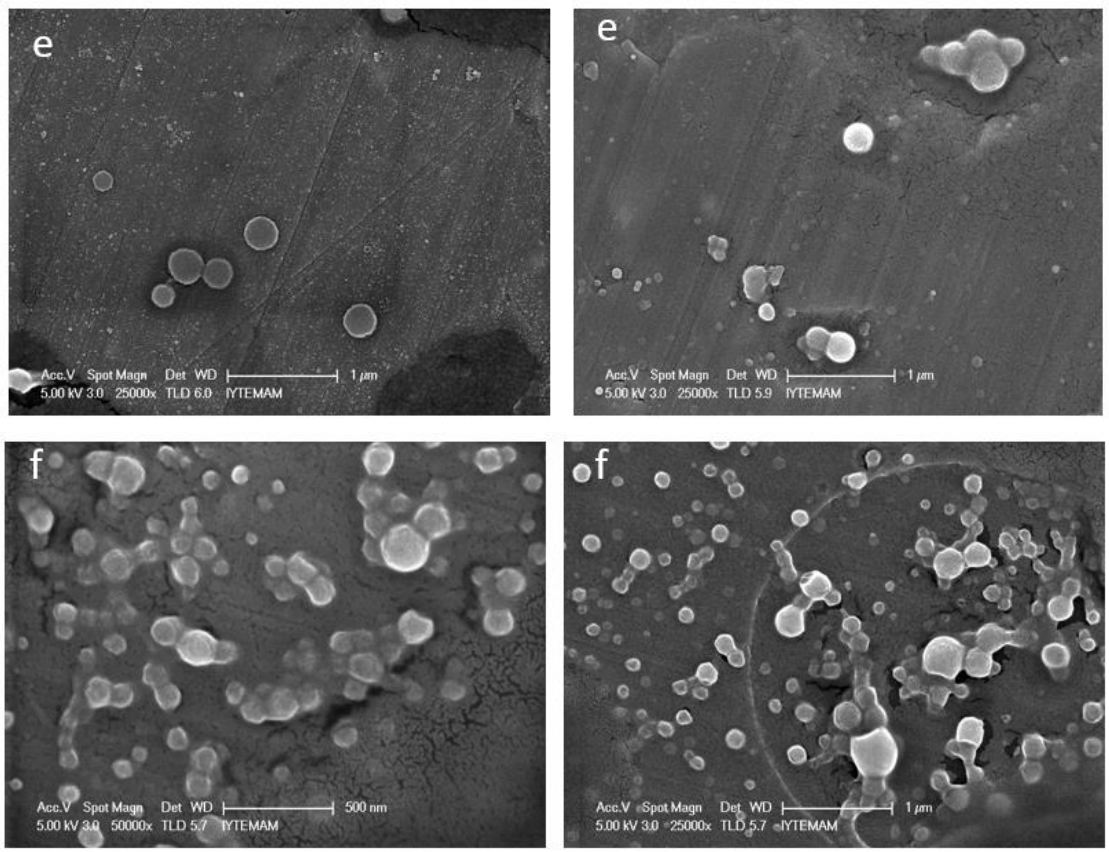

Figure 3.33. SEM analysis of different IPDI/PPG ratios accordingly mole; a) 1.00/1.00, b) 1.05/1.00, c) 1.10/1.00, d) 1.15/1.00, e) 1.20/1.00, f) 1.25/1.00.

Synthesis and characterization of nanocups was repeated at the mole ratio IPDI/PPG 1.10/1.00. Because the best result was observed at this ratio. Figure 3.34 shows structure and size of nanocups. According to images, synthesis of nanocups was repeated successfully, and size was measured as shown in Figure 3.34.

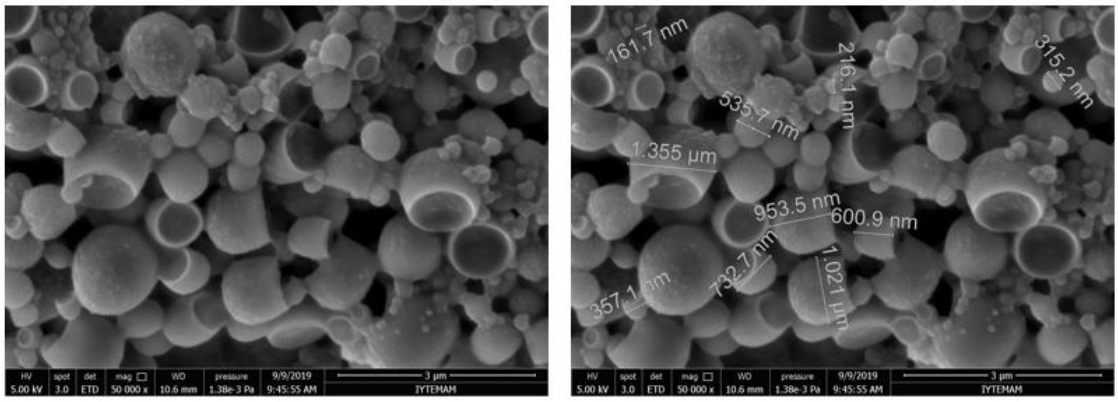

Figure 3.34. SEM analysis of nanocups which have certain IPDI/PPG ratios (1.10/1.00).

Size and zeta potential was measured by DLS. The analysis was done at the same dilution ratio (1/2000). Figure 3.35 shows size analysis of nanocups at 1.10/1.00 (IPDI/PPG) mole ratio. According to result, average hydrodynamic radius was measure approximately as 200 nm. Also, Table 3.1 shows zeta potential analysis. According to measurement, zeta potential was measured as -40.2 mV.

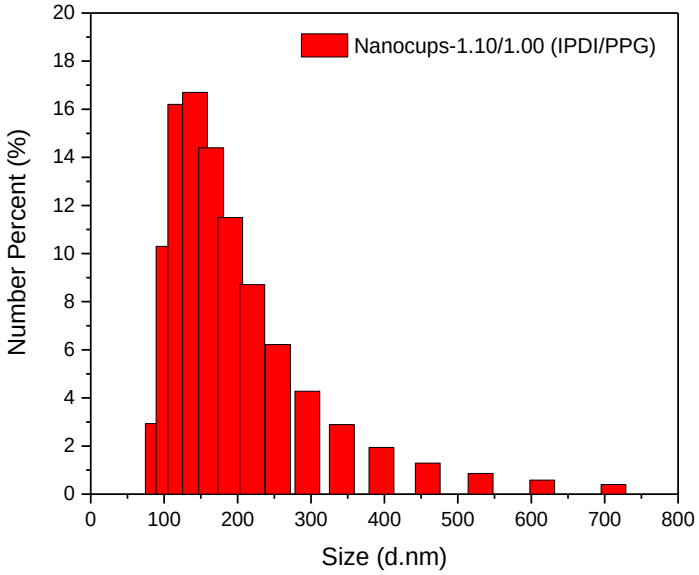

Figure 3.35. Size analysis of nanocups at 1.10/1.00 (IPDI/PPG) mole ratio.

Table 3.1. Zeta Potential Results of Nanocups

Name of Sample	ZP mV	Mob µmcm/Vs	Cond mS/cm
Nanocups-1.10/1.00 (IPDI/PPG) mole ratio	-40.2	-3.152	0.019867

In addition to these studies, various synthesizes was performed by one-pot miniemulsion polymerization technique. Firstly, prepolymer was used in order to synthesize nanosphere which was synthesized by two-step technique. After synthesizing, product was analyzed by FTIR-ATR spectroscopy as shown in Figure 3.36. According to the spectrum, nanosphere has NCO at 2265 cm^{-1}, NH_2 at 3460 cm^{-1}, and OH at range of 3550-3200 cm^{-1} functional groups on its surface. Also, SEM analysis was done as shown in Figure 3.37. According to images, nanospheres was not observed efficiently.

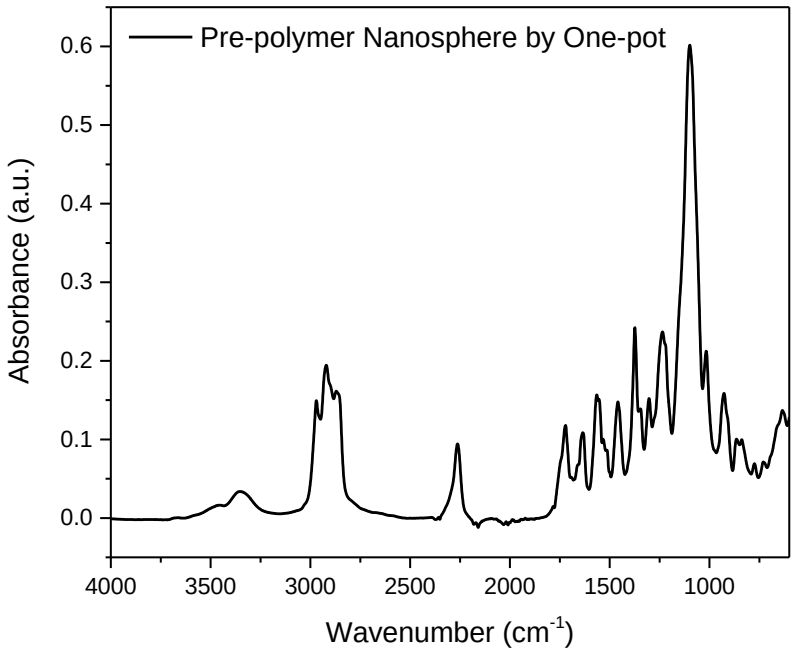

Figure 3.36. FTIR-ATR spectrum of prepolymer nanosphere by one-pot technique.

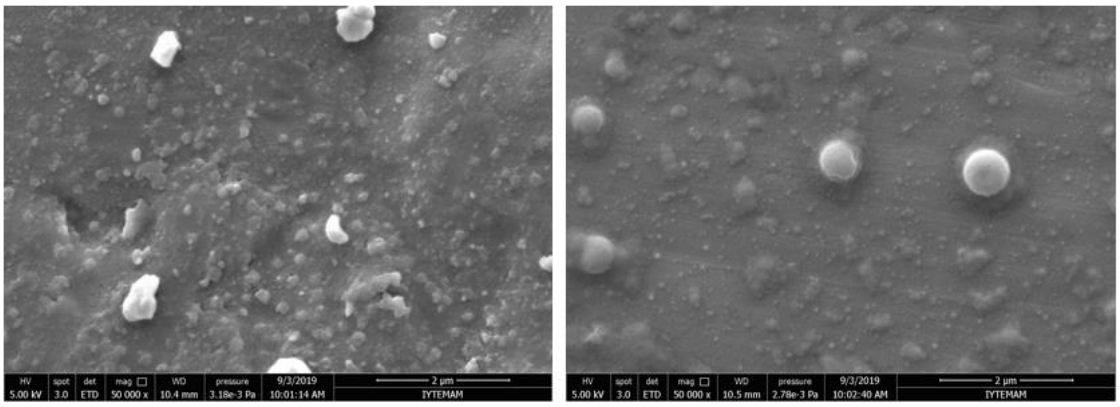

Figure 3.37. SEM images of prepolymer nanospheres by one-pot technique.

Secondly, ethyl-lysine-diisocyanate (ELDI) was used instead of IPDI in synthesis. ELDI/PPG nanospheres was synthesized by one-pot technique. Product was characterized by FTIR-ATR spectroscopy as shown in Figure 3.38. According to the spectrum, unlike synthesis using prepolymer, we cannot mention the presence of NCO in the product of the synthesis using ELDI. However, it can be said that it has a serious carbonyl bond and

it has a polyurethane structure. Also, SEM images was obtained as shown in Figure 3.39. According to images, morphology has not sufficiently nanosphere structure.

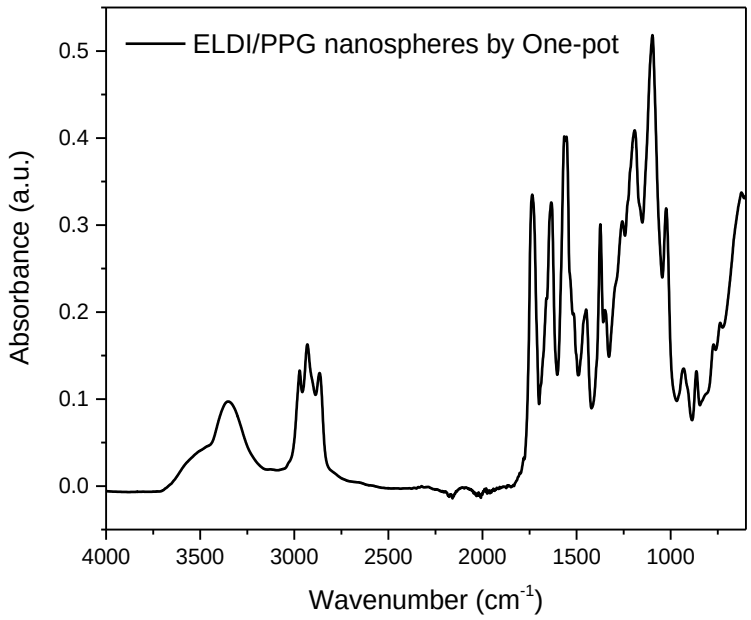

Figure 3.38. FTIR-ATR spectrum of ELDI/PPG nanospheres by one-pot technique.

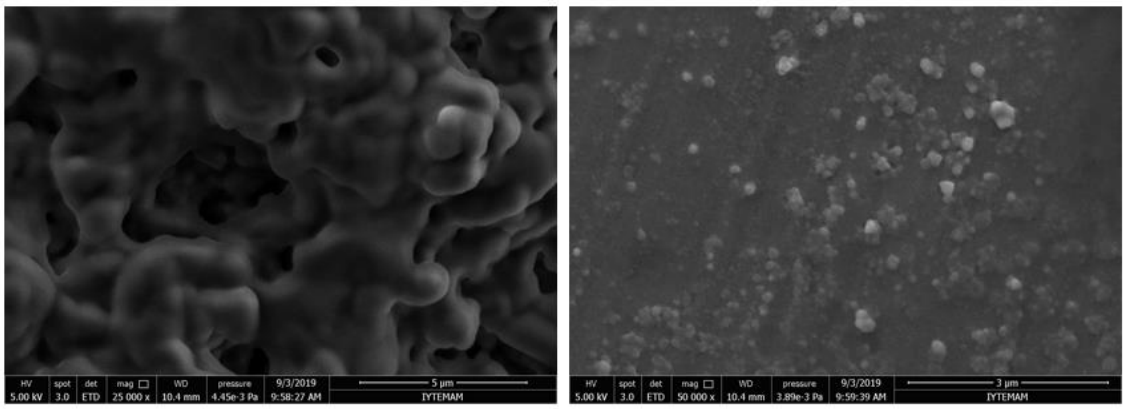

Figure 3.39. SEM images of ELDI/PPG nanospheres by one-pot technique.

Then, ethylenediamine (EDA) was used instead of PPG in synthesis. IPDI/EDA nanospheres was synthesized by one-pot technique. Product was characterized by FTIR-ATR spectroscopy as shown in Figure 3.40. According to this analysis, it is possible to talk about polyurethane and polyurea structures. In addition, the presence of NCO is

noteworthy. If the formation of nanospheres is observed, we can imagine that a large part of its surface is covered with NH_2 functional groups. However, SEM images was obtained as shown in Figure 3.41. According to images, morphology has not sufficiently nanosphere structure.

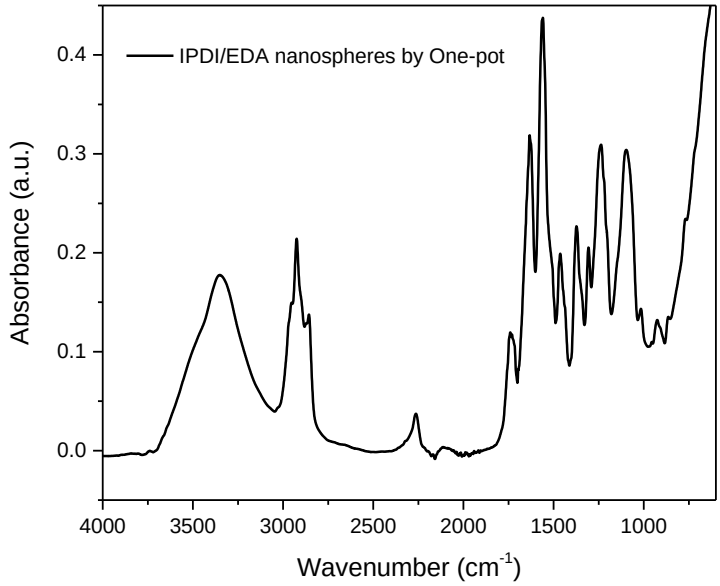

Figure 3.40. FTIR-ATR spectrum of IPDI/EDA nanospheres by one-pot technique.

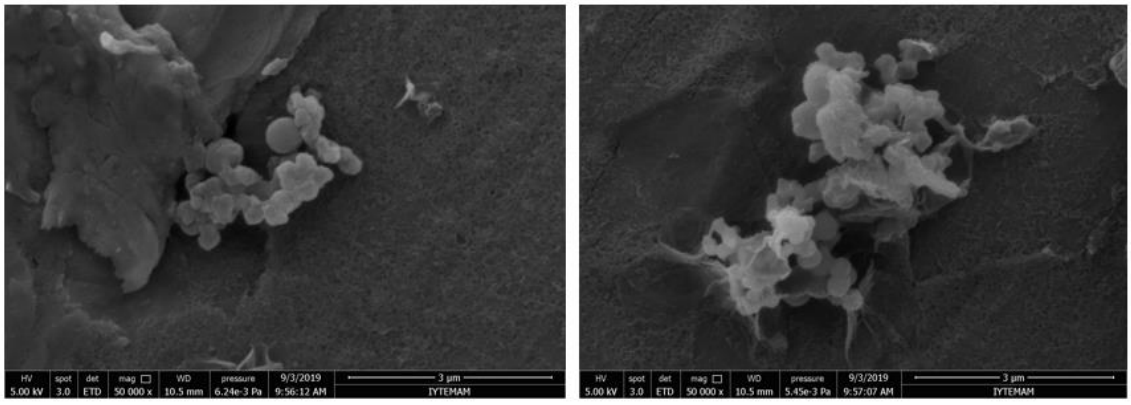

Figure 3.41. SEM images of IPDI/EDA nanospheres by one-pot technique.

Finally, polyethyleneimine 25000 mw (PEI) was used instead of PPG in synthesis. IPDI/PEI nanospheres was synthesized by one-pot technique. Product was characterized by FTIR-ATR spectroscopy as shown in Figure 3.42. The result of analysis, the range of 3500-3400 cm^{-1} band refers to primary amine (-N-H), 3400-3250 cm^{-1} band refers to secondary and tertiary amine, 3000-2840 cm^{-1} band refers to -C-H (sp^2-sp^3). Specifically,

1630 cm^{-1} band refers to -N-(C=O)-N- stretching which shows polyurea groups in the structure of nanospheres. In addition, SEM images was obtained as shown in Figure 3.43. According to images, morphology was formed by nanospheres.

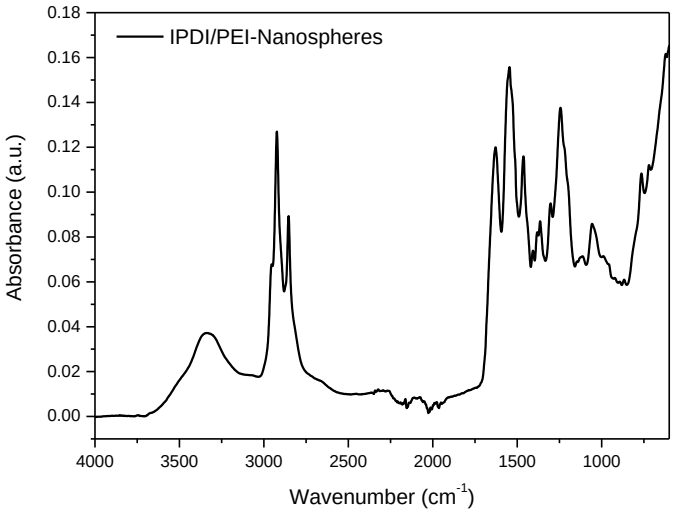

Figure 3.42. FTIR-ATR spectrum of IPDI/PEI nanospheres by one-pot technique.

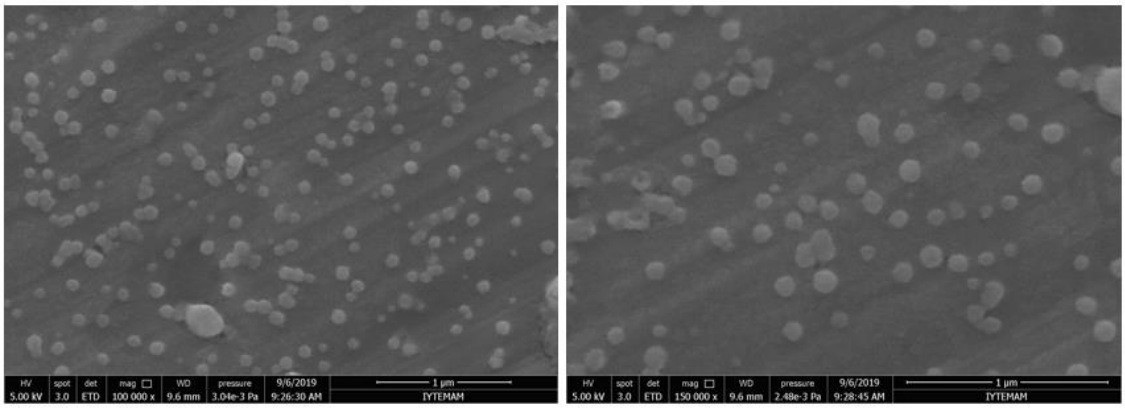

Figure 3.43. SEM images of IPDI/PEI nanospheres by one-pot technique.

After SEM characterization, DLS was used to measure size and zeta potential of IPDI/PEI nanospheres. Size results was shown in Figure 3.44. According to the results, size was measured as a range of 250-550 nm. Also, zeta potential was measured as shown in Table 3.2. According to measurement, zeta potential was measured as -23.8 mV.

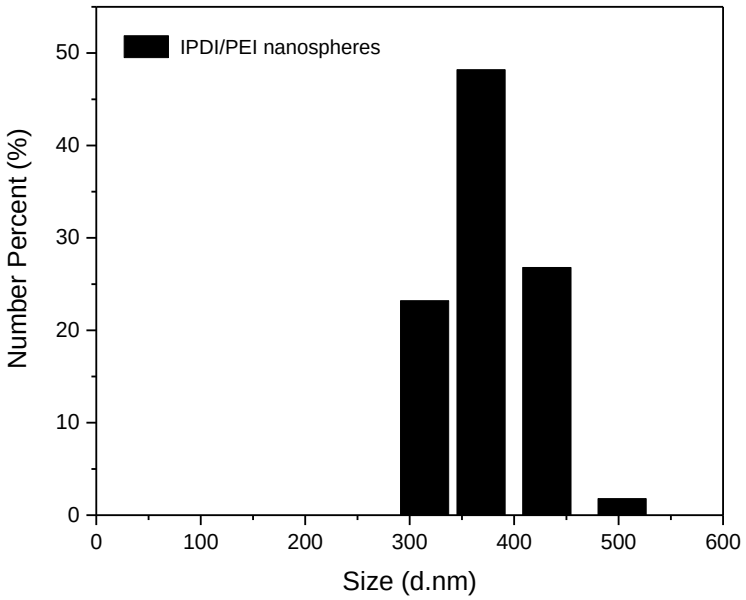

Figure 3.44. Size measurement of IPDI/PEI nanospheres.

Table 3.2. Zeta potential measurements of IPDI/PEI nanospheres.

Sample Name	Zeta Potential (mV)	Mobility (µmcm/Vs)	Conductivity (mS/cm)
IPDI/PEI nanospheres	-23.8	-1.865	0.015

In these synthesis, PPG, EDA, and PEI were used and different nanospheres were synthesized which have different properties in order to use in different applications. These materials can be compared by various perspectives. Firstly, PPG and PEI were successful in obtaining spherical morphology, but EDA was not successful. Also, PPG caused to negative charge on the nanospheres, however, PEI caused to positive charge on the nanospheres. Therefore, both of them were used in different application area because of their charge.

In addition to these, PLGA (85:15)/PEI nanospheres was synthesized in order to create an alternative to nanosphere synthesis and increase biocompatibility. In the synthesis, 290 mg PLGA dissolved in chloroform as an organic phase and 500 mg

polyvinyl alcohol and 84 mg SDS in the water phase were dissolved in 10 ml of ultrapure water. After mixing the two phases, 10 mg of polyethyleneimine was added to the medium. The organic phase was evaporated after ultrasonication. As the process can be seen, it is similar to two-step miniemulsion polymerization technique. The sample was then prepared in two different ways for SEM analysis (by dilution and precipitation from the solution). Some of the images of SEM analysis was shown in Figure 3.45. According to the images, nanosphere morphology was obtained. However, size of nanospheres was measured higher value than other synthesized nanospheres.

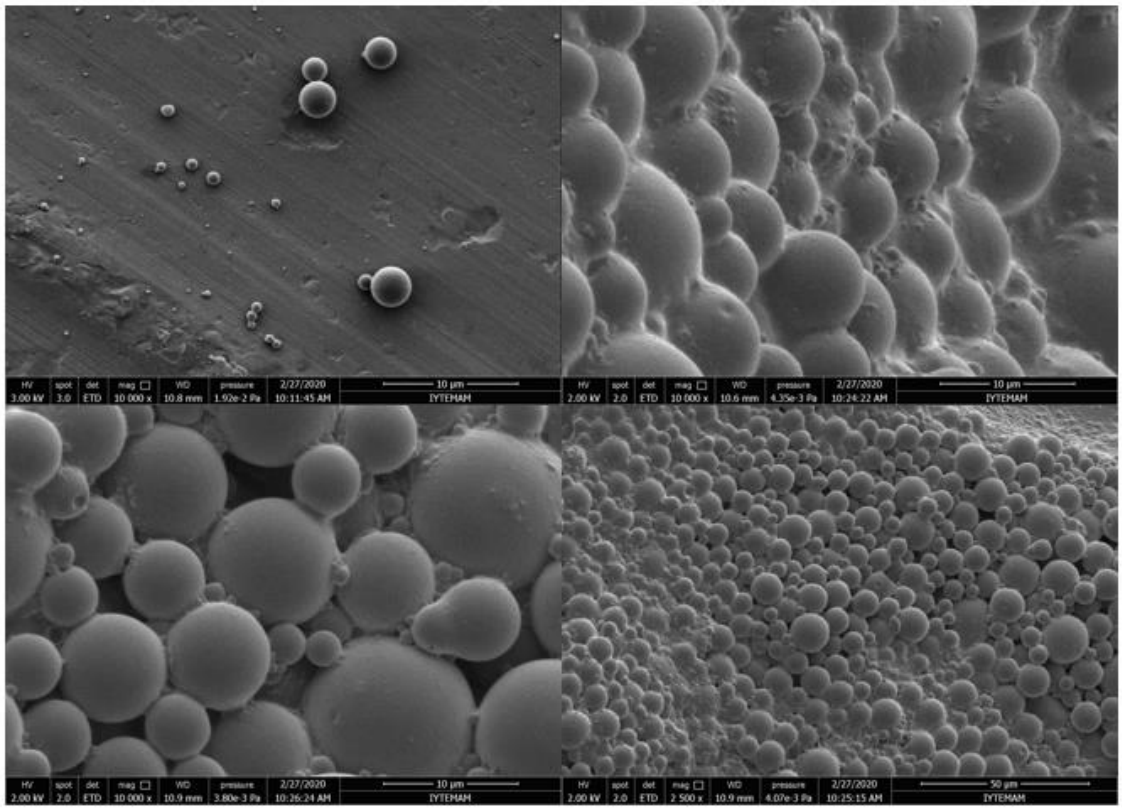

Figure 3.45. SEM images of PLGA (85:15)/PEI nanospheres.

3.3. Applications

Synthesis of conjugated polythiophene and polyurethane nanosphere derivatives was completed. Then, applications was performed as anionic-cationic complexation, and dual modal (fluorescent, magnetic) agents. Aim of doing these applications are to investigate bioimaging agents.

3.3.1. Anionic-Cationic Polythiophene Polyelectrolyte Complexation

Anionic polythiophene (PTAA) has negative charge and cationic polythiophene (PT4) has positive charge. Thanks to their opposite charge properties, anionic-cationic polythiophene complexation was done in order to examine complexation results and complex-ssDNA interaction. Thus, questions were answered such as how strongly the anionic-cationic complex was formed, whether ssDNA will join this complex or will it disrupt the complex polymer structure and create a duplex structure with PT4 instead of PTAA. Firstly, PT4 was synthesized and characterized by UV-visible, and fluorescence spectroscopy. However, PT4's maximum wavelengths was measured as 370 nm in UV-visible spectrum. Generally, PT4 has maximum wavelengths at approximately 400 nm. The reason of this situation is related to having less monomer unit than other derivatives. PT4 was analyzed in range pH 3-11 by UV-visible spectroscopy like PTAA (Figure 3.12) as shown in Figure 3.46. Also, PT4 was analyzed by fluorescence spectroscopy like PTAA (Figure 3.14) at the same way as shown in Figure 3.47.

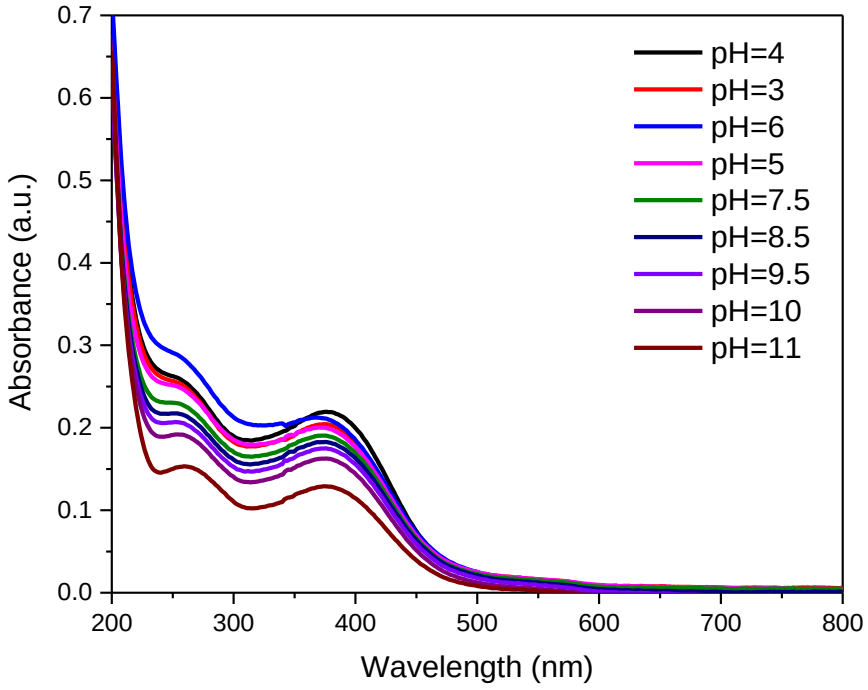

Figure 3.46. UV-Visible absorbance spectrum of PT4 aqueous solution (0.5 mg/2 ml) for pH=3-11.

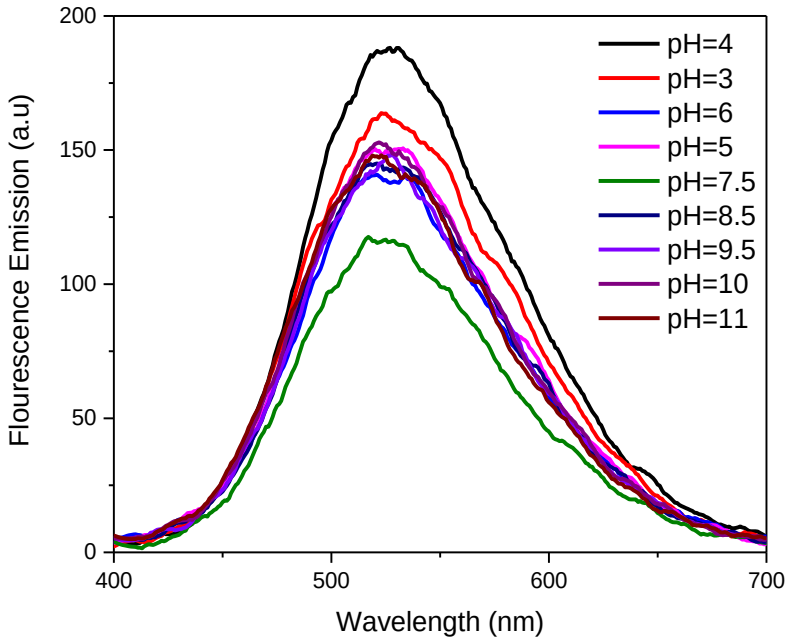

Figure 3.47. Fluorescence emission spectra of PT4 aqueous solution (0.5 mg/ 2 ml) for pH=3-11.

According to Figure 3.46 and Figure 3.47, PT4 was not affected too much by the pH changes, and the resulting differences are due to dilution during pH adjustment. In addition, no significant changes were observed in the maximum wavelengths of both the absorbance and emission spectrum in this experiment. As a result, it was understood that the main source of the changes that will occur when the cationic and anionic polythiophenes form a complex will be anionic polythiophene. Because the pH of the anionic polythiophene dissolved in the basic medium could be affected by cationic polythiophene. Thus, it made sure that the cationic PT4 was not affected by the pH of the anionic PTAA.

PT4 was titrated with PTAA (pH:9) in different concentrations in order to form anionic-cationic complex. Titration procedure was done by UV-visible and fluorescence spectroscopy. Firstly, UV-visible spectroscopy was used to observe forming complex. Figure 3.48 shows that concentration ratio was adjusted as 2.2:1 (PT4: PTAA) for PT4, and PTAA respectively 1.86 mM, and 0.85 mM. Then, concentration ratio was adjusted as 0.5:1 (PT4: PTAA) for PT4 (0.45 mM) and PTAA (0.85 mM). In Figure 3.48 and Figure 3.49, volume of anionic and cationic polymers was prepared as equal for 200 µL.

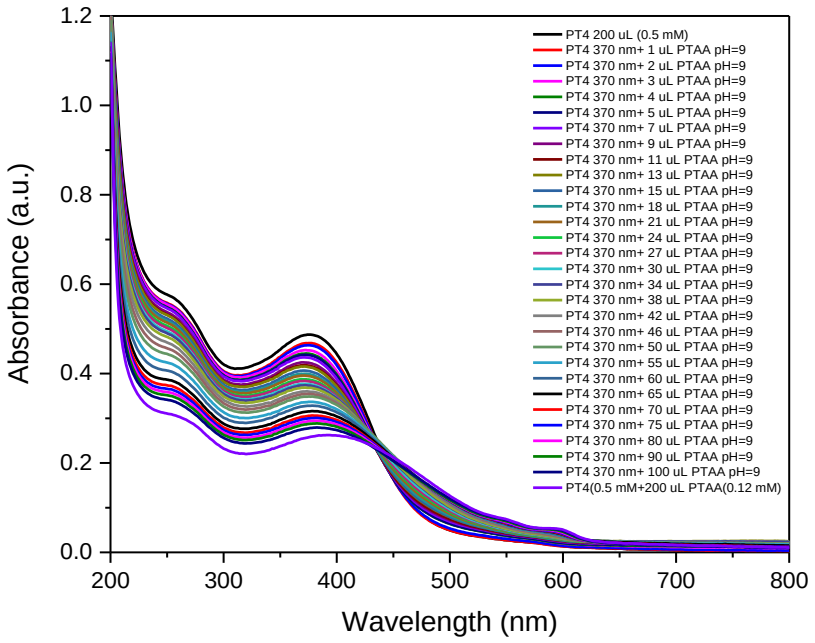

Figure 3.48. UV-Visible absorbance spectrums of PT4-PTAA titrations (ratio 2.2:1).

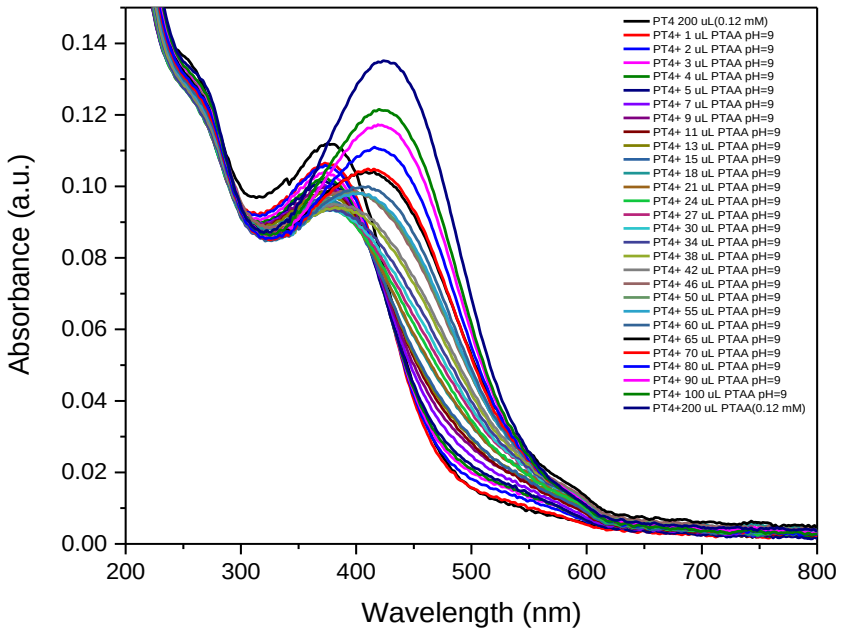

Figure 3.49. UV-Visible absorbance spectrums of PT4-PTAA titrations (ratio 0.5:1).

First trial has concentration ratio 4:1 between PT4 and PTAA. According to Figure 3.48, absorbance intensity of PT4 decreased at maximum wavelength 370 nm by addition of PTAA. Also, maximum wavelength shifted to right slightly. When titration was completed, new maximum wavelength shifted at 410 nm. In addition, even it was small, new peak was observed at 600 nm. On the other hand, a point like an isosbestic was observed at 435 nm. All of result of this spectrums shows that anionic-cationic complex was formed and planarization of PT4 was observed. After first trial, concentration ratio was adjusted 0.5:1 as shown in Figure 3.49. According to spectrums, isosbestic point disappears and final maximum wavelength was 430 nm. Figure 3.49 shows complex formation like a Figure 3.48.

Then, fluorescence spectroscopy was used to observe forming complex. Figure 3.50 shows that concentration ratio was adjusted as 2.2:1 (PT4: PTAA) for PT4, and PTAA respectively 1.86 mM, and 0.85 mM. Then, concentration ratio was adjusted as 0.5:1 (PT4: PTAA) for PT4 (0.45 Mm) and PTAA (0.85 mM). In Figure 3.50 and Figure 3.51, volume of anionic and cationic polymers was prepared as equal for 200 µL.

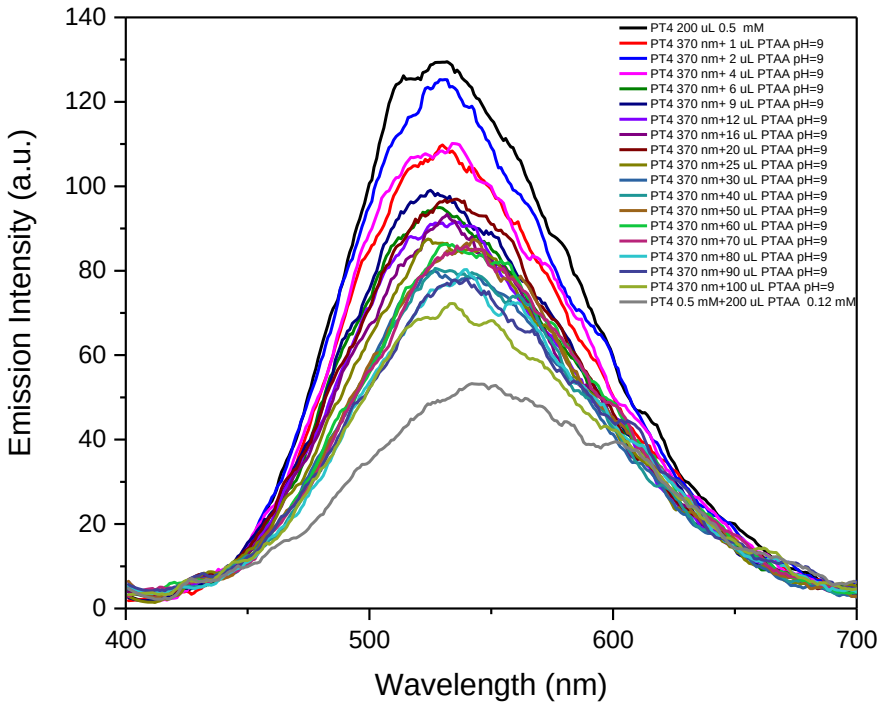

Figure 3.50. Flourescence emission Spectrums of PT4-PTAA titrations (ratio 2.2:1).

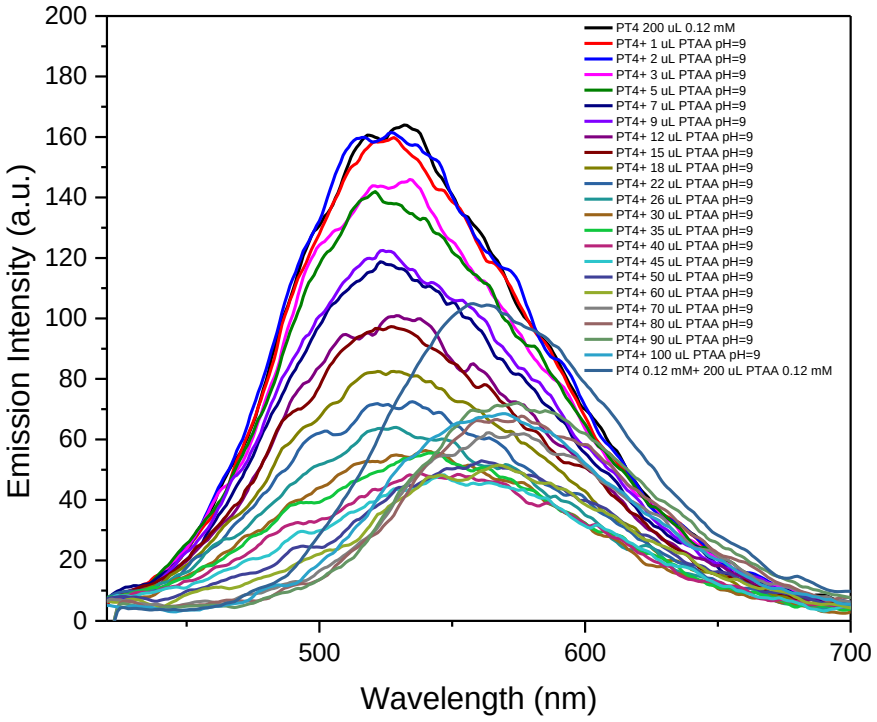

Figure 3.51. Flourescence emission Spectrums of PT4-PTAA titrations (ratio 0.5:1).

First trial has concentration ratio 2.2:1 between PT4 and PTAA. According to Figure 3.50, emission intensity of PT4 decreased at maximum wavelength 525 nm by addition of PTAA. Also, maximum wavelength shifted to right slightly. When titration was completed, new maximum wavelength shifted at 550 nm. In addition, even it was small, new peak was observed at 600 nm. All of result of this spectrums shows that anionic-cationic complex was formed and planarization of PT4 was observed. Because fluorescent quenching was observed when PTAA was added to the PT4. After first trial, concentration ratio was adjusted 0.5:1 as shown in Figure 3.51. According to spectrums, final maximum wavelength was 570 nm. Figure 3.51 shows complex formation like a Figure 3.50.

In addition, anionic-cationic interaction effect was examined by DLS. Size of polymers were measured. Firstly, PT4 and PTAA was measured at $16x10^{-3}$ mM concentration as shown in Figure 3.52. Results shows that average hydrodynamic radius of PT4 was measured approximately 13 nm and average hydrodynamic radius of PTAA was measured as 8 nm. Then, size of anionic-cationic complex polymer (after PT4-PTAA titration) was measured as shown in Figure 3.53 at the same concentration. According to

the results, when anionic-cationic titration was done, conformation of polymers changed random coil to planar form. Thus, PT4 and PTAA formed complex polymer structure.

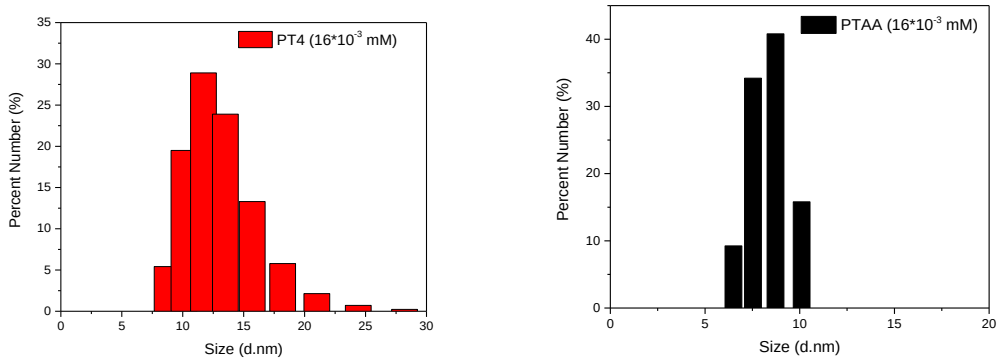

Figure 3.52. Size results of PT4 and PTAA by DLS.

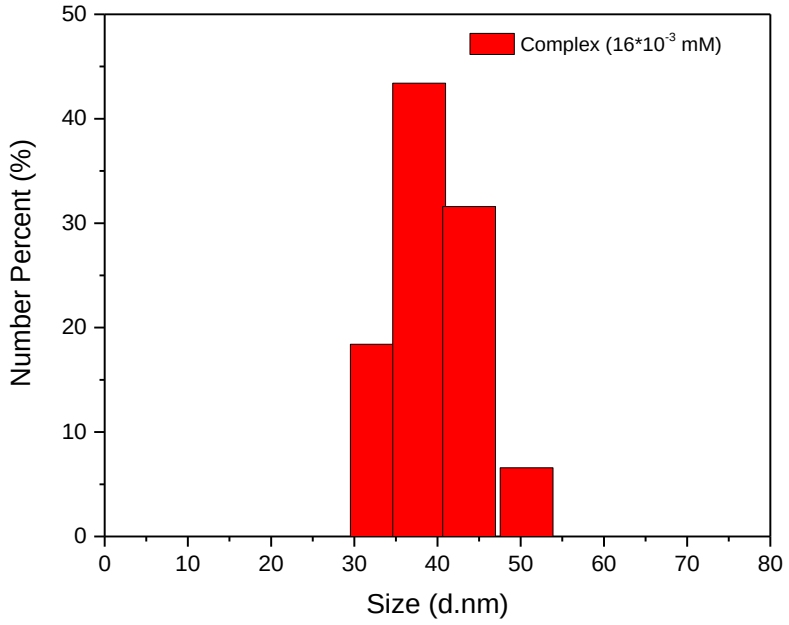

Figure 3.53. Size result of complex polymer by DLS.

After above trials, complex mixture ratios was determined by zeta potential analysis. Purpose of this experiment is to make sure ratio of complexation for PT4 and PTAA. After this analysis, it was seen that 70% of the mixture was cationic (PT4) and

30% of the anionic (PTAA) was suitable in order to form neutral complex. Because the zeta potential in this mixture was measured as 3.5 mV, this was the closest result to zero in this experiments as shown in Figure 3.54. In this experiment, PT4 and PTAA has the concentration as respectively 0.45 Mm and 0.85 mM for PT4 and PTAA.

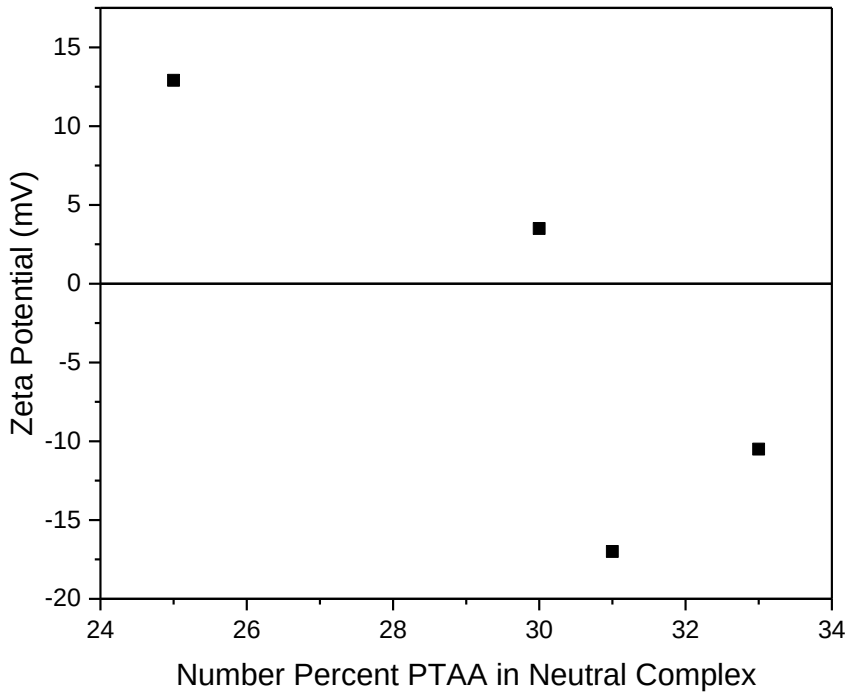

Figure 3.54. Zeta potential measurements for determination of polymer ratio in complex.

After determination of neutral complex ratio, PT4 (cationic), PTAA (anionic), and complex polymers were analyzed by UV-visible spectroscopy (Figure 3.55). In analysis, PT4 and PTAA has concentration as respectively 0.45 Mm and 0.85 mM for PT4 and PTAA. Also, pH of PTAA was adjusted to 9. Complex polymer was prepared as neutral complex ratio (PT4: PTAA, %70/%30, 210 µL PT4: 90 µL PTAA). According to spectrums, maximum wavelengths were measured as 376nm, 471nm and 416nm, respectively. In addition to this experiment, fluorescence resonance energy transfer (FRET) partner investigation was done for PT4 and PTAA as shown in Figure 3.56. According to results, there is FRET partner between PTAA absorbance and PT4 emission. Because complex polymer has higher maximum wavelength than PT4 and PTAA in fluorescence spectrums. Thus, there is an energy transfer between PT4 and PTAA.

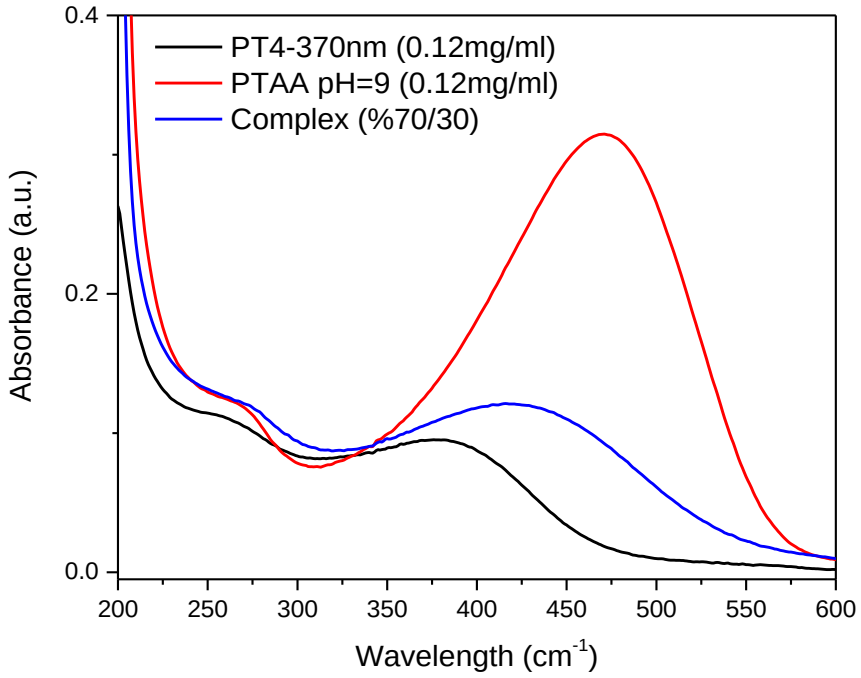

Figure 3.55. UV-Visible absorbance spectrum of PT4, PTAA and their complex.

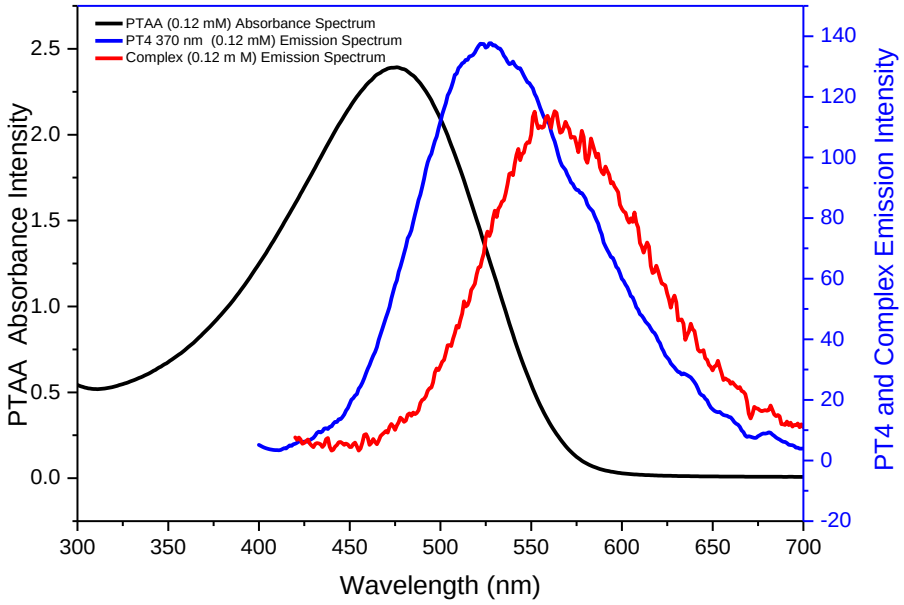

Figure 3.56. Investigation of FRET partner between PT4 and PTAA.

PT4 and PTAA was titrated at neutral complex ratio by UV-visible spectroscopy as shown in Figure 3.57. According to Figure 3.57, absorbance intensity of PT4 decreased at maximum wavelength 376 nm by addition of PTAA. Also, maximum wavelength shifted to right slightly. When titration was completed, new maximum wavelength shifted at 416 nm. In addition, even it was small, new peak was observed at 600 nm. On the other hand, a point like an isosbestic was not observed. All of result of this spectrums shows that anionic-cationic complex was formed and planarization of PT4 was observed slightly.

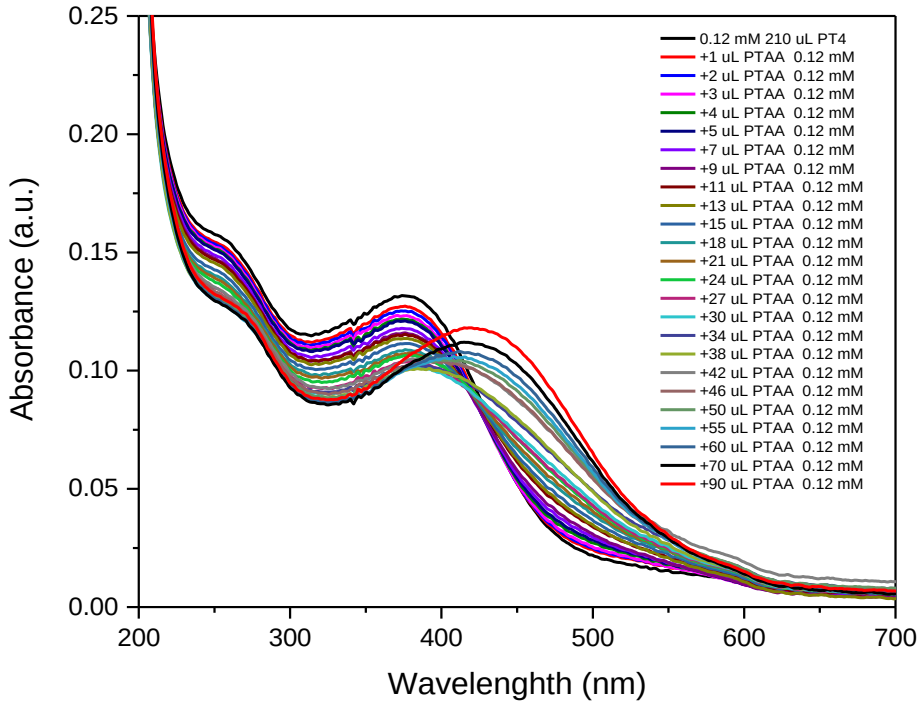

Figure 3.57. UV-visible absorbance spectrums of 210 µL PT4(370nm)-90 µL PTAA titration.

Then, neutral complex was titrated with 10 uL ssDNA sample in order to examine interaction of complex polymers and ssDNA. Figure 3.58 shows that interaction of complex polymers and ssDNA didn't has any spectroscopic change about ssDNA effect. Only, there is change at 260 nm which refers addition of ssDNA. According to the result, ssDNA was not able to interact with complex polymers because ssDNA didn't has enough charge in order to decompose the anionic-cationic complex, therefore, it didn't join to the complex interaction.

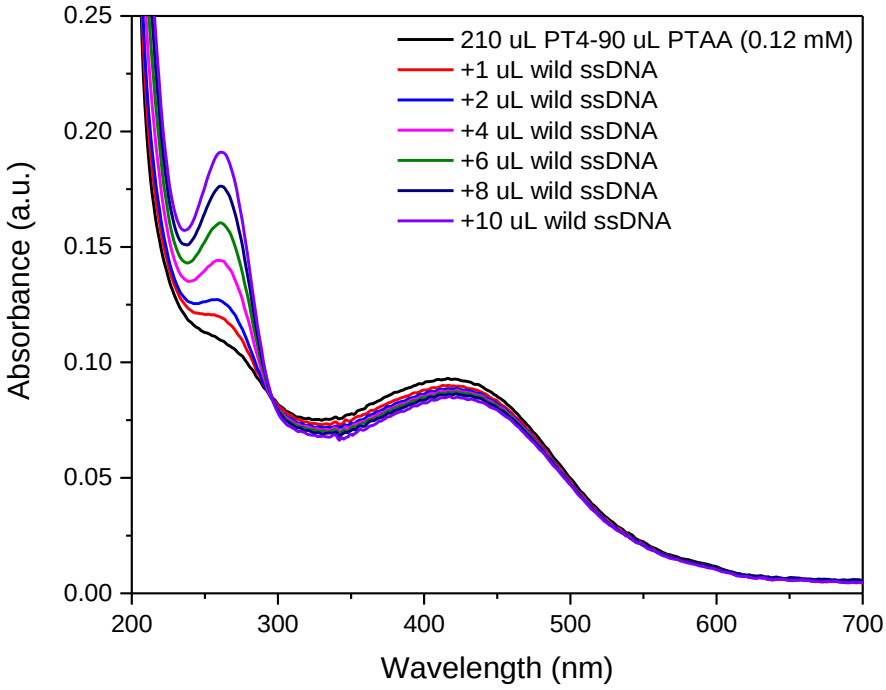

Figure 3.58. UV-visible absorbance spectrums of 210 µL PT4(370nm)-90 µL PTAA+10uL ssDNA titration.

PT4 and PTAA was titrated at neutral complex ratio by fluorescence spectroscopy as shown in Figure 3.59. According to Figure 3.59, emission intensity of PT4 decreased at maximum wavelength 525 nm by addition of PTAA. Also, maximum wavelength shifted to right. When titration was completed, new maximum wavelength shifted at 575 nm. All of result of this spectrums shows that anionic-cationic complex was formed and planarization of PT4 was observed. Because fluorescent quenching was observed when PTAA was added to the PT4. Then, neutral complex was titrated with 10 uL ssDNA sample in order to examine interaction of complex polymers and ssDNA by fluorescence spectroscopy. Figure 3.60 shows that interaction of complex polymers and ssDNA didn't has any spectroscopic change about ssDNA effect. Only, there is a small decrease at maximum wavelength. The reason of decreasing is related to dilution of neutral complex with addition of ssDNA. Thus, as seen in both absorbance and emission spectrum, ssDNA could not make any interaction to the complex polymer structure. The reason for this situation is entirely related to the fact that the anionic-cationic polymer interaction is very strong, and the ssDNA is not strong enough to join complex interaction.

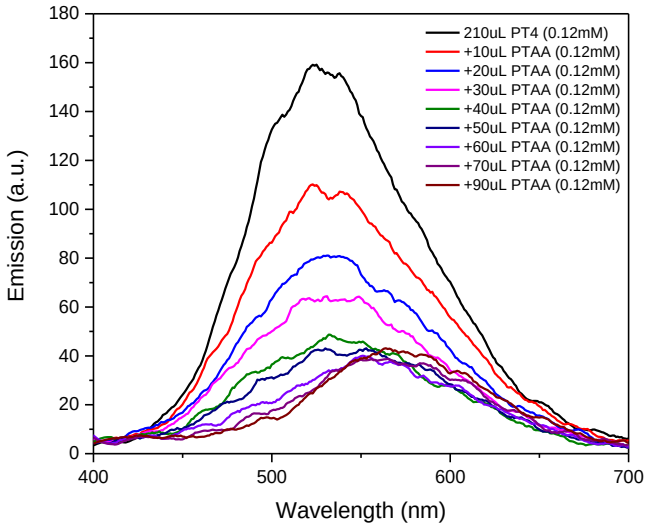

Figure 3.59. Flourescence emission spectrums of 210 µL PT4(370nm)-90 µL PTAA titration.

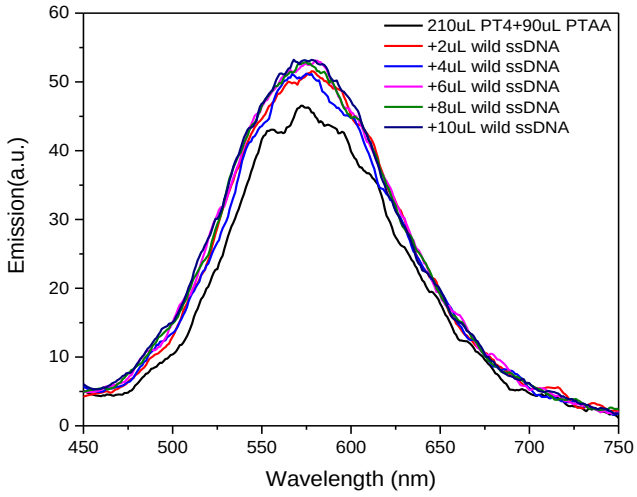

Figure 3.60. Flourescence emission spectrums of 210 µL PT4(370nm)-90 µL PTAA+10uL ssDNA titration.

After spectroscopic investigation, PT4 (cationic), PTAA (anionic), and neutral complex polymers were analyzed in order to measure zeta potential by DLS. Also, 10 µL ssDNA was added into the neutral complex and PT4 for zeta potential analysis. In

addition, 15 µL ssDNA was diluted to 1.5 ml ultrapure water and analyzed. All polymer concentration was adjusted to $16*10^{-3}$ mM except ssDNA. When Table 3.3 was examined, ssDNA affected to neutral complex. Neutral complex shows a decrease from 0.38 mV to -21.8 mV when 10 µL ssDNA was added. The reason of this condition is related to addition of ssDNA which have negative charge as shown in Table 3.3 and Figure 3.61. Thus, negative zeta potential was obtained. Then, neutral complex was titrated with ssDNA in order to make sure about the interaction as shown in Figure 3.61. According to the results, while ssDNA was adding, zeta potential of neutral complex decreased.

Table 3.3. Zeta Potential analysis results of polymer and polymer-ssDNA interaction

Sample Name	Zeta Potential (mV)	Mob (µmcm/Vs)	Cond (mS/cm)
PTAA	-23	-1.800	14.8
PT4	34.5	2.702	0.0245
Neutral Complex (PT4/PTAA)	0.38	0.029	5.68
Neutral Complex+10 µL ssDNA	-21.8	-1.713	5.7
PT4+10 µL ssDNA	0.19	0.0151	0.0434
15 µL ssDNA in 1.5 ml water	-18.2	-1.429	0.0585

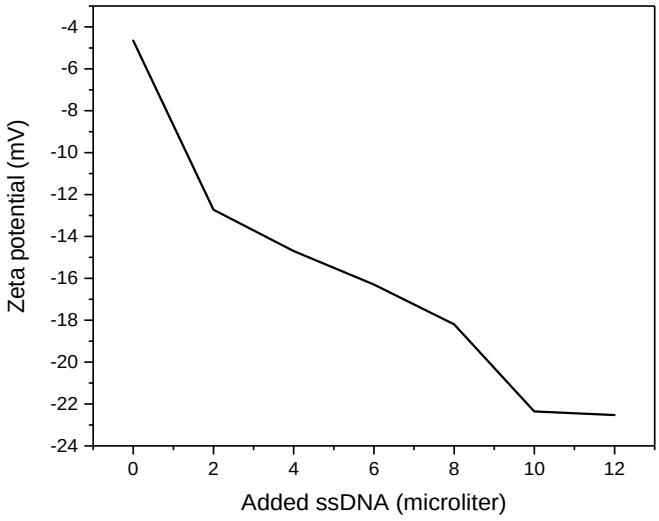

Figure 3.61. Zeta potential results of DNA titration with the complex polymer.

3.3.2. Magnetic Levitation Studies on the Nanospheres

IPDI-PEI nanospheres was prepared by one-pot miniemulsion technique which was used to synthesize dual mode agent for aimed in bioimaging applications such as fluorescence and magnetic imaging as shown in Figure 2.16. In this study, IPDI/PEI polyurea nanospheres was functionalized with conjugated polythiophene PTAA and gadolinium (Gd) metal ions. Thus, the nanospheres was prepared as fluorescent and magnetic agent for bioimaging. The purpose of this study is to ease characterization and increase working range of bioimaging agents. First of all, IPDI/PEI/PTAA nanospheres was analyzed by fluorescence spectroscopy at excitation wavelength 475 nm (475 nm was absorbance maximum wavelength of PTAA) as shown in Figure 3.62. Emission maximum wavelength of IPDI/PEI/PTAA nanospheres was measured as 570 nm. According to the result, it was observed to yield a value above the fluorescence intensity of the PTAA polymer.

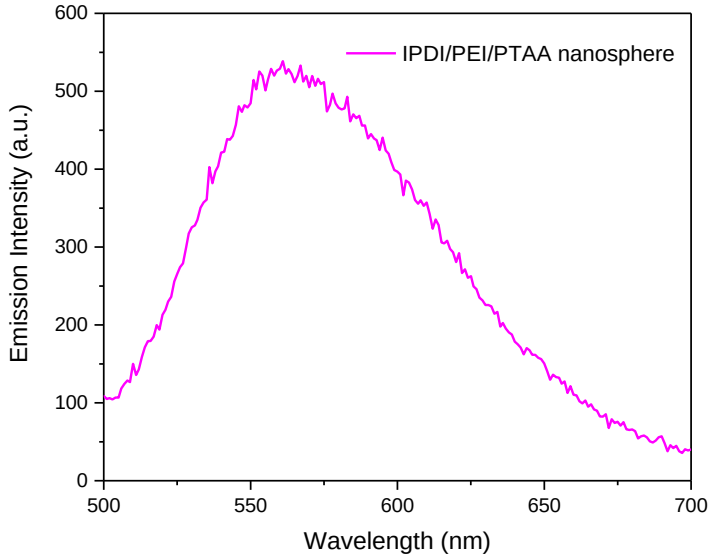

Figure 3.62. Emission spectrum of IPDI/PEI/PTAA nanospheres.

Size and zeta potential measurements of nanospheres were measured by DLS. As seen in Figure 3.63, the average hydrodynamic radius of IPDI / PEI / PTAA nanospheres was measured approximately as 25 nm. Then, zeta potential analyzes were measured for 3 times as shown in Table 3.4. As a result of the analysis, the average zeta potential value

of IPDI/PEI/PTAA nanospheres was measured as 11.8 mV. The results shows that PTAA changed the properties of IPDI / PEI nanospheres because IPDI / PEI have greater size without PTAA (at size range 250-400 nm (Figure 3.44)) and IPDI / PEI nanospheres have negative zeta potential value (-23.8 mV (Table 3.2)).

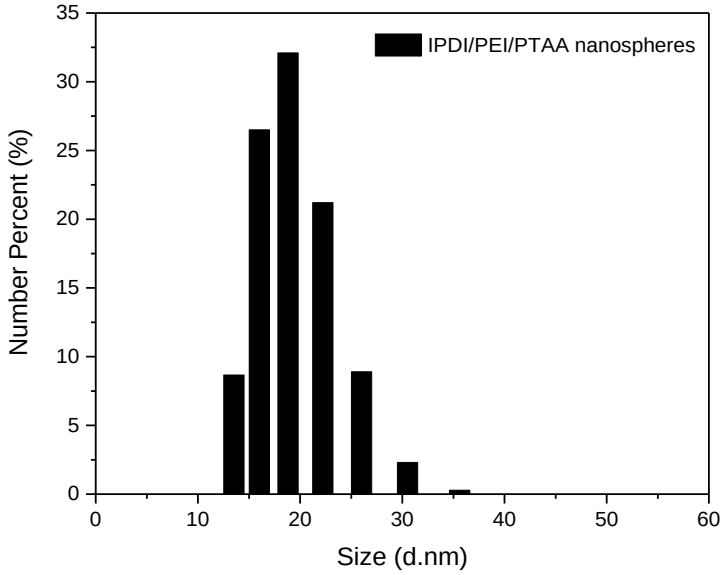

Figure 3.63. Size result of IPDI/PEI/PTAA nanospheres.

Table 3.4. Zeta potential results of IPDI/PEI/PTAA nanospheres.

Sample	ZP	Mob	Cond
	mV	µmcm/Vs	mS/cm
IPDI/PEI/PTAA 1	11.2	0.8756	0.103
IPDI/PEI/PTAA 2	12.4	0.9708	0.104
IPDI/PEI/PTAA 3	11.7	0.9191	0.104

In addition to these characterizations, SEM analysis was performed by dilution of IPDI/PEI/PTAA nanospheres at dilution ratio 1/1000. The images are shown in Figure 3.64. Also, size measurements was done in order to compare with DLS measurements.

When images were examined, nanosphere morphology was seen and size measurement of SEM was similar to size measurement of DLS. Also, IPDI/PEI/PTAA nanospheres was imaged by fluorescence microscope as shown in Figure 3.65. Figure 3.65 shows an images which are non-diluted, 1/100 diluted, and precipitated sample at 5X zoom. According to the images, IPDI/PEI/PTAA nanospheres have yellow-green fluorescence brightness.

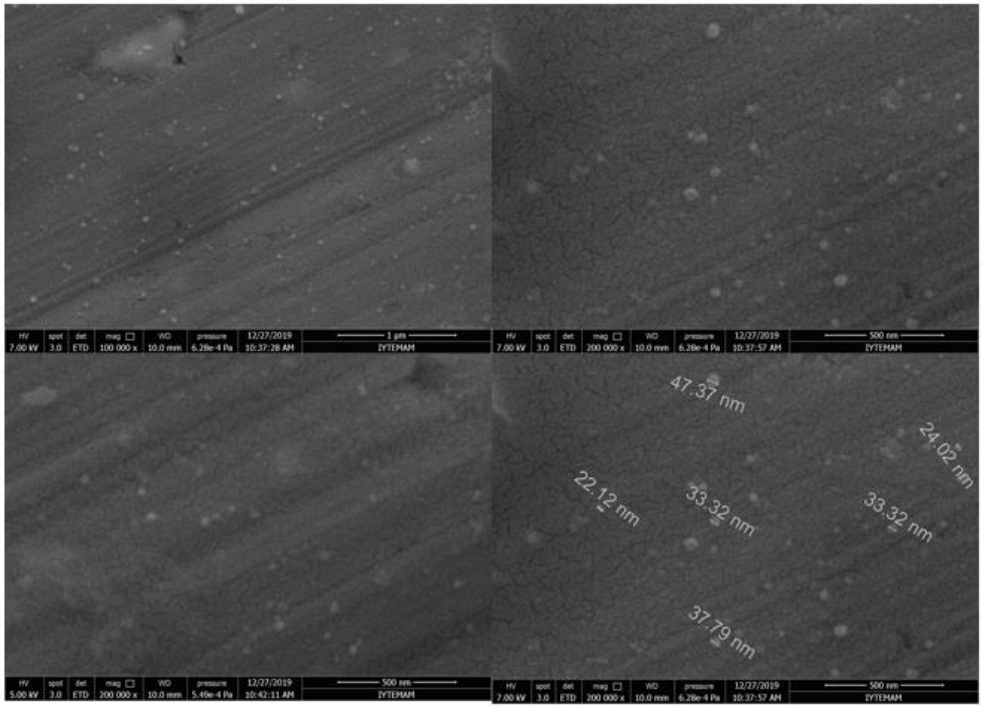

Figure 3.64. SEM images of IPDI/PEI/PTAA nanospheres.

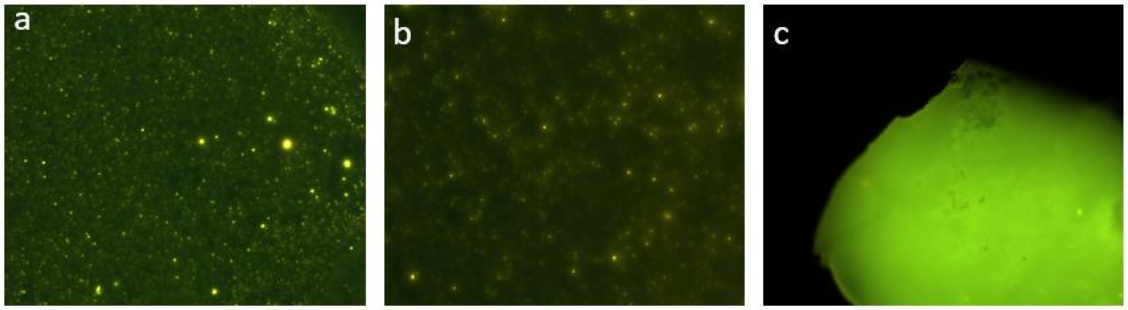

Figure 3.65. IPDI/PEI/PTAA fluorescence microscope images, (a) non-diluted sample 5X, (b) 1/100 diluted sample 5X, (c) precipitated sample 5X.

By the completion of the full characterization of IPDI/PEI/PTAA nanospheres then, magnetic properties was provided by bounding of gadolinium metals. After dual mode agents was prepared, determination of free Gd metal ion was done by ICP-OES. Samples were taken from each dialysis media. As shown in Figure 3.66, it was seen that the amount of free gadolinium has almost moved away from the media after the 5th repetition.

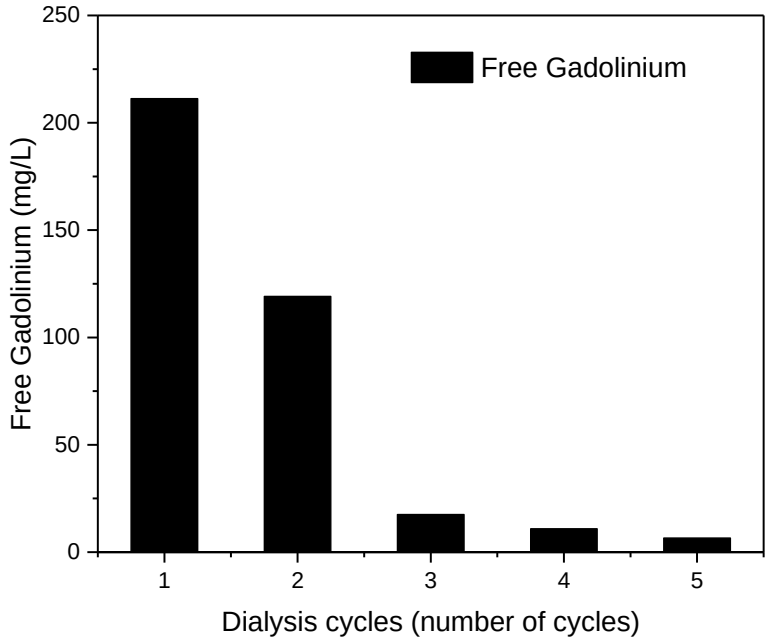

Figure 3.66. Free gadolinium determination results in dialysis cycles for dual mode agents.

IPDI/PEI/PTAA/DOTA-NHS/Gd (Dual mode (fluorescence and magnetic)) agents was analyzed at excitation wavelength 475 nm by fluorescence spectroscopy (Figure 67). As a result of spectrum, the majority of the fluorescence intensity of IPDI/PEI/PTAA nanospheres seems to have been lost, but it has been observed that it has a fluorescence intensity at a maximum wavelength of 575 nm. Also, size and zeta potential measurements of dual mode agents were performed by DLS. As seen in Figure 3.68, the average hydrodynamic radius of the agents was measured around 8 nm. Afterwards, zeta potential analyzes were performed for 3 times as shown in Table 3.5. As a result of the analysis, the average zeta potential value of the agents was measured as 6.1 mV. These results were observed to be lower than the results of IPDI/PEI/PTAA nanospheres.

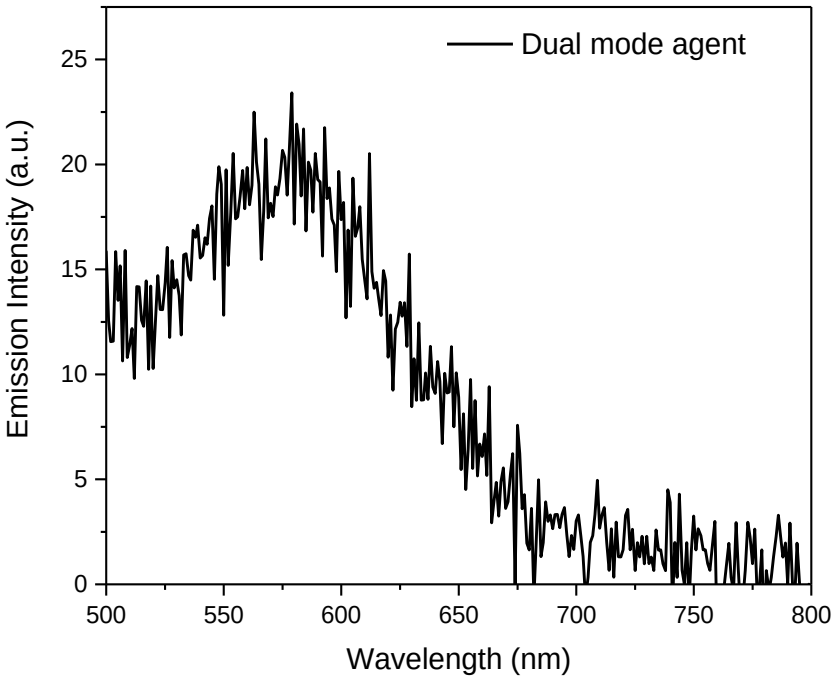

Figure 3.67. Fluorescence spectrum of dual mode agents.

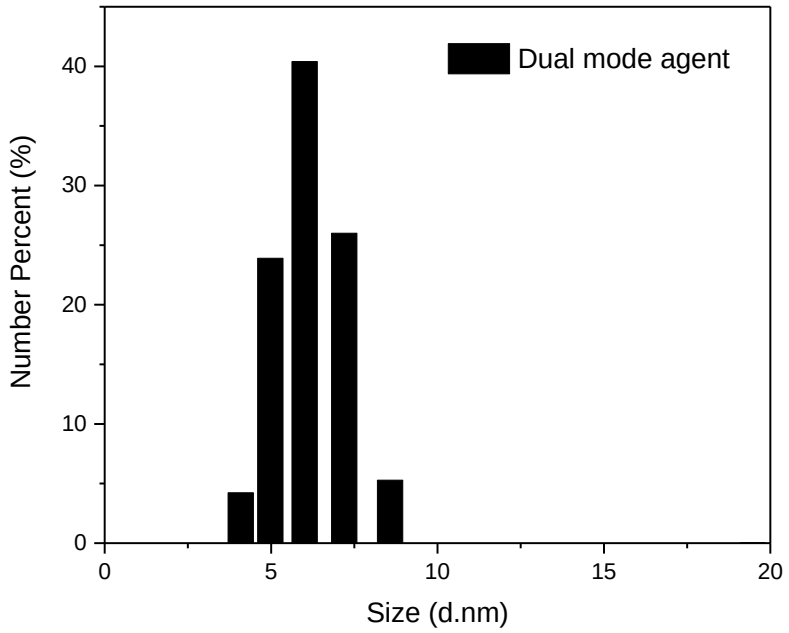

Figure 3.68. Size measurement of dual mode agents.

Table 3.5. Zeta potential measurements of dual mode agents.

Sample	ZP	Mob	Cond
	mV	µmcm/Vs	mS/cm
Dual mode agent 1	4.84	0.3792	0.105
Dual mode agent 2	6.69	0.5242	0.106
Dual mode agent 3	6.78	0.5315	0.108

In addition to these characterizations, SEM analysis was performed at the dilution ratio of 1/1000. The images are shown in Figure 3.69. When images were examined, nanosphere morphology depraved slightly. Also, size measurement of SEM was not similar to size measurement of DLS for dual mode agents. Size of agents was similar to IPDI/PEI/PTAA nanospheres.

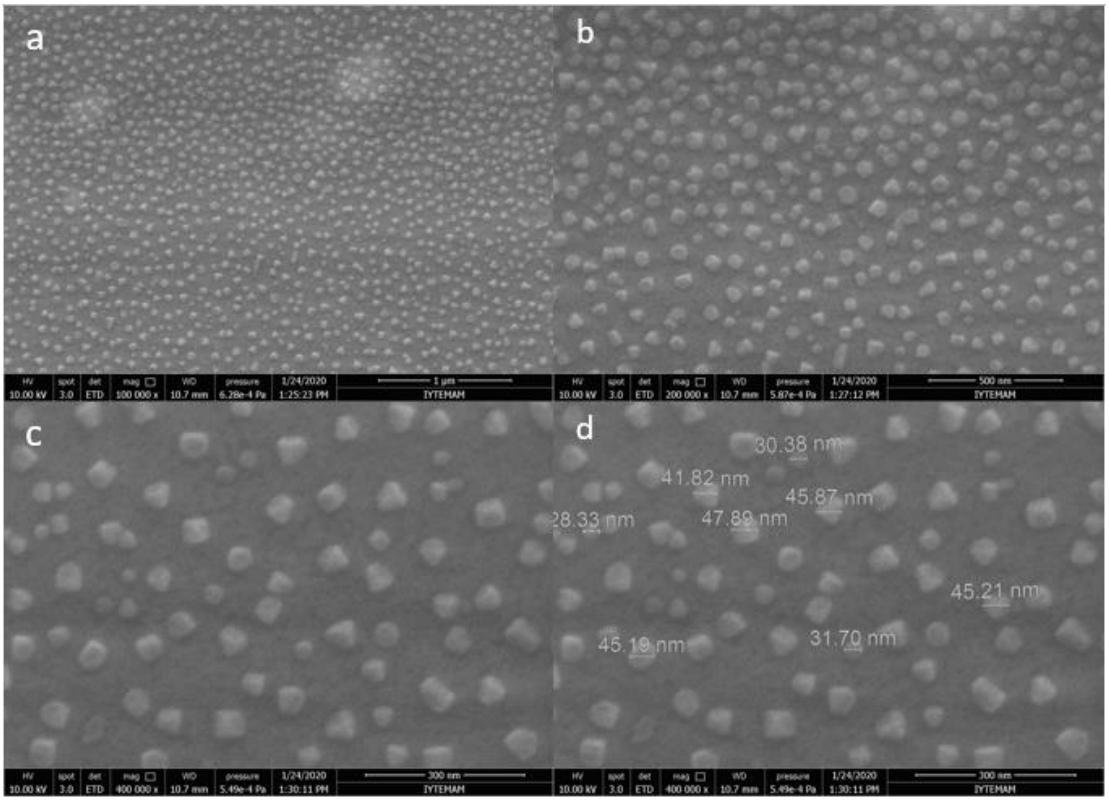

Figure 3.69. SEM images of dual mode; a) 1 um, b)500 nm, c)300 nm, and d)300 nm.

Dual mode agent was analyzed by modelled magnetic levitation systems (Figure 3.70). Also, fluorescent microbeads were used in order to show magnetic effect. When

images were examined, polyurea fluorescent-magnetic agents was successfully synthesized for bioimaging applications. In Figure 3.70.a, cloudy structure was observed as green-yellow color which refers dual mode agents. In addition to this study, the movement of agents was tested with thin rod magnet. As seen in Figure 3.71, dual mode agents took the shape of the magnet over 1 day. This test shows that dual mode agents able to move by magnetic effect. This movement able to display by fluorescence microscope.

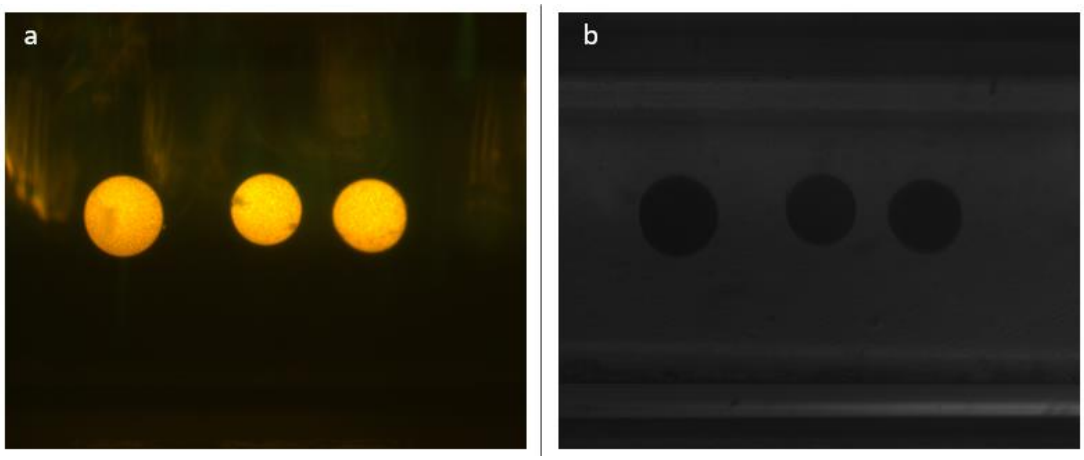

Figure 3.70. Analysis of dual mode agent in magnetic levitation system, a) Blue channel image, b) Black and White image.

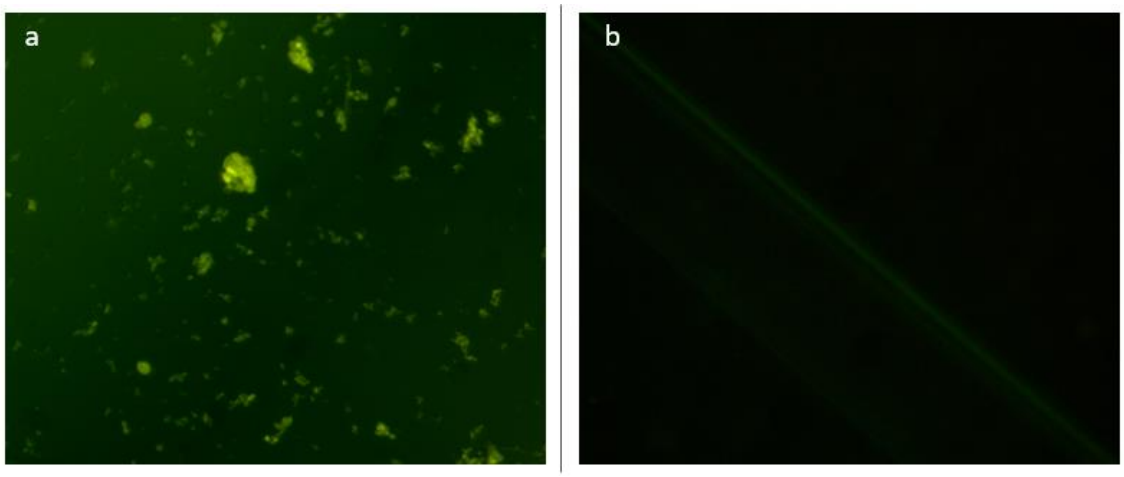

Figure 3.71. Response of the dual mode agent to magnet, a) Before magnet, b) After magnet (after 1 day).

3.3.3. Functionalization of Nanospheres

Two kind technique was used to synthesize functional nanospheres which are EDC-NHS coupling and one pot miniemulsion techniques. Also, PTAA was used as an anionic conjugated polymers in one pot miniemulsion technique in order to increase working applications and areas. The results of techniques was detailed below topics.

3.3.3.1. EDC-NHS Coupling Technique on the Nanospheres

First of all, IPDI/PEI nanospheres was functionalized with PTAA by EDC-NHS coupling technique. IPDI/PEI/PTAA nanospheres and PEI was analyzed in order to compare two of them by FTIR-ATR spectroscopy (Figure 3.72). When the spectrum was examined, it was observed that the broad band at 3600-3000 cm^{-1} range, which refers carboxylic acid -OH groups in the PTAA structure. In addition, it was observed that the carboxylic acid C=O groups at 1720 cm^{-1} overlapped within the peak. According to these results, IPDI/PEI/PTAA fluorescence nanospheres have been successfully synthesized.

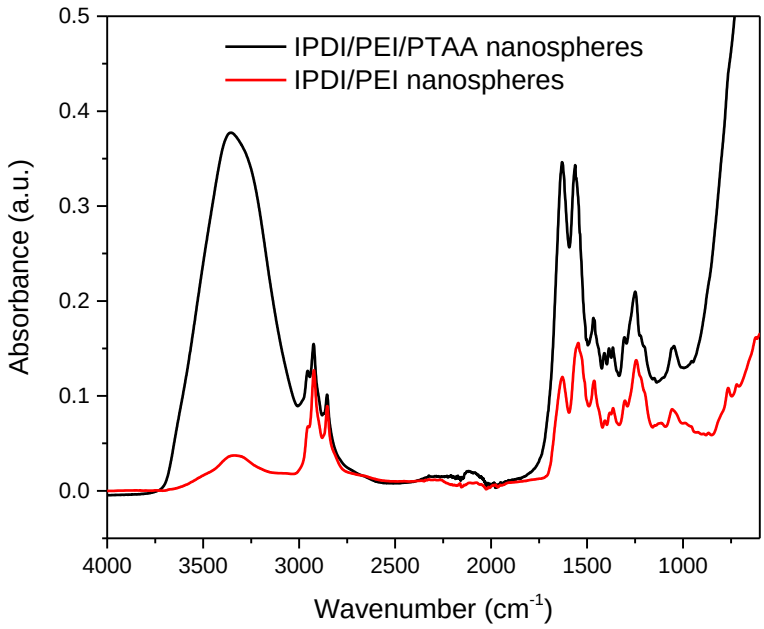

Figure 3.72. Comparative FTIR-ATR spectrums of IPDI/PEI and IPDI/PEI/PTAA nanospheres.

After FTIR-ATR characterization, UV-visible spectroscopy analysis was done for PTAA and IPDI/PEI/PTAA nanospheres as shown in Figure 3.73. According to the spectrum, IPDI/PEI/PTAA caused to scattering and so, baseline was affected. Also, nanospheres have shifting to left at the maximum wavelength of absorbance. New maximum wavelength shifted from 470 nm to 420 nm.

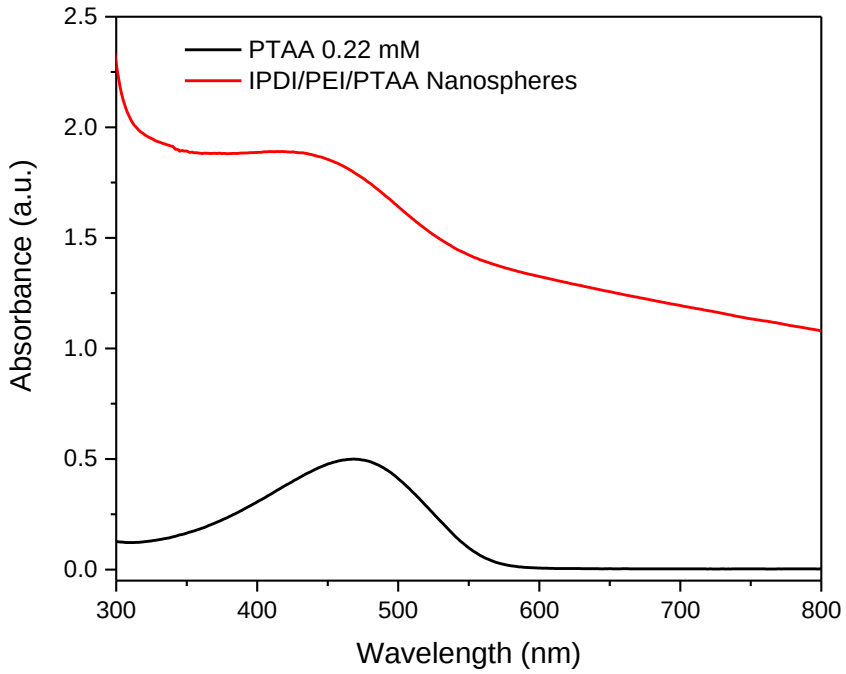

Figure 3.73. UV-visible absorbance spectrum of PTAA and IPDI/PEI/PTAA nanospheres.

Fluorescence spectroscopy analysis was done for PTAA and IPDI/PEI/PTAA nanospheres as shown in Figure 3.74. When spectrum was examined, IPDI/PEI/PTAA has more fluorescence intensity than PTAA. The reason of this situation is related to scattering of light. Nanospheres are able to scatter the light, therefore, intensity of emission increases. Also, nanospheres have shifting to left at the maximum wavelength of emission. New maximum wavelength shifted from 600 nm to 575 nm.

According to UV-visible and fluorescence spectroscopy analysis, it was decided to titrate IPDI/PEI/PTAA nanospheres with PT4 (cationic conjugated polythiophene). For this purpose, excitation wavelength was adjusted at 420 nm (Figure 3.75) for fluorescence spectroscopy. When graph was examined, complexation was observed on nanosphere's

surface and slight quenching was observed with addition of PT4 at the maximum wavelength of spectrum. However, no strong quenching was observed in the complex titrations.

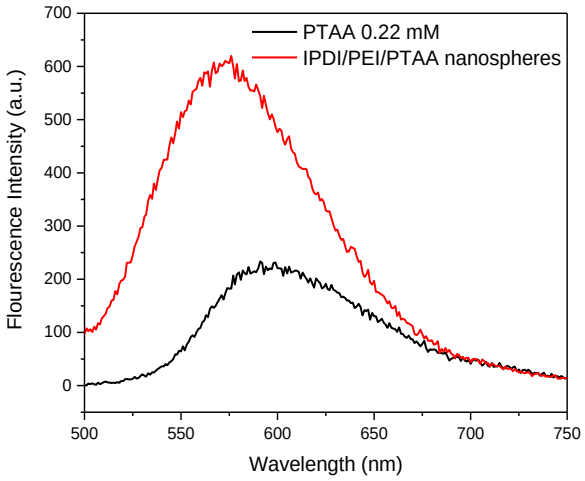

Figure 3.74. Fluorescence emission spectrum of PTAA and IPDI/PEI/PTAA nanospheres.

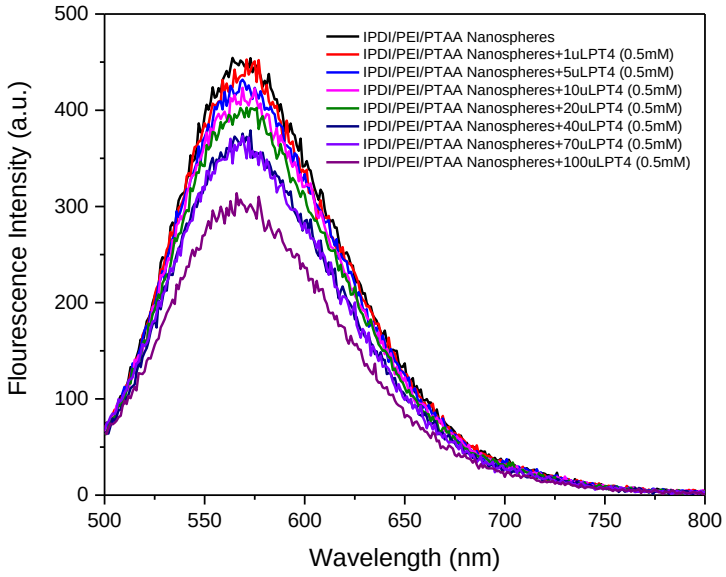

Figure 3.75. Spectroscopic titration between IPDI/PEI/PTAA nanospheres and PT4(0.5mM) by fluorescence spectroscopy (Excitation Wavelength:420 nm).

After complexation test, IPDI/PEI/PTAA nanospheres was imaged by fluorescence microscopy. Figure 3.76 shows several images which was obtained from IPDI/PEI/PTAA suspension sample. According to the images, nanospheres formed a clusters between each other.

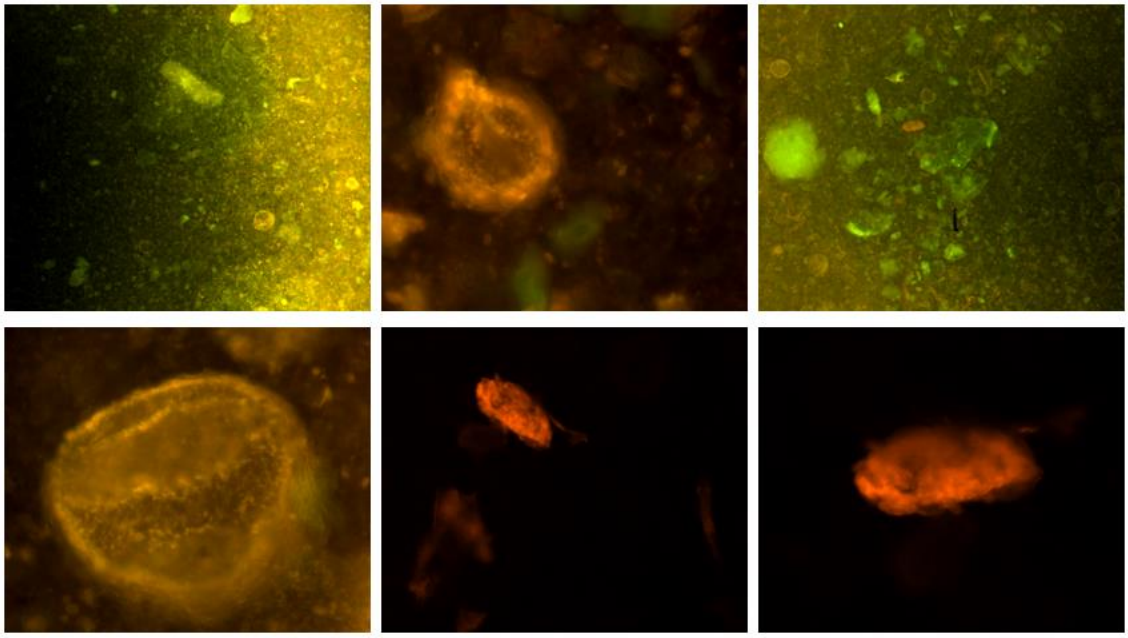

Figure 3.76. Flourescence microscopic images of IPDI/PEI/PTAA nanospheres from suspension.

IPDI/PEI/PTAA nanospheres and PTAA were analyzed to measure quantum yield. Table 3.6 shows that while PTAA's quantum yield was measured as 9.69 %, IPDI/PEI/PTAA nanosphere's quantum yield was measured as 14.7 %. As a result of quantum yield, increase was observed when nanospheres was functionalized with PTAA. The reason of this increase is related to scattering of nanospheres.

Table 3.6. Quantum Yield analysis of PTAA, IPDI/PEI/PTAA nanospheres.

Sample	Quantum Yield (%)
PTAA-0.22 mM	9.69 %
IPDI/PEI/PTAA-0.22 mM	14.7 %

In addition to these characterization, zeta potential measurement was done by DLS. PTAA, IPDI/PEI/PTAA nanospheres and IPDI/PEI/PTAA/PT4 nanospheres were analyzed to measure zeta potential. Table 3.7 demonstrates the result of measurements. Firstly, IPDI/PEI nanosphere's zeta potential measurement was measured as 20.5 mV. Then, IPDI/PEI/PTAA nanosphere shows -13.5 mV thanks to anionic polythiophene PTAA. Lastly, IPDI/PEI/PTAA/PT4 sample was measured as -10.3 mV. It was formed by addition of 100 µL PT4 (cationic polythiophene) to IPDI/PEI/PTAA nanospheres. While PTAA decreased the zeta potential of nanospheres, PT4 contributed as positive to zeta potential. Thus, complexation of PT4 and PTAA was observed slightly on the IPDI/PEI nanospheres.

Table 3.7. Zeta potential measurement results.

Sample Name	Zeta Potential (mV)	Mobility (µmcm/Vs)	Conductivity (mS/cm)
IPDI/PEI nanospheres	20.5	1.606	0.039
IPDI/PEI/PTAA nanospheres	-13.5	-1.061	1.41
IPDI/PEI/PTAA/PT4 nanospheres	-10.3	-0.805	1.02

3.3.3.2. One-pot Technique with conjugated polymers

In this study, PPG 1000 was used instead of PEI 25000. Thus, IPDI/PPG/PTAA nanospheres was prepared. Firstly, absorbance analysis was done by UV-Visible spectroscopy. However, desired spectrum was not obtained because IPDI/PPG/PTAA nanospheres was so concentrated, that's why, the light was scattered. Although dilution was performed, results didn't change. Thus, the absorbance spectrum of IPDI/PPG/PTAA was not shown in this thesis. Then, emission analysis was performed by fluorescence

spectroscopy. Excitation wavelength was chosen between the range 400 and 500 nm in order to optimize the emission of nanospheres. Figure 3.77 shows florescence spectrum of IPDI/PPG/PTAA nanospheres. According to this figure, excitation wavelength was found 450 nm and florescence maximum wavelength was 565nm. On the other hand, IPDI/PPG/PTAA nanospheres have higher fluorescence intensity than PTAA. The reason of this situation is related to increasing the quantum yield because of nanospheres.

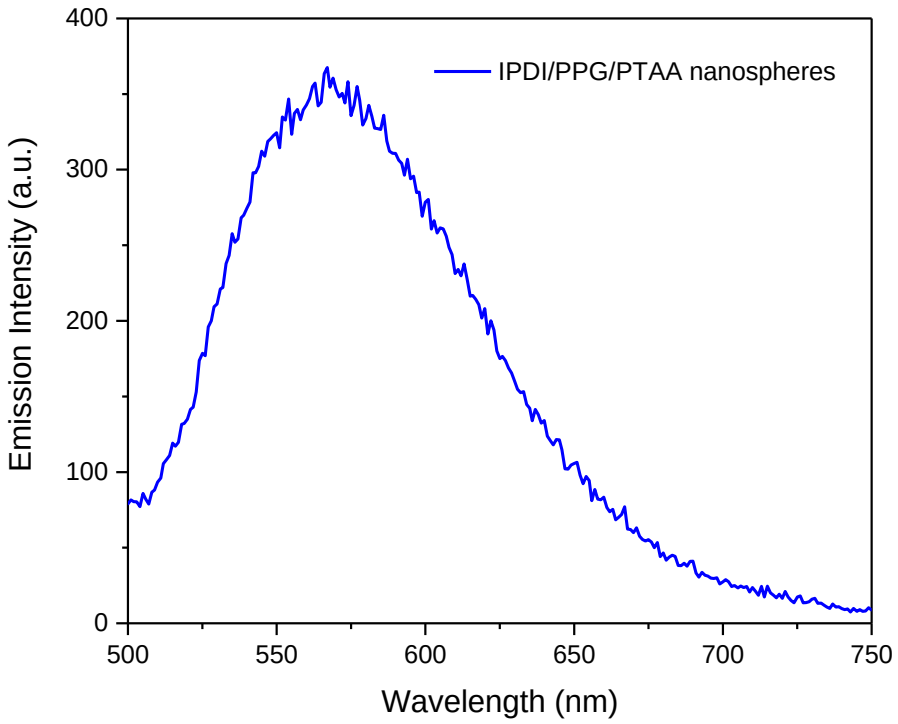

Figure 3.77. Fluorescence emission spectrum of IPDI/PPG/PTAA nanospheres.

After fluorescence analysis, DLS analysis was performed for measurement of size and zeta potential. Size analysis of IPDI/PPG/PTAA nanospheres was shown in Figure 3.78. According to the results, average hydrodynamic radius was found as approximately 60 nm. Also, zeta potential analysis was performed for 3 times, and Table 3.8 shows results. When table was examined, average zeta potential value was measured as -59.6 mV. Nanospheres have negative charge on the surface of nanospheres.

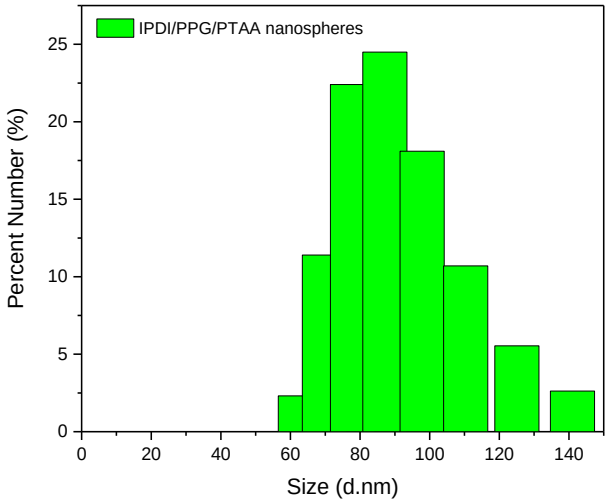

Figure 3.78. Size measurement of IPDI/PPG/PTAA nanospheres

Table 3.8. Zeta potential measurement results of IPDI/PPG/PTAA nanospheres.

Sample Name	ZP	Mob	Cond
	mV	µmcm/Vs	mS/cm
IPDI/PPG/PTAA 1	-58.8	-4.609	0.0663
IPDI/PPG/PTAA 2	-57.8	-4.533	0.0672
IPDI/PPG/PTAA 3	-62.2	-4.878	0.0711

In addition to these, SEM analysis was done in order to observe morphology as shown in Figure 3.79. Samples were prepared with 1/1500 dilution ratio. Several images were shown which shows spherical morphology. Also, size measurement was done by SEM and result shows that DLS size results similar to SEM size results.

In addition to SEM analysis, fluorescence microscopy was used to investigate the IPDI/PPG/PTAA nanospheres. Several images was obtained with different zoom and dilution ratios. Firstly, Figure 3.80.a was prepared with no dilution which shows intensive fluorescence image. Figure 3.80.b was prepared with 1/10 dilution ratio which was obtained as rare according to Figure 3.80.a. Lastly, IPDI/PPG/PTAA was precipitated and examined in Figure 3.80.c. When image was investigated, the image like a surface of sun.

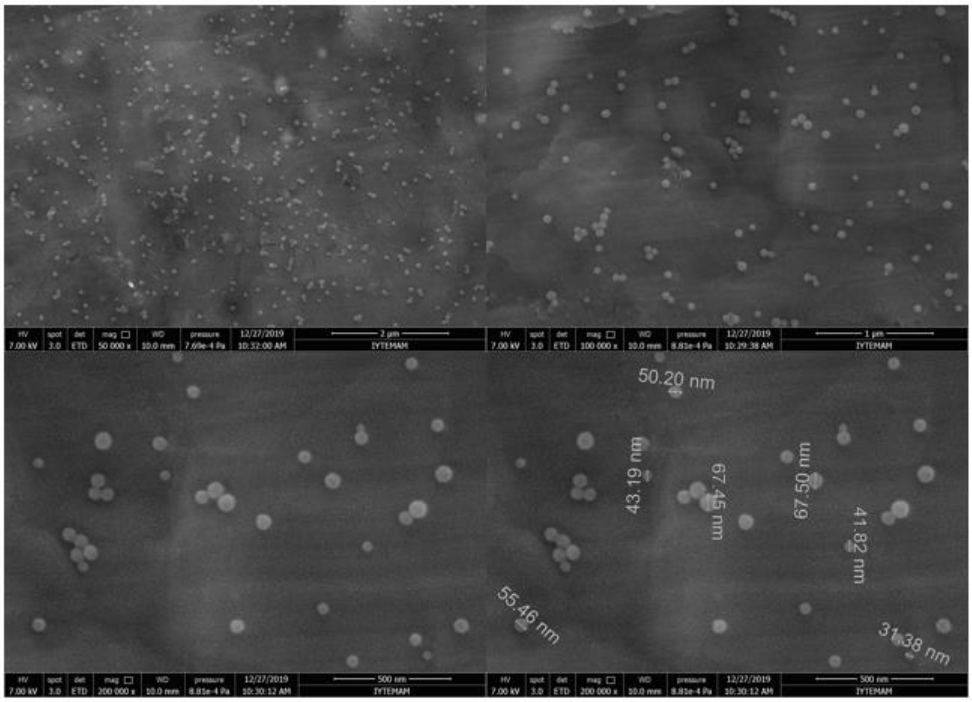

Figure 3.79. SEM images of IPDI/PPG/PTAA nanospheres.

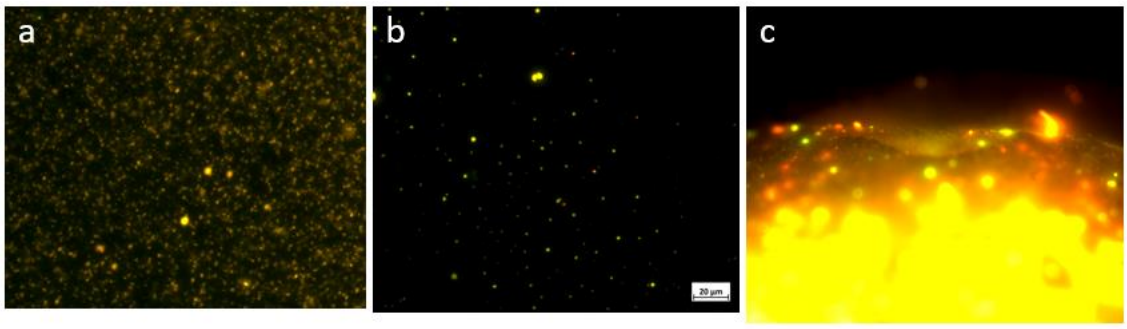

Figure 3.80. Flourescence microscopy images of IPDI/PPG/PTAA nanospheres, (a) no dilution 40X, (b) 1/10 dilution 40X, (c) precipitate 5X.

Also, ELDI was used instead of IPDI. Thus, ELDI/PPG/PTAA and ELDI/PEI/PTAA nanospheres were synthesized at the same protocol. Products were characterized with same way. Their results depended its polymers such as PPG and PEI. Generally, ELDI/PPG/PTAA nanospheres was similar to IPDI/PPG/PTAA nanospheres. At the same way, ELDI/PEI/PTAA nanospheres was similar to IPDI/PEI/PTAA nanospheres. That's why, their characterization results was not shown in this thesis in order to don't repeat same results and discussions.

CHAPTER 4

CONCLUSIONS

In this thesis, the synthesis of polythiophene-polyurethane soft nanoparticles was carried out for bioimaging applications. Firstly, conjugated polythiophenes synthesized and characterized by ^{1}H NMR analysis, UV-visible and fluorescence spectrophotometer. Synthesized conjugated polythiophenes were classified to two groups which are anionic and cationic polythiophenes. PTAA was synthesized as anionic polythiophene and PT3-PT4-PT5 was synthesized as cationic polythiophene. PT4 was used as cationic polythiophene in this thesis. Therefore, PTAA and PT4 were used to carry out polyelectrolyte-polyelectrolyte complexation. According to the results, PTAA and PT4 formed anionic-cationic complex polymer. Also, the complex polymers were titrated with ssDNA sample in order to examine relationship between complex polymer and ssDNA. As a result of examination, complex polymers and ssDNA didn't give a reaction in the spectroscopic investigation, but they responded in size measurement and zeta potential analysis. As can be known, ssDNA have negative charge, therefore, when neutral complex polymer was titrated with ssDNA, size increased, and zeta potential values decreased. The purpose of this study was to examine usability of complex polymers in bioimaging applications. Thus, complex polymers can be used to detection of any charged biomaterial in bioimaging applications.

Secondly, polyurethane nanosphere derivatives were synthesized by miniemulsion polymerization technique. When synthesis was performed, two techniques were experienced as two step and one pot miniemulsion technique. As a result of synthesis, one pot miniemulsion technique has been found to be more suitable than other technique in this thesis. Because, it provided easy processing, and time saving. Several derivatives of polyurethane nanospheres were synthesized and characterized by SEM, and DLS. As a result of the synthesis, the nanospheres were successfully synthesized in the range of 10-500 nm. Also, several experimental conditions were investigated on the polyurethane nanospheres which were ultrasonication time, concentration of surfactant,

crosslinking agent effect, amounts and types of isocyanates, and amounts and types of polyol groups. Especially, types of isocyanates and polyol groups have great significance in this study. Two kinds of isocyanates were used, and they were IPDI, and ELDI. Also, PPG 1000 and PEI 25000 were used in synthesis. When PPG 1000 was used, polyurethane nanospheres were prepared and when PEI 25000 was used, polyurea nanospheres were prepared. Polyurea nanospheres have $-NH_2$ functional groups on the surface of nanospheres. Therefore, polyurea nanospheres were used to synthesize functional bioimaging agents.

In conclusion, bioimaging agents were prepared by different techniques and they were characterized by SEM, fluorescence microscopy, UV-visible and fluorescence spectroscopy, and magnetic levitation systems. They had fluorescent and magnetic properties with using conjugated polythiophene and gadolinium metals on the synthesized polyurea nanospheres. As a result of these studies, bioimaging agents were ready to use in imaging applications. They can be used to investigate different biological structures.

REFERENCES

1. Liong, M.; Lu, J.; Kovochich, M.; Xia, T.; Ruehm, S. G.; Nel, A. E.; Tamanoi, F.; Zink, J. I., Multifunctional inorganic nanoparticles for imaging, targeting, and drug delivery. *ACS nano* 2008**,** *2* (5), 889-896.

2. Björk, P.; Nilsson, K. P. R.; Lenner, L.; Kågedal, B.; Persson, B.; Inganäs, O.; Jonasson, J., Conjugated polythiophene probes target lysosome-related acidic vacuoles in cultured primary cells. *Molecular and cellular probes* 2007**,** *21* (5-6), 329-337.

3. Zhu, C.; Yang, Q.; Liu, L.; Wang, S., A potent fluorescent probe for the detection of cell apoptosis. *Chemical Communications* 2011**,** *47* (19), 5524-5526.

4. Xu, Q.; Zhu, L.; Yu, M.; Feng, F.; An, L.; Xing, C.; Wang, S., Gadolinium (III) chelated conjugated polymer as a potential MRI contrast agent. *Polymer* 2010**,** *51* (6), 1336-1340.

5. Atkins, K. M.; Martínez, F. M.; Nazemi, A.; Scholl, T. J.; Gillies, E. R., Poly (para-phenylene ethynylene) s functionalized with Gd (III) chelates as potential MRI contrast agents. *Canadian Journal of Chemistry* 2011**,** *89* (1), 47-56.

6. Seo, J.; Kim, Y.-s., Ultrasound imaging and beyond: recent advances in medical ultrasound. Springer: 2017.

7. Passerotti, C.; Chow, J. S.; Silva, A.; Schoettler, C. L.; Rosoklija, I.; Perez-Rossello, J.; Cendron, M.; Cilento, B. G.; Lee, R. S.; Nelson, C. P., Ultrasound versus computerized tomography for evaluating urolithiasis. *The Journal of urology* 2009**,** *182* (4S), 1829-1834.

8. Schuster, D. M.; Nieh, P. T.; Jani, A. B.; Amzat, R.; Bowman, F. D.; Halkar, R. K.; Master, V. A.; Nye, J. A.; Odewole, O. A.; Osunkoya, A. O., Anti-3-[18F] FACBC positron emission tomography-computerized tomography and 111In-capromab pendetide single photon emission computerized tomography-computerized tomography for recurrent prostate carcinoma: results of a prospective clinical trial. *The Journal of urology* 2014**,** *191* (5), 1446-1453.

9. Wu, C.; Bull, B.; Szymanski, C.; Christensen, K.; McNeill, J., Multicolor conjugated polymer dots for biological fluorescence imaging. *ACS nano* 2008**,** *2* (11), 2415-2423.

10. Li, K.; Liu, B., Polymer-encapsulated organic nanoparticles for fluorescence and photoacoustic imaging. *Chemical Society Reviews* 2014**,** *43* (18), 6570-6597.

11. Zhu, C.; Liu, L.; Yang, Q.; Lv, F.; Wang, S., Water-soluble conjugated polymers for imaging, diagnosis, and therapy. *Chemical reviews* 2012**,** *112* (8), 4687-4735.

12. Chiang, C. K.; Fincher Jr, C.; Park, Y. W.; Heeger, A. J.; Shirakawa, H.; Louis, E. J.; Gau, S. C.; MacDiarmid, A. G., Electrical conductivity in doped polyacetylene. *Physical review letters* 1977**,** *39* (17), 1098.

13. Diaz, A.; Kanazawa, K., Electrochemical Polymerization of Pyrrole, JCS Chem. *Comm* 1979**,** *635*, 636.

14. Yassar, A.; Roncali, J.; Garnier, F., Preparation and electroactivity of poly (thiophene) electrodes modified by electrodeposition of palladium particles. *Journal of electroanalytical chemistry and interfacial electrochemistry* 1988**,** *255* (1-2), 53-69.

15. Tourillon, G.; Garnier, F., New electrochemically generated organic conducting polymers. *Journal of Electroanalytical Chemistry and Interfacial Electrochemistry* 1982**,** *135* (1), 173-178.

16. Bates, N.; Cross, M.; Lines, R.; Walton, D., Flexible and heat-processable conductive films of polypyrrole. *Journal of the Chemical Society, Chemical Communications* 1985**,** (13), 871-872.

17. Delamar, M.; Lacaze, P.-C.; Dumousseau, J.-Y.; Dubois, J.-E., Electrochemical oxidation of benzene and biphenyl in liquid sulfur dioxide: formation of conductive deposits. *Electrochimica Acta* 1982**,** *27* (1), 61-65.

18. Rault-Berthelot, J.; Simonet, J., The anodic oxidation of fluorene and some of its derivatives: Conditions for the formation of a new conducting polymer. *Journal of electroanalytical chemistry and interfacial electrochemistry* 1985**,** *182* (1), 187-192.

19. Barbarella, G.; Melucci, M.; Sotgiu, G., The versatile thiophene: an overview of recent research on thiophene-based materials. *Advanced Materials* 2005**,** *17* (13), 1581-1593.

20. Mishra, A.; Ma, C.-Q.; Bauerle, P., Functional oligothiophenes: molecular design for multidimensional nanoarchitectures and their applications. *Chemical reviews* 2009**,** *109* (3), 1141-1276.

21. Ashraf, R. S.; Meager, I.; Nikolka, M.; Kirkus, M.; Planells, M.; Schroeder, B. C.; Holliday, S.; Hurhangee, M.; Nielsen, C. B.; Sirringhaus, H., Chalcogenophene comonomer comparison in small band gap diketopyrrolopyrrole-based conjugated polymers for high-performing field-effect transistors and organic solar cells. *Journal of the American Chemical Society* 2015**,** *137* (3), 1314-1321.

22. Liu, X.; Wang, H. Q.; Li, Y.; Gui, Z.; Ming, S.; Usman, K.; Zhang, W.; Fang, J., Regular Organic Solar Cells with Efficiency over 10% and Promoted Stability by Ligand-and Thermal Annealing-Free Al-Doped ZnO Cathode Interlayer. *Advanced Science* 2017**,** *4* (8), 1700053.

23. Friend, R.; Gymer, R.; Holmes, A.; Burroughes, J.; Marks, R.; Taliani, C.; Bradley, D.; Dos Santos, D.; Bredas, J.; Lögdlund, M., Electroluminescence in conjugated polymers. *Nature* 1999**,** *397* (6715), 121-128.

24. Nielsen, C. B.; Ashraf, R. S.; Treat, N. D.; Schroeder, B. C.; Donaghey, J. E.; White, A. J.; Stingelin, N.; McCulloch, I., 2, 1, 3-Benzothiadiazole-5, 6-Dicarboxylic Imide–A Versatile Building Block for Additive-and Annealing-Free Processing of Organic Solar Cells with Efficiencies Exceeding 8%. *Advanced Materials* 2015**,** *27* (5), 948-953.

25. Kaya, H. Detection of DNA methylation of multiple tumor supressor p16INK4a gene by polythiophene based optical sensor. İzmir Institute of Technology, 2018.

26. Yildiz, U. H.; Alagappan, P.; Liedberg, B., Naked eye detection of lung cancer associated miRNA by paper based biosensing platform. *Analytical chemistry* 2013**,** *85* (2), 820-824.

27. Chai, R.; Xing, C.; Qi, J.; Fan, Y.; Yuan, H.; Niu, R.; Zhan, Y.; Xu, J., Water-Soluble Conjugated Polymers for the Detection and Inhibition of Protein Aggregation. *Advanced Functional Materials* 2016**,** *26* (48), 9026-9031.

28. Kim, B.; Chen, L.; Gong, J.; Osada, Y., Titration behavior and spectral transitions of water-soluble polythiophene carboxylic acids. *Macromolecules* 1999**,** *32* (12), 3964-3969.

29. Rajwar, D.; Ammanath, G.; Cheema, J. A.; Palaniappan, A.; Yildiz, U. H.; Liedberg, B., Tailoring conformation-induced chromism of polythiophene copolymers for nucleic acid assay at resource limited settings. *ACS applied materials & interfaces* 2016**,** *8* (13), 8349-8357.

30. Bertrand, P.; Jonas, A.; Laschewsky, A.; Legras, R., Ultrathin polymer coatings by complexation of polyelectrolytes at interfaces: suitable materials, structure and properties. *Macromolecular rapid communications* 2000**,** *21* (7), 319-348.

31. Radeva, T., *Physical chemistry of polyelectrolytes*. CRC Press: 2001; Vol. 99.

32. Feng, L.; Zhu, J.; Wang, Z., Biological functionalization of conjugated polymer nanoparticles for targeted imaging and photodynamic killing of tumor cells. *ACS applied materials & interfaces* 2016**,** *8* (30), 19364-19370.

33. Braeken, Y.; Cheruku, S.; Ethirajan, A.; Maes, W., Conjugated polymer nanoparticles for bioimaging. *Materials* 2017**,** *10* (12), 1420.

34. Feng, L.; Zhu, C.; Yuan, H.; Liu, L.; Lv, F.; Wang, S., Conjugated polymer nanoparticles: preparation, properties, functionalization and biological applications. *Chemical Society Reviews* 2013**,** *42* (16), 6620-6633.

35. Özenler, S.; Yucel, M.; Tüncel, O. z.; Kaya, H.; Özçelik, S.; Yildiz, U. H., Single Chain Cationic Polymer Dot as a Fluorescent Probe for Cell Imaging and Selective Determination of Hepatocellular Carcinoma Cells. *Analytical chemistry* 2019**,** *91* (16), 10357-10360.

36. Li, K.; Ding, D.; Huo, D.; Pu, K. Y.; Thao, N. N. P.; Hu, Y.; Li, Z.; Liu, B., Conjugated polymer based nanoparticles as dual-modal probes for targeted in vivo fluorescence and magnetic resonance imaging. *Advanced Functional Materials* 2012**,** *22* (15), 3107-3115.

37. Feng, X.; Lv, F.; Liu, L.; Tang, H.; Xing, C.; Yang, Q.; Wang, S., Conjugated polymer nanoparticles for drug delivery and imaging. *ACS applied materials & interfaces* 2010**,** *2* (8), 2429-2435.

38. Giorgetti, E.; Giusti, A.; Arias, E.; Moggio, I.; Ledezma, A.; Romero, J.; Saba, M.; Quochi, F.; Marceddu, M.; Gocalinska, A. In *In Situ production of polymer-capped silver nanoparticles for optical biosensing*, Macromolecular symposia, Wiley Online Library: 2009; pp 167-173.

39. Tebaldi, M. L.; Belardi, R. M.; Montoro, S. R., Polymers with Nano-Encapsulated Functional Polymers: Encapsulated Phase Change Materials. In *Design and Applications of Nanostructured Polymer Blends and Nanocomposite Systems*, Elsevier: 2016; pp 155-169.

40. Hanemann, T.; Szabó, D. V., Polymer-nanoparticle composites: from synthesis to modern applications. *Materials* 2010**,** *3* (6), 3468-3517.

41. Landfester, K., Miniemulsions for nanoparticle synthesis. In *Colloid chemistry II*, Springer: 2003; pp 75-123.

42. Rao, J. P.; Geckeler, K. E., Polymer nanoparticles: preparation techniques and size-control parameters. *Progress in polymer science* 2011**,** *36* (7), 887-913.

43. Mallakpour, S.; Behranvand, V., Polymeric nanoparticles: Recent development in synthesis and application. *Express Polymer Letters* 2016**,** *10* (11), 895.

44. Wang, Y.-J.; Larsson, M.; Huang, W.-T.; Chiou, S.-H.; Nicholls, S. J.; Chao, J.-I.; Liu, D.-M., The use of polymer-based nanoparticles and nanostructured materials in treatment and diagnosis of cardiovascular diseases: Recent advances and emerging designs. *Progress in Polymer Science* 2016**,** *57*, 153-178.

45. Nasir, A.; Kausar, A.; Younus, A., A review on preparation, properties and applications of polymeric nanoparticle-based materials. *Polymer-Plastics Technology and Engineering* 2015**,** *54* (4), 325-341.

46. He, G.; Pan, Q.; Rempel, G. L., Synthesis of poly (methyl methacrylate) nanosize particles by differential microemulsion polymerization. *Macromolecular rapid communications* 2003**,** *24* (9), 585-588.

47. Nagavarma, B.; Yadav, H. K.; Ayaz, A.; Vasudha, L.; Shivakumar, H., Different techniques for preparation of polymeric nanoparticles-a review. *Asian J. Pharm. Clin. Res* 2012**,** *5* (3), 16-23.

48. Li, C. Y.; Chiu, W. Y.; Don, T. M., Preparation of polyurethane dispersions by miniemulsion polymerization. *Journal of Polymer Science Part A: Polymer Chemistry* 2005**,** *43* (20), 4870-4881.

49. Reis, C. P.; Neufeld, R. J.; Ribeiro, A. J.; Veiga, F., Nanoencapsulation I. Methods for preparation of drug-loaded polymeric nanoparticles. *Nanomedicine: Nanotechnology, Biology and Medicine* 2006**,** *2* (1), 8-21.

50. Tiarks, F.; Landfester, K.; Antonietti, M., One-step preparation of polyurethane dispersions by miniemulsion polyaddition. *Journal of Polymer Science Part A: Polymer Chemistry* 2001**,** *39* (14), 2520-2524.

51. Barrère, M.; Landfester, K., High molecular weight polyurethane and polymer hybrid particles in aqueous miniemulsion. *Macromolecules* 2003**,** *36* (14), 5119-5125.

52. Wang, C.; Chu, F.; Graillat, C.; Guyot, A., Hybrid Acrylic-Polyurethane Latexes by Miniemulsion Polymerization. *Polymer Reaction Engineering* 2003**,** *11* (3), 541-562.

53. Tang, P.; Sudol, E.; Silebi, C.; El-Aasser, M., Miniemulsion polymerization—a comparative study of preparative variables. *journal of applied polymer science* 1991**,** *43* (6), 1059-1066.

54. Miller, C.; Blythe, P.; Sudol, E.; Silebi, C.; El-Aasser, M., Effect of the presence of polymer in miniemulsion droplets on the kinetics of polymerization. *Journal of Polymer Science Part A: Polymer Chemistry* 1994**,** *32* (12), 2365-2376.

55. Alduncin, J. A.; Forcada, J.; Barandiaran, M. J.; Asua, J. M., On the main locus of radical formation in emulsion polymerization initiated by oil-soluble initiators. *Journal of Polymer Science Part A: Polymer Chemistry* 1991**,** *29* (9), 1265-1270.

56. Alduncin, J. A.; Forcada, J.; Asua, J. M., Miniemulsion polymerization using oil-soluble initiators. *Macromolecules* 1994**,** *27* (8), 2256-2261.

57. Landfester, K.; Bechthold, N.; Tiarks, F.; Antonietti, M., Miniemulsion polymerization with cationic and nonionic surfactants: a very efficient use of surfactants for heterophase polymerization. *Macromolecules* 1999**,** *32* (8), 2679-2683.